PolyPublie
Polytechnique Montréal

POLYTECHNIQUE MONTRÉAL
UNIVERSITÉ D'INGÉNIERIE

Titre: Title:	Machinability of Titanium Metal Matrix Composites (Ti-MMCs)
Auteur: Author:	Maryam Aramesh
Date:	2015
Type:	Mémoire ou thèse / Dissertation or Thesis
Référence: Citation:	Aramesh, M. (2015). Machinability of Titanium Metal Matrix Composites (Ti-MMCs) [Thèse de doctorat, École Polytechnique de Montréal]. PolyPublie. https://publications.polymtl.ca/1772/

Document en libre accès dans PolyPublie
Open Access document in PolyPublie

URL de PolyPublie: PolyPublie URL:	https://publications.polymtl.ca/1772/
Directeurs de recherche: Advisors:	Marek Balazinski, Helmi Attia, & Hossam Kishawy
Programme: Program:	Génie mécanique

Ce fichier a été téléchargé à partir de PolyPublie, le dépôt institutionnel de Polytechnique Montréal
This file has been downloaded from PolyPublie, the institutional repository of Polytechnique Montréal

https://publications.polymtl.ca

UNIVERSITÉ DE MONTRÉAL

MACHINABILITY OF TITANIUM METAL MATRIX COMPOSITES (Ti-MMCs)

MARYAM ARAMESH

DÉPARTEMENT DE GÉNIE MÉCANIQUE

ÉCOLE POLYTECHNIQUE DE MONTRÉAL

THÈSE PRÉSENTÉE EN VUE DE L'OBTENTION

DU DIPLÔME DE PHILOSOPHIAE DOCTOR

(GÉNIE MÉCANIQUE)

JUIN 2015

© Maryam Aramesh, 2015.

UNIVERSITÉ DE MONTRÉAL

ÉCOLE POLYTECHNIQUE DE MONTRÉAL

Cette thèse intitulée :

MACHINABILITY OF TITANIUM METAL MATRIX COMPOSITES (Ti-MMCs)

présentée par: ARAMESH Maryam

en vue de l'obtention du diplôme de : Philosophiae Doctor

été dûment acceptée par le jury d'examen constitué de:

M. LAKIS Aouni A., Ph. D., président

M. BALAZINSKI Marek, Docteur ès sciences, membre et directeur de recherche

M. ATTIA Helmi, Ph. D., membre et codirecteur de recherche

M. KISHAWY Hossam A., Ph. D., membre et codirecteur de recherche

M. VADEAN Aurelian, Doctorat, membre

M. KOSHY Philip, Ph. D., membre

DEDICATION

I would like to dedicate my thesis to my dearest parents Parvin and Mehdi, beloved husband Ali and wonderful brother Nima.

ACKNOWLEDGEMENTS

I would like to express my profoundest gratitude to my supervisor Prof. Marek Balazinski, for his invaluable guidance, advice and support whilst encouraging me to peruse my own ideas throughout all these years. He has always been an inspiration to me in all aspects of my life for his wisdom, kindness and trust.

I would also like to thank sincerely my co-supervisors Profs. Helmi Attia and Hossam Kishawy for their continuous guidance, help and support. This work would not succeed without their precious advice.

I acknowledge the NSERC Canadian Network for Research and Innovation in Machining Technology (CANRIMT) for their financial support.

I would like to thank the aerospace structures, materials and manufacturing laboratory of the National Research Council Canada (NRC) for hosting me as a guest worker and providing me with their facilities. My deepest special thanks goes to Prof. Attia and his team for their endless support which is priceless.

I would like to thank my colleagues and office-mates Mehrdad Givi, Paul Provencher, Anna Los and Xavier Rimpault for their help and support. I also wish to thank my dear friends Shagha Rouzmeh, Shagha Attar and Mojdeh Tirehdast for their friendship, kindness and encouragements during all these years.

My sincere thanks goes to my family and my husband Ali Alem for their love, support and continuous encouragements.

RÉSUMÉ

Les composites à matrices métalliques de titane (Ti-MMCs), en tant que nouvelle génération de matériaux, ont plusieurs applications potentielles dans les domaines industriels de l'aérospatiale, et l'automobile. La présence de particules de céramique améliore les propriétés mécaniques et physiques de la matrice. Cependant, ces particules sont dures et abrasives par leur nature, ce qui cause de multiples difficultés pour leur usinabilité. L'usure sévère des outils ainsi que la vie utile très brève de ceux-ci représentent les inconvénients les plus importants de leur usinabilité. La littérature indique très peu d'études concernant leur usinabilité, en particulier pour l'estimation de la durée de vie utile et de l'usure des outils de coupe. Les outils de diamant polycristallin (PCD) semblent être le meilleur choix pour usiner les MMCs du point de vue des chercheurs. Malgré ceci, en raison de leur coût élevé, des alternatives abordables sont fort souhaitables. Les plaquettes de nitrure de bore cubique (CBN) demeurent les outils les plus durs après celles de PCD, démontrent d'excellentes qualités dont une grande résistance à l'usure, une bonne dureté à température élevée, un bas coefficient de friction et une température de fusion élevée. Toutefois, les outils de CBN n'ont pas encore été étudiés dans le contexte de l'usinage des Ti-MMCs. La présente étude élabore en profondeur les mécanismes d'usure des plaquettes de CBN durant le tournage des Ti-MMCs. La morphologie unique des faces usées des outils a été étudiée pour la première fois, menant à une nouvelle compréhension dans l'identification des mécanismes d'usure chimiques durant l'usinage des Ti-MMCs. De plus, la pleine exploitation de la vie utile des outils de coupe est critique en raison des dépenses importantes liées au remplacement non-optimal des outils de coupe. Ceci encourage fortement le développement d'une modèle fiable pour l'estimation de la vie utile pour toutes conditions de coupe. Cette étude élabore une nouvelle méthode découlant de la méthodologie d'analyse de survie (survival analysis) pour estimer les états d'usures successives des outils pour toutes conditions d'usinage des Ti-MMCs. Ce modèle statistique prend en compte la durée de l'usinage en plus des effets des paramètres de coupe. De cette manière, les résultats obtenus ont démontré un excellent accord avec les résultats expérimentaux. De surcroît, un modèle plus avancé a été développé en rajoutant l'usure des outils comme variable au modèle précédent. Il en sort un nouveau modèle proposé pour estimer la durée de vie utile restante des plaquettes usées pour des conditions d'usinage variables, en incluant l'usure actuelle des outils dans les données d'entrée. Les résultats de ce modèle ont été validés par expérimentation et le modèle concorde très bien avec les essais expérimentaux.

ABSTRACT

Titanium metal matrix composites (Ti-MMCs), as a new generation of materials, have various potential applications in aerospace and automotive industries. The presence of ceramic particles enhances the physical and mechanical properties of the alloy matrix. However, the hard and abrasive nature of these particles causes various issues in the field of their machinability. Severe tool wear and short tool life are the most important drawbacks of machining this class of materials. There is very limited work in the literature regarding the machinability of this class of materials especially in the area of tool life estimation and tool wear.

By far, polycrystalline diamond (PCD) tools appear to be the best choice for machining MMCs from researchers' point of view. However, due to their high cost, economical alternatives are sought. Cubic boron nitride (CBN) inserts, as the second hardest available tools, show superior characteristics such as great wear resistance, high hardness at elevated temperatures, a low coefficient of friction and a high melting point. Yet, so far CBN tools have not been studied during machining of Ti-MMCs. In this study, a comprehensive study has been performed to explore the tool wear mechanisms of CBN inserts during turning of Ti-MMCs. The unique morphology of the worn faces of the tools was investigated for the first time, which led to new insights in the identification of chemical wear mechanisms during machining of Ti-MMCs.

Utilizing the full tool life capacity of cutting tools is also very crucial, due to the considerable costs associated with suboptimal replacement of tools. This strongly motivates development of a reliable model for tool life estimation under any cutting conditions. In this study, a novel model based on the survival analysis methodology is developed to estimate the progressive states of tool wear under any cutting conditions during machining of Ti-MMCs. This statistical model takes into account the machining time in addition to the effect of cutting parameters. Thus, promising results were obtained which showed a very good agreement with the experimental results.

Moreover, a more advanced model was constructed, by adding the tool wear as another variable to the previous model. Therefore, a new model was proposed for estimating the remaining life of worn inserts under different cutting conditions, using the current tool wear data as an input. The results of this model were validated with the experimental results. The estimated results were well consistent with the results obtained from the experiments.

TABLE OF CONTENTS

LIST OF TABLES

LIST OF FIGURES

INTRODUCTION

Metal matrix composites (MMCs) offer such an outstanding combination of preferred characteristics that cannot be excluded from our daily life anymore. In order to achieve a valuable modification in various properties of materials, metallic matrices are reinforced with additional phases upon extra requirements on chemical and/or physical properties. The resultant custom-made materials offer desired characteristics such as light weight, high wear resistance, high physical, thermal and mechanical properties. Thus, they demonstrate various potentials in different industries such as aerospace, transportation and automotive (Kainer, 2006).

Titanium metal matrix composites (Ti-MMCs) benefit from both desired characteristics of the titanium alloy matrix such as light weight, high temperature and wear resistance, in addition to high toughness provided by the TiC reinforcing particles (Pramanik et al., 2008). Thus, they exhibit a combination of preferable mechanical and physical properties. Despite all these brilliant characteristics, these materials suffer from poor machinability mostly due to the presence of extremely hard and abrasive reinforcements. The interaction between the tool and reinforcing particles induces a complex deformation behavior in MMC structures, resulting in propagation of cracks and voids on the surface of the material and consequent low accuracy and poor surface finish. In addition, low thermal conductivity, low modulus of elasticity and chemical reactivity of titanium alloys rise additional challenges in the field of their machinability (Davim, 2008; Hosseini & Kishawy, 2014).

Severe tool wear and very short tool life are technically the most important drawbacks of machining of Ti-MMCs. Thus, analyses of tool life and tool wear could be considered as one of the most important criteria for their machinability. Polycrystalline diamond (PCD) tools have been introduced as the most effective tools for machining MMCs (Heath, 2001). However, their high cost strongly motivates seeking out more cost effective alternatives. Cubic boron nitride (CBN) inserts, as the second hardest available tools, show potentials as an alternative for machining of MMCs. Yet, there is no literature regarding the tool wear mechanisms of these inserts during machining of Ti-MMCs.

Huge costs associated with sub-optimal tool replacements are a call for the development of a reliable model for estimating the remaining life of inserts under different cutting conditions. This is

even more crucial for machining Ti-MMCs, where severe tool wear results in a very short life. Moreover, non-homogeneous distribution of reinforcing particles results in considerable variability of the tool wear data. Therefore, developing a model based on the theory of probability appears to be the best option for modelling the progressive states of tool wear for this class of materials.

Reliable and safe reuse of worn inserts would not be possible without an accurate estimation of their remaining lives till failure. Yet, so far no model has been proposed for predicting the remaining life of worn inserts, using the tool wear data as the input. Development of a model capable of fulfilling this task significantly contributes in cost reduction and productivity increase in machining processes.

Problem definition

High tool wear, short tool life and poor surface quality are the most important issues which are of concern during machining of Ti-MMCs. Hard and abrasive nature of the reinforcing particles are responsible for severe abrasive tool wear. Two-body abrasion wear takes over when the reinforcing particles abrade the cutting tool material while they are tightly confined in the matrix material. Whereas in three-body abrasion, tool wear could also occur when the debonded particles from the matrix roll between the tool and the workpiece. Consequently holes and cavities are generated on the tool surface (H. A. Kishawy et al., 2005). Also, debonding, fracture and cracking of particles would cause voids and cavities on the surface of the workpiece which will highly affect the surface integrity and result in poor surface finish.

Titanium alloy matrix also rises its own machining challenges, mainly due to its thermal and chemical characteristics such as poor thermal conductivity and chemical reactivity at elevated temperatures (Hosseini, Kishawy, et al., 2014).

Due to a very low thermal conductivity of the titanium alloy matrix, extremely high local temperatures are generated in a very small area around the cutting edge. The extremely high contact temperature will result in high tool wear rates during their machining operations. Moreover, oxidation and other chemical wear mechanisms will be involved and further reduce the tool life.

During machining of Ti MMCs, segmented chips are produced that can induce force fluctuations and tool wear variations leading to lack of accuracy. Serrated chips on the trailing edge and

material side flow are also two phenomena which occur during machining MMCs and result in surface deterioration.

Research objectives

Main objective

There is a significant lack of data in the field of machinability analysis of Ti-MMCs. The main objective of this study is to perform a comprehensive study for tool wear and tool life estimation during machining of Ti-MMCs, since these studies are considered as the most important criteria in any machinability analysis.

Specific objectives

- **A comprehensive study on the tool wear mechanisms of CBN inserts during turning of Ti-MMCs.**

Tool wear mechanisms of CBN inserts, as the second candidate for machining of MMCs, during turning of titanium metal matrix composites (Ti-MMCs) were investigated. Adhesion, abrasion, chemical interactions and their effects on the wear surface morphology were investigated in detail.

- **Estimating the progressive states of tool wear for machining of Ti-MMCs with variable cutting conditions.**

A novel model based on the survival analysis methodology is developed for estimating the progressive states of tool wear under different cutting conditions during machining of Ti-MMCs. The model accounts for the machining time in addition to the effect of cutting variables, thus it delivers accurate results.

- **Estimating the remaining useful tool life of worn tools under different cutting conditions.**

Another more advanced survival model is developed for estimating the remaining life of worn inserts under different cutting conditions. The data regarding the tool wear itself was added as a variable into the model, in addition to the cutting parameters. Thus, the new model was capable of predicting the remaining life of worn inserts, using the current tool wear value as the input data.

Hypotheses

- **Maximum flank wear length, VB_{Bmax}, is an accepted measure for quantification of the tool life.**

VB_{Bmax} is often used for tool life analysis, since it is easy to quantify and also due to its influence on the accuracy and surface integrity of the machined part (Davim & Astakhov, 2008)

- **Maximum flank wear length, VB_{Bmax}, at the second transition point of the tool wear curve is considered as the tool *failure* criterion in machinability analyses**

Severe vibration, temperature and cutting forces are induced at the third state of tool wear curve. Thus, during any machining process, entering this state should be avoided in order to prevent any serious detriments to the tool and machined surface. The tool wear associated with the transition between the second and third state is often regarded as the tool life criterion (Astakhov, 2013).

- **Tool life and tool wear are affected by the cutting conditions**

Several factors could affect the tool life and tool wear. Yet, cutting conditions specially the cutting speed are of prime concerns, due to their significant effect on the tool wear and consequently the tool life (Astakhov, 2013).

THESIS ORGANIZATION

General technical overview

For the purpose of clarifying the thesis organization, the following provides a general technical overview of the thesis.

This study contains two major phases. In the first phase (Chapter 2), the tool wear mechanisms of CBN inserts, as the second potential alternative tools for machining of Ti-MMCs, were discussed in detail.

In the second phase, the tool life estimation was performed, using survival analysis methodology. The second phase include three steps:

At the first step (Chapter 3), a fixed cutting condition was adopted and only the effect of aging was considered in the Weibull model. The time to reach each state of tool wear and the total sojourn time spent in each state was calculated.

At the second step (Chapter 4), a proportional hazards model with a Weibull baseline was developed. Thus, the effect of cutting conditions in addition to the effect of aging were reflected in the model. Therefore, the time to reach each state under variable cutting conditions were obtained.

In the third step (Chapter 5), tool wear was also added to the previous model. Thus, the remaining life of worn cutting inserts under different cutting conditions was calculated. Due to the importance of the second tool wear transition point, this point was used as the failure criterion for the last model.

At the end (Chapter 6), a complementary analysis was also performed to find the optimum cutting conditions during machining of Ti-MMCs.

Each chapter stated above contains a journal paper corresponding to the mentioned topic.

Following the aforementioned steps and the objectives of this study, more details regarding the chapters' contents are provided below.

Chapters' contents

1- Chapter 1 provides the literature review on the most important aspects of the machinability of MMCs including the chip shape, surface integrity and tooling. A comprehensive literature review is provided on the tool selection for machining of MMCs and the previous researches performed on the CBN inserts for machining of MMCs. Moreover, the current proposed methods for tool life estimations are discussed in this section. This study provides insight into the existing research, the existing problems and missing links thereof which should be addressed.

2- Chapter 2 provides the results of the comprehensive study on the tool wear mechanisms of CBN inserts during turning of Ti-MMCs. Various tool wear mechanisms, including adhesion, abrasion and chemical wear mechanisms were investigated and their effects on the unique wear morphology of the inserts were discussed. Furthermore, for the first time, the embrittlement of titanium alloys during machining of Ti-MMCs was studied. The root causes were investigated and the effect on the wear surface morphology and also on the machined surface was investigated.

3- Chapter 3 provides the steps required to estimate the progressive states of tool wear for a constant cutting condition. The condition used is typical for this tool and material, based on the recommendation of the tool supplier. Thus, only the effect of aging (t) is reflected in the Weibull model used in this study. The mean residual life (MRL) function is also introduced. The procedure for estimating the transition time between each state of tool wear, in addition to the total sojourn time spent in each state are explained.

4- Chapter 4 introduces the novel method for estimating the progressive states of tool wear of *new* inserts for any cutting conditions using a proportional hazards model (PHM) with a Weibull baseline. Applying the PHM as the predictive model, the effect of cutting conditions and aging are taken into account. Thus, an accurate model is developed for estimating the transition time between each state of tool wear under different cutting conditions. It should be mentioned that since Ti-MMCs are produced near net shape, usually only semi-finishing tests are required for the final product. Thus, only cutting speed (V) and feed rate (f) are considered as the controllable variables of this study.

5- Chapter 5 introduces a more advanced novel method for estimating the remaining useful life of *worn* cutting inserts under different cutting conditions during turning of Ti-MMCs, using the current tool wear value (VB) of the worn tool as the input data. Tool wear at the transition point between the second and third states of tool wear is considered as the failure criterion. Tool wear data is added as another variable (monitoring variable) to the PH model (explained in chapter 4) in addition to cutting conditions. Thus, the valuable information regarding the remaining life of worn inserts under different cutting conditions are obtained.

6- Chapter 6 presents the results of a complementary research performed in collaboration with Dr. Ashraf at American University of Cairo. Optimization of cutting conditions is also considered as a very important piece of data which complements the machinability analysis. Furthermore, there is no data regarding the multi-objective optimization of cutting conditions during machining of Ti-MMCs. Multi objective optimization has been performed to find the cutting conditions that result in minimum tool wear and surface roughness, while preserving the highest productivity. For this study, cutting speed (V), feed rate (f) and depth of cut (a_p) were considered as variables; and surface roughness (R_a) and tool wear (VB) were selected as the response parameters.

7- General discussions including the originality of the work and contributions to the knowledge are provided in chapter 7.

8- In chapter 8, the general conclusions of the present work, list of publications as well as suggestions for the future works are presented.

In order to better visualize the different phases of this study and to illustrate the different variables and methodologies involved in each phase, the outline of this research is summarized in Figure 1.

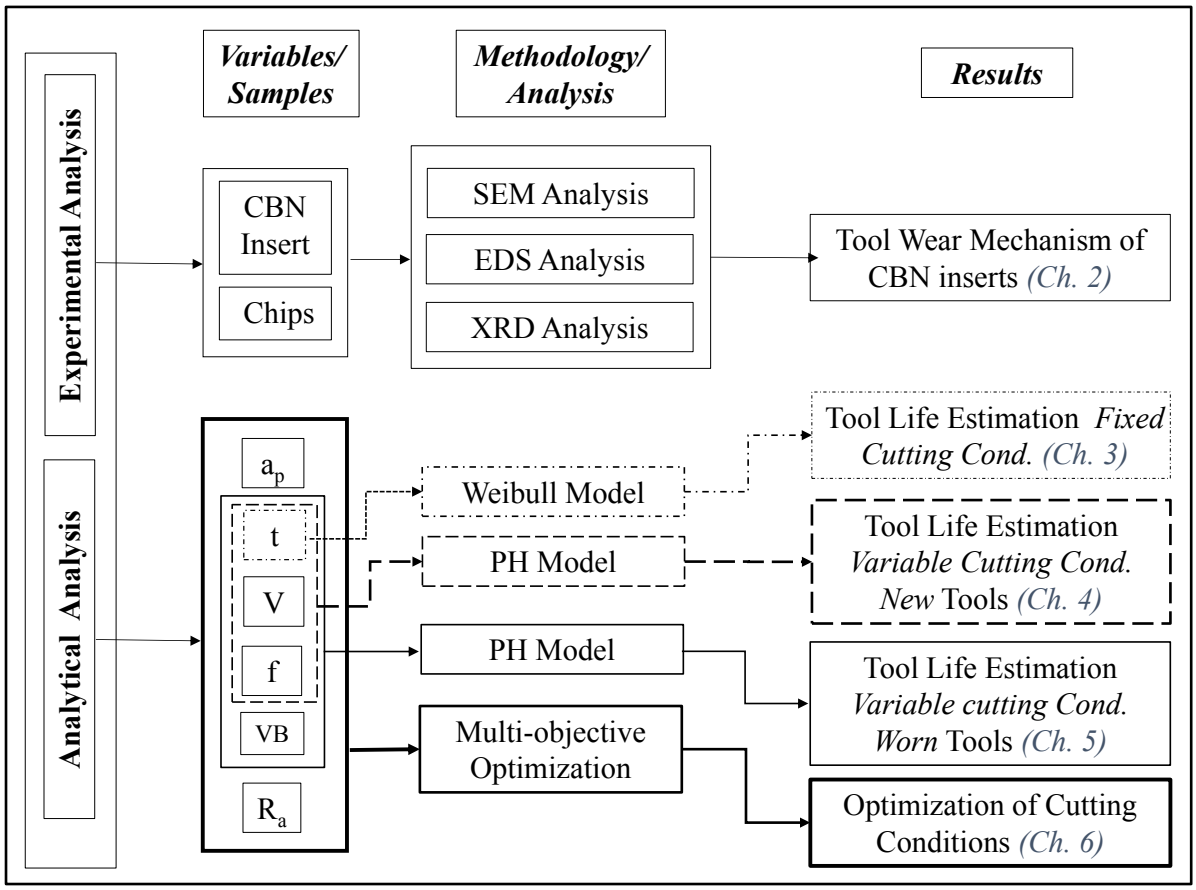

Figure 1: Research outline

Chapter 1 LITERATURE REVIEW

1.1 Introduction

It is reported that the first research on machinability of metal matrix composites goes back to 1985, on the investigation of wear mechanisms during machining of aluminum metal matrix composite, performed by Burn et al. (Brun et al., 1985). In 1990s deep investigation on the machining of MMCs started (Davim, Pramanik, et al., 2008; Songmene et al., 1999). However, most of the research efforts regarding the machinability of the MMCs are focused on aluminum MMCs and there is a significant lack of data regarding the machinability analysis of Ti-MMCs. In the upcoming section, the contributions on the most important parameters of machinability of MMCs in the open literature are discussed. Chip shape, surface integrity, tool wear and tool life estimation which are considered as the main concerns of any machinability analysis, are covered in the literature review.

1.2 Metal matrix composites (MMCs)

Metal matrix composites (MMCs) are composed of non-metallic reinforcements in metal matrices, and show higher properties in comparison to the monolithic materials. MMCs can be either reinforced with particles, continuous long fibers or discontinuous ones in the form of whiskers. The most commonly used materials for reinforcing the metal matrix composites are ceramic fibers which inherit superior stiffness, strength and temperature stability (Seshan et al., 1996). Yet, production process of particulate composites is simpler and more cost effective than that of fiber reinforced composites. In comparison to whiskers, particles can be merged together more efficiently and with a higher volume percentage. No health concern has been reported yet in applying micrometer particles. Furthermore, applying them yields in less breakage of reinforcements in comparison to whiskers (Srivatsan et al., 2006).

Particles can be in any size, shape or configuration. They can have random or preferred orientations. Mostly the particles are distributed randomly, thus particulate composites show isotropic characteristics.

In general, particles are employed as reinforcements in composites in order to improve material properties such as stiffness, resistance to abrasion at elevated temperatures, and decrease of shrinkage (Berthelot, 1999). Improvement in the mechanical properties of the material via reinforcing the matrix with particles can be attributed to dispersion strengthening and blocking of the dislocation movements (Seshan et al., 1996). Blocking the dislocation motion means lower plastic deformation and consequently higher strength. Sometimes they are employed in the material just as a filler and in order to minimize the cost while maintaining the characteristics. Generally, particles are chosen as reinforcements based on the desired properties which are expected. For example ductile materials are often reinforced with brittle metals such as tungsten and molybdenum in order to improve their temperature behavior while maintaining the ductility at room temperature (Berthelot, 1999).

Regarding the application of MMCs, their application in aeronautic and aerospace industries comes back to 1970s. At 1980 they were utilized in the automotive industry (Paulo Davim et al., 2000). Nowadays they are widely used in different industries due to their superior characteristics over monolithic materials. Examples of their applications in various industries are listed below (Heath, 2001):

- Automotive: engine-connecting rods, propeller shaft and brake disk.
- Aerospace: blade sleeves, fuel access and door covers
- Turbine-compressor engineering
- Leisure industry: tennis racquet and bicycle frames
- Thermal and electric transportation: cooking wave and heat sinks

1.2.1 Titanium Metal Matrix Composites (Ti-MMCs)

Ti-MMCs used in this study are produced by Dynamet Technology, Inc., and are made of Ti-6Al-4V alloy matrix reinforced with 10-12% volume fraction of TiC particles with irregular shapes and 10-20 μm size. They are usually made near net shape through a process known as CHIP (Cold and Hot Pressing).

The process includes: blending of raw material powders; CIP (Cold Isostatic Pressing), applying a high hydrostatic pressure at room temperature to compact the blended powders in a tool; vacuum sintering at high temperature in vacuum below the melting point to densify the material

and diffuse the powders to form the alloy or MMC; followed by HIP (Hot Isostatic Pressing) which is used to close the small residual porosities and improve the mechanical properties of the products via applying a combination of moderate temperature and hot argon gas pressure. Other traditional metal working processes such as extrusion could be also performed on the CHIP process materials to form the final product. A schematic of the process is shown in Figure 1-1.

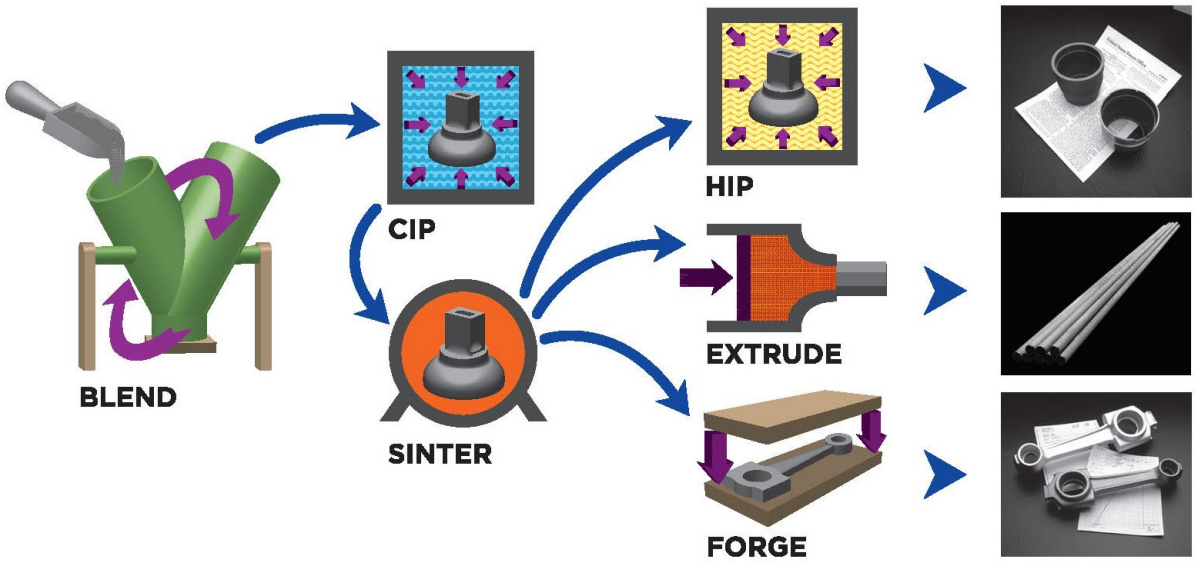

Figure 1-1: Schematic of CHIP process used for production of near-net shape components (Dynamet Technology, Inc.)

The mechanical properties of the Ti-MMC used in this study is provided in Table 1-1.

Table 1-1: Mechanical properties of Ti-MMC used in this study (Dynamet Technology, Inc.)

Yield Strength	Tensile Strength	Elastic Modulus	Shear Modulus	Thermal Conductivity	Specific Heat	Density
1014 MPa	1082 MPa	135 GPa	51.7 MPa	5.8 W/mK	610 J/kgK	4500 kg/m^3

Titanium Alloy reinforced with TiC particles take the advantage of both titanium and ceramics, thus possess superior characteristics such as high strength, high temperature resistance of titanium with an increase in stiffness provided by the ceramic reinforcement (Pramanik et al., 2008). Thus, they are considered as viable materials in various industries

such as aerospace and automotive. Some applications of titanium metal matrix composites are listed below and shown in Figure 1-2:

- Manufacturing structural components of the F-16 jet's landing gear
- Turbine engine components (fan blades, actuator pistons, synchronization rings, connecting links, shafts, discs)
- Automotive engine components
- Drive train parts
- General machine components

Figure 1-2: Some applications of metal matrix composites such as turbine engine blades, space shuttle struts, F-16 landing gear, automotive engine components, and diesel engine pistons

Though Ti-MMCs are produced near net shape, finish machining is required to obtain the acceptable surface quality of the parts. However, these materials suffer from poor machinability due to the hard and abrasive nature of the reinforcing particles, in addition to the low thermal conductivity, low elastic modulus and high chemical reactivity of titanium alloy matrix (S Kannan et al., 2006; Nikham, 2014). Severe tool wear and poor surface finish are considered as the most important drawbacks of machining MMCs.

1.3 Chip morphology

The study of chip morphology goes back to the beginning of the 20th century and the investigations of Mallock (Mallock, 1881) and Taylor (Taylor, 1906). Since then chip morphology analysis has been always of interest due to its importance and its influence on the other machining parameters. This study will provide us with the sufficient knowledge of cutting forces, tool wear and surface integrity; therefore, it can be beneficial in optimizing cutting conditions in order to get better surface finish and longer tool life.

Different properties of the workpiece material such as its yield strength, strain hardening, ductility and hardness are responsible for formation of different chip types. For example during machining materials with very high ductility, due to the severe plastic deformation of the chips, long and continuous chips are generated. Whereas in brittle materials such as gray cast iron, lack of ductility, hence insufficient plastic deformation results in the generation of discontinuous or segmented chips (Miracle et al.). Different cutting parameters also affect the formation of chips. Changes in the crack initiation and propagation as well as changes in the shear localization can lead to different chip formation under different cutting conditions. For example during cutting of titanium alloys different chip formation has been observed as continuous chips at low speeds around 50 m/min, segmented chips at speeds around 100 m/min, and shear localized chips at speed of 125 m/min and above (Daymi et al., 2009). Segmented (saw-toothed) chips are generated during turning of titanium metal matrix composites, which belong to the category of cyclic (serrated) chips (R Bejjani et al., 2011). Cyclic chips are defined as "continuous chips with a periodic variation in thickness" and can be classified into four types of wavy chips, segmented chips, catastrophic shear chips, and discontinuous chips (H. A. Kishawy, M. A. Elbestawi, 1997).

Segmented chips will affect the surface integrity, it may cause tool wear on the trailing edge of the tool and also it affects the accuracy of machining and the variability of the tool wear data, due to the force fluctuations which are induced (H. A. Kishawy, M. A. Elbestawi, 1997). Brittleness of the workpiece material, instability of the cutting process, periodic crack generation and catastrophic shear instability can be counted as the root cause of the generation of saw-toothed chips (Komanduri et al., 1981; Komanduri et al., 1984; Recht, 1964; M. C. Shaw et al., 1993). During machining MMCs due to the high induced strain rates, creation of adiabatic shear bands is also responsible for the generation of segmented chips.

Adiabatic shear bands are formed as a result of microscopic failure of materials especially for the materials that are exposed to high strain rates. At high strain rates, a change in the homogeneous plastic deformation pattern into inhomogeneous one, induces extensive local heating and as a result material softening. This phenomenon leads to the generation of the localized deformations (Dai et al., 2004). Particles have an important role in generation of adiabatic shear bands. Plastic deformation takes place only in the matrix and the reinforced particles only deform elastically. The smaller particle spacing as a result of the smaller particle size induces higher strain gradient. As mentioned before, strain gradients strongly affect shear banding generation and higher strain gradients lead to the generation of adiabatic shear bands (Rittel, 2009).

1.4 Surface roughness

Surface roughness is one of the most important components of surface integrity. The selection of optimum cutting parameters in order to achieve the required surface quality has been always a challenging matter among researchers. Different factors affect the surface roughness during machining. Cutting conditions, tool characteristics and the workpiece material are among the most important factors.

Tool-particle interactions during machining of MMCs significantly influence the surface roughness of the workpiece material due to the generation of voids and cavities as a result of particle fracture and/or debonding. This interaction is mainly affected by the variation of the feed. If during machining of MMCs the feed is set approximately equal to the particle size, severe surface deterioration will take place due to the particle fracture, particle debonding and particle pull out phenomena (Davim, 2008).

The influence of the feed rate on the surface roughness is reported to be greater than that of cutting speed and volume fraction of particles in machining MMCs (Bhushan et al., 2010). Besides, contradictory effects of feed on the surface roughness have been observed which should be considered. Decreasing the feed can result in better surface finish due to the generation of smaller feed marks. On the other hand severe plastic deformation and probability of material side flow are the consequences of decreasing feed which would lead to the inferior surface finish. This opposing manner has been also reported in increasing the feed during machining of MMCs

showing declining of the surface finish by increasing the feed in to a specific value and then increasing with further raising of the feed (Pramanik et al., 2008).

Cutting speed also has a significant effect on the surface roughness. Better surface finish has been reported during machining of MMCs with higher cutting speeds due to the facile removal of the hard reinforcement particles (Bhushan et al., 2010).

Tool wear during machining also affects the surface roughness. By an increase in tool wear and consequently by an increase in the tool-edge radius, a flat area will be formed along the clearance face. This will in one hand; increase the tool-workpiece contact area and on the other hand; generate high temperatures which both will result in deterioration of surface performance. This effect has been demonstrated in the Figure 1-3 (W. Grzesik, 2010).

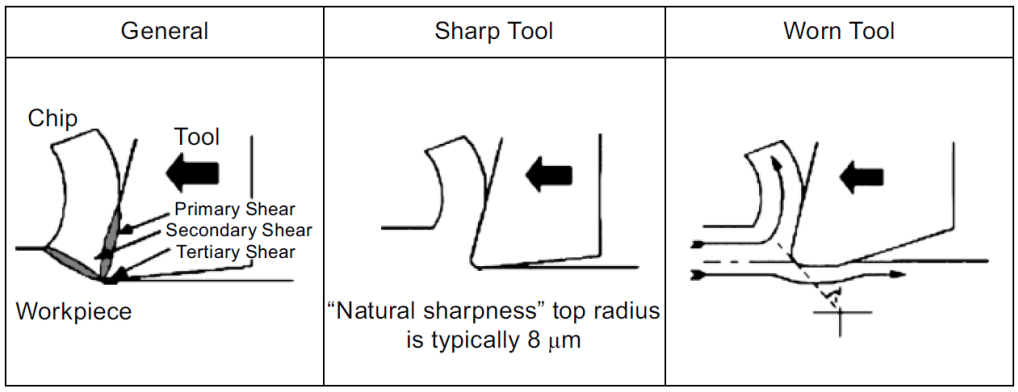

Figure 1-3: The effect of tool wear on the surface roughness (W. Grzesik, 2010)

Adhesion property of the tool is also an important factor which affects the surface roughness and should be considered (Bhushan et al., 2010).

Zhang et al. noticed an acceptable surface finish during machining of Al-MMC under a specific feed rate and depth of cut. They also revealed that a further increase in the feed rate and the depth of cut would result in the micro-cracks initiation in the interface of the SiC particles and the aluminum matrix and then gradual formation of macro-cracks on the machined surface. This will result in the deterioration of the surface finish. They also found the SiC grains to be responsible in preventing the dislocation movements and as a result, the macro deformation and dislocation pile-up at the matrix-particle interface (Zhang et al., 2009).

Improvement of mechanical properties of the workpiece material can contribute to better surface finish and surface quality due to declining the plastic deformation and chip bonding (Zhang et al., 2009). MMCs show lower strength in comparison to monolithic materials at all the machining conditions. It can be addressed to the generation of cracks as a result of the presence of particles in the shear plane and tool-chip interface (Pramanik et al., 2008). Strengthening behavior of the MMCs is dependent on the particle size showing higher flow stress with smaller reinforcing particles. This higher strengthening effect can be explained by the higher strain gradient with a smaller particle size (Dai et al., 2004). Strength of the workpiece material in the deformation zones can be affected by the cutting speed and feed via changes in the temperature, strain and strain rate. The reason can be explained by the reduction of work hardening of the MMCs with the temperature raise and its augmentation with the increase of strain rate (Davim, Pramanik, et al., 2008).

1.5 Cutting tools for machining MMCs

Tool life and tool wear tests are regarded as one of the most commonly used criteria for evaluating the machinability. The study will not only reveal the performance of the tool but also the evaluation of the workpiece material can be achieved through the analysis (W. H. Cubberly, 1989).

High hardness, good toughness and wear resistance are the characteristics that are expected from an ideal tool (Astakhov, 2013; Byrne et al., 2003). Hardness of the tool, which is greatly linked to its strength, is considered as a measure to its resistance to deformation. The ability to retain hard at high temperatures (called high hardness) is also considered as an important characteristic of a cutting tool (Astakhov, 2013). Polycrystalline diamond (PCD) and cubic boron nitride (CBN) inserts are the hardest tools in the market.

High fracture toughness of the tool will result in shock resistance, less chipping and fracture of the tool (Astakhov, 2013). As an example, the compromise between the hardness and toughness in cemented carbide tools has ranked them as one of the most useful and successful cutting tools in the various industries (Heath, 2001).

Generally, it is preferred to develop very hard tool materials with increased toughness. Thus, coatings and layered materials are used in order to make a tool with a very hard surface and a

tough core, in order to preserve the high wear resistance of the surface in addition to the high fracture toughness and damage resistance of the core (Dobrzański et al., 2010).

Wear resistance is defined as the ability of the tool in attaining its high integrity and acceptable tool life (Hosseini & Kishawy, 2014). Hung et al. (Hung et al., 1996) compared polycrystalline boron nitride (PCBN) and PCD inserts with WC tools in terms of wear resistance during machining of MMCs. They found that PCBN and PCD tools are superior than WC inserts in the order of magnitude of one and two.

Generally, a balanced combination of mentioned characteristics are expected from a desired tool (Hosseini & Kishawy, 2014). Considering all these factors, different tool materials for cutting of MMCs have been tested till now. PCD tools appear to be the best choice from researcher's point of view where abrasive wear is the dominant wear mechanism (Heath, 2001). Their abrasion resistance is approximately 500 times more than tungsten carbide (Davim & Astakhov, 2008).

During machining of MMCs, abrasive nature of reinforcements induces high abrasive wear on cutting tools, which shows increase with the augmentation of the reinforcement ratio (Bhushan et al., 2010; Songmene et al., 1999). Two-body and three-body abrasive wear are reported to be the main wear mechanisms during machining of MMCs (H. A. Kishawy et al., 2005; Li et al., 2001). Moreover, these particles are harder than most of the common tool materials. However, diamond is exceptionally hard and capable of resisting to the reinforcing particles (Davim, 2002).

PCD tools also inherit superior chemical, physical and mechanical properties such as high strength, resistance to corrosion, low tendency to adhere to the work material, low coefficient of friction and low thermal expansion (Bhushan et al., 2010; Byrne et al., 2003).

Bejjani et al (Bejjani, 2012) found that PCD tools are more suitable for machining of Ti-MMCs, compared to carbide tools in terms of tool life and surface roughness. They found that higher cutting speeds in the range of 170 m/min could be applied with PCD tools, comparing to carbide tools (around 90 m/min). However they found that there is a severe fire hazards above cutting speed of 180 m/min, which should be avoided.

Due to the high cost of PCD tools, researches have been conducted to find the proper cutting conditions which makes it possible to apply other economical tools with the same productivity (Bhushan et al., 2010). Other more cost effective alternatives are CBN, CVD diamond-coated, TiCN/TiN-coated carbide, triple-layer $TiC/Al_2O_3/TiCN$-coated carbide and uncoated carbide (Davim, Pramanik, et al., 2008).

CBN inserts show high characteristics such as high hardness and ability to retain a sharp cutting edge, hence preserving the desired surface integrity. They also exhibit high melting point and low friction coefficient and show good chemical stability and wear resistance (Angseryd et al., 2011; Barry et al., 2001; H. M. Lin et al., 2008). Thus, they are proven to be viable alternatives for machining hard-to-cut materials such as metal matrix composites (Aouici et al., 2012; Hung et al., 1998). In terms of hardness, thermal characteristics and fracture resistance, they show superior performance over ceramic and cemented carbide tools, during machining of MMCs (Ravi et al., 2014). It has been reported that CBN tools offer the highest machining performance during machining of Al/SiC MMCs (Ravi et al., 2014). However, there is very limited research performed with CBN inserts for Machining of MMCs, and there is not any study performed on the Ti-MMCs. These were among our motivation for performing a comprehensive study on the different tool wear mechanisms of CBN inserts during machining of Ti-MMCs. In the next section, a literature review on their wear mechanisms are provided.

1.5.1 Tool wear mechanisms of CBN inserts

Cubic boron nitride is the second hardest material after diamond. In general CBN content varies from ~ 50 vol% CBN in "low content CBN" to ~ 80-90 %vol CBN in "high content CBN", depending on the desired application (Klimczyk et al., 2011). Obtaining a high density CBN is tough due to the strong covalent bonding of B and N and their low self- diffusion coefficients (Klimczyk et al., 2011). Furthermore, CBN is thermodynamically metastable at normal pressures and transforms to hexagonal, graphite like phase with low hardness at high temperatures. Therefore sintering of PCBN under high temperature- high pressure should be performed (Hotta et al., 2008; Klimczyk et al., 2011).

Direct or binder assisted sintering processes are conducted to consolidate the PCBN insert. Superior characteristics of CBN can be achieved through binder assisted sintering processes while the process further allows consolidating the PCBN in comparatively lower temperature and pressure compared to the direct sintering method (Monteiro et al., 2013). Different elements such as metallic elements like Al, Co and Ni as well as ceramic binders such as TiC, TiN and Al_2O_3 have been recommended for improving the sintering process (Chiou et al., 2013). However, the low melting point of metallic elements limits their usage for high-temperature applications. In addition, the high toughness of ceramic binders will compensate the lower fracture toughness of

CBN. Hence the high hardness of CBN in addition to the high toughness of ceramic binders will contribute to excellent mechanical properties of the CBN inserts (Hotta et al., 2008).

Combination of different tool wear mechanisms have been reported to be involved during machining with CBN inserts (Lahiff et al., 2007).

Chain of physical, chemical and thermo-mechanical phenomena are responsible for the formation of cutting tool wear. High thermal and mechanical loads produced during machining, through generation of considerable amount of cutting heat, pressure and strain, account for the generation of different tool wear mechanisms (Astakhov, 2013). Hard and abrasive reinforcing particles in the metal matrix composites are further detrimental to the cutting tools and will induce higher tool wear.

Flank wear is reported as the dominant wear mechanism during machining of SiC/Al MMCs with CBN, which is highly affected by the particle size. Severe nose and cutting edge fracture was observed during machining with high particle size (110 μm). When machining with small particle size around 30-40 μm, abrasion and adhesion were found to be dominant. Furthermore, an increase in the amount of flank wear was observed with the increase of cutting speed, which was addressed to the built-up edge (BUE) generation and higher adhesion of the workpiece material at higher cutting speeds (Ciftci et al., 2004).

Ding et al. (X. Ding et al., 2005) also found flank wear as the dominant wear mechanism during machining of Al-SiC MMCs with CBN, which occurred jointly with the surface cracking. Intergranular fracture was also observed on the rake face. A significant increase in the adhesion of the workpiece material at high cutting speeds was observed during dry machining. Nonetheless, the application of coolant at low cutting speed reduced the adhesion of the material, but on the other hand, increased the abrasion between the tool flank face and the machined surface. They also found the lowest amount of tool flank wear using binderless PCBN inserts.

Yanming et al reported edge and corner breakage of CBN inserts during cutting of Al-SiC MMC with CBN. They found more severe corner breakage and less tool life when machining workpieces with higher volume fraction or coarser sizes of SiC particles (Yanming et al., 2000).

Regarding the machining parameters, higher values compared to WC inserts are reported during machining of Al-MMCs with CBN (D. K. Das et al., 2014). Considering the tool geometry, Dabade et al. found lower cutting forces and less surface damage with wiper geometry on the

CBN inserts, which was addressed to higher contact length and as a result higher thermal softening (Dabade et al., 2007).

Other wear mechanisms such as chemical wear (Angseryd et al., 2011; Barry et al., 2001) melt wear (Farhat, 2003) and fracture of the tool binder material (Ezugwu et al., 2005) were also reported during machining with CBN tool but with different materials rather than MMCs:

During machining of steel, abrasion wear was reported as the dominant mechanism at low cutting speeds. Yet, a switch from mechanical wear to chemically driven wear mechanisms, such as diffusion and oxidation wear at high cutting speeds were reported (Kramer et al., 1986).

Angseryd et al. (Angseryd et al., 2011) reported an increase in the chemical wear with the increase in the cutting speed, during machining of hardened steel. They found that at low cutting speeds only the surface of the tool was affected, whereas at higher speeds, an area beneath the wear surface was also involved.

During machining of P20 tool steel, diffusion and melt wear were reported as the dominant and secondary wear mechanisms respectively. Melt wear was described as the formation of low melting point Cr and Mn compounds with the insert material and the consequent removal from the cutting zone (Farhat, 2003).

Ezugwu et al. (Ezugwu et al., 2005) found lower performance of different grades of CBN inserts in terms of tool life, in comparision to uncoated carbide tools during machining of Ti-6Al-4V. This was adressed to the excessive chipping and rapid notching of the CBN cutting edge. They also found that high diffusive wear resulted in the reduction of the bond strength of the insert substrate. More reduction in the tool life was observed with an increase in the CBN content.

Luo et al (Luo et al., 1999) found the abrasion of the insert binder material by the workpiece carbide particles as the main wear mechanism during machining of AISI 4340 steel. Furthermore, a protective layer was found on the chip-tool interface, which was a solution of the workpiece material and tool material binder.

Barry et al (Barry et al., 2001) found the chemical tool wear to be the dominant wear mechanism of CBN inserts during machining of BS 817M40 steel. Fragments of oxidized workpiece material were found on the crater surface. Lin et al (H. Lin et al., 2008) reported abrasion wear as the dominant wear mechanism at low cutting speeds during machining of hardened steel. Formation

of a protective oxide layer on the tool face was reported at higher cutting speeds. Transformation of continuous chip to saw-toothed chip under high cutting speeds was also mentions as another phenomenon affecting the wear mechanism of CBN inserts.

1.6 Tool life estimation

Tool life estimation is regarded as one of the most important elements of any machinability analysis. One important reason is the huge costs which are incurred as a result sub-optimal utilization of cutting inserts. It has been reported that only 38% of the time the tools are used up to their full capacity which imposes extra costs as high as $10 billion per year for US industry alone (Umbrello et al., 2004b). The cost could be related to in-service failures such as poor surface quality, scraped parts or machine tool damage, as the result of overestimation of tool life; in addition to the reduction in the overall productivity of the operation and excess machine downtime, due to the underestimation of the tool life. This is even more critical when machining of difficult-to-machine materials such as MMCs (Salonitis et al., 2014).

The first model for tool life estimation is proposed by Taylor (Taylor, 1906) more than hundred years ago, and is still used widely in various machining studies even at the level of national and international standards (Astakhov, 2014). However, the validity of the model for any cutting material rather than carbon steels and high speed steels and for cutting speeds higher than 25 m/min is still questionable (Davim & Astakhov, 2008; Mamalis et al., 2002).

At 1993, Ravinda et al. (Ravindra et al., 1993) described the correlation between the cutting forces and the progressive tool wear and tool failure and introduced it as an indicator of the wear process. Owing to this recognition, several analytical models for tool life estimation and tool wear monitoring were developed later, applying different methodologies (Bhattacharyya et al., 2007; Braun et al., 1999; S. Das et al., 1996; Dimla Snr, 2000; Huang et al., 2007; Lee et al., 1998; Sikdar et al., 2002).

Numerous studies have also been performed by correlating tool wear to different signals such as tool temperature (Mathew, 1989; Wanigarathne et al., 2005), vibration (Dimla Sr et al., 2000; Orhan et al., 2007), surface roughness (de Agustina et al., 2014), power signals (Oh et al., 2004) and optical measurements of tool wear (Gadelmawla et al., 2014) extracted from different sensors such as dynamometers, acoustic emission and accelerometers (de Agustina et al., 2014; Dimla

Snr, 2000). Several tool wear monitoring were also developed using finite element analysis (Xie et al., 2005; Yen et al., 2004).

Although success was claimed in these studies, the random nature of the tool wear was neglected in these model, which may adversely affect their precision (Martin, 1994). Considerable variability of the tool wear data could exist due to various factors such as differences in the physical and mechanical properties of different batches of workpiece and tool materials. During machining of composite materials, significant variation could exist even within a single batch of material as a result of nonhomogeneous distribution of the reinforcing phases. Thus, for this class of material development of models based on the theory of probability is highly recommended.

In 1977, DeVor et al. (DeVor et al., 1977), studied the probabilistic nature of the cutting tool life. Afterwards, several models were proposed for the reliability analysis of cutting inserts, implementing different probability distributions of tool failure data such as normal, lognormal and Weibull (DeVor et al., 1977; Hitomi et al., 1978; Mazzuchi et al., 1989; Negishi, 1976; J. G. Wager et al., 1971; K.-S. Wang et al., 2001).

Generally, in a reliability analysis two states are considered for a system which is intended to perform a function: good, if it performs the function; and defective if it is not capable of performing the function. These states are interpreted statistically. Time to failure (TTF), which is the interval between the time at which the system started its function till the moment it failed, is considered as a random variable ($x \geq 0$), which could have different distributions. If the time to failure possess the distribution of $F(t) = P\{x \leq t\}$, then the system reliability is:

$$R(t) = 1 - F(t) = P\{x > t\} \qquad (2\text{-}1)$$

Thus, F(t) is the probability that the system fails before time t; and R(t) is the probability of not having the failure at least till time t (Papoulis, 1990).

During a machining process, a cutting tool could also have two possible states: an operating state and a failure state. In the operating state machining tool is properly capable of fulfilling the intended machining function. While the failure state, which is considered as an opposing event to the operating state, occurs when the cutting tool is unable to cut properly or when the detriments to the surface outweighs the tool replacement cost. This failure state is usually defined, in terms of permissible maximum tool wear defined on the tool wear curve. The tool wear curve

demonstrates three states called as initial, steady and rapid states. Severe vibration, cutting forces and temperature occur at the third (rapid) state. Thus, tool should be replaced before entering this state in order to avoid detriments to the tool and workpiece. The tool wear at the transition point between the first and second states is often considered as the tool wear criterion (Astakhov, 2006).

Considering the time to failure of cutting inserts as a random variable (DeVor et al., 1977), reliability of cutting inserts could be formulated and used for the investigating the performance of the tools.

Klim et. al. (Klim et al., 1996) developed a reliability model in order to investigate the effect of feed rate variation on the tool life. Furthermore, he developed a tool replacement strategy based on the reliability characteristics of the tool life data (Aramesh et al., 2013). Lin (Lin, 2008) studied the reliability curve variation under different cutting speeds. Rodriguez et al. (Patiño Rodriguez et al., 2010) developped a policy for tool replacement in turning and milling operations based on the reliability analysis. Wang et al. (K. S. Wang et al., 2001) developped a reliability dependent failure rate model for estimating the cutting tool reliability. Rodrigez et al (Patiño Rodriguez et al., 2010) developed the reliability function for the turning and milling operations, and used it to define the changing time of the cutting tools.

Mazzuci et al. (Mazzuchi et al., 1989) introduced proportional hazards model (PHM) in machining for reliability assessments of cutting tools. PHM is an effective model for survival analysis which mostly used in medical science. In tool reliability analysis, this model accounts for aging and cumulative tool wear in addition to the effect of the cutting conditions, which are reflected in the covariates of the model.

Tool wear is highly dependent on the cutting conditions, especially cutting speed and feed rate (Jemielniak et al., 1985). Furthermore, tool wear has an aging behavior, meaning that the probability of failure increases over time during the machining operation. Implementing these effects in the model, PHM stands out above the models introduced even later for tool reliability analysis.

Feng et al. (Feng et al., 2011) developed a PH model for tool reliability assessment, using tool vibration signal feature extraction. Liu et al. (Liu et al., 1996) used a PH model and developed a general formula for tool reliability calculation, assuming a constant parameter values of hazard

function during a cutting process. Tail et al. developed a PH model for predicting the time to replacement of cutting tools based on the fixed reliability and hazard threshold (Tail et al., 2010).

Another advantage of PH models is that different variables including controllable variables monitoring variables could be added to the model.

Controllable covariates are those that can be controlled during a process such as cutting speed, feed rate and depth of cut in machining. Monitoring or uncontrollable covariates mostly change in response to the controllable ones and are monitored during a process. They have influence on the process but cannot be adjusted during a process, such as surface roughness and tool wear in machining process. This was in fact a motivation for us to add tool wear as a monitoring variable to the model in order to estimate the remaining life of worn inserts under different cutting conditions. It should be mentioned that very limited work has been done to calculate the remaining life of worn inserts (Ao et al., 2010; Baruah et al., 2005; Gokulachandran et al., 2012; Karandikar et al., 2013; Wang et al., 2012). However, to the best of our knowledge, so far no model has been introduced implementing the tool wear itself as a variable in the model in addition to the cutting conditions, thereby being able to predict the remaining life of *worn* inserts based on the current tool wear value.

1.7 Conclusions of the literature review

The results of the investigations performed on the open literature suggests that there is a significant lack of knowledge in the machinability of Ti-MMCs, and there exist a huge potential in different areas especially in surface integrity and tooling.

- Chemical wear mechanisms especially the oxidation mechanism during machining of Ti-MMCs were not studied before. Some work has been done on different mechanisms of Ti-MMCs during machining with PCD tools. But the chemical wear mechanisms were not studied before and the oxidation mechanism which is responsible for severe flaming and fire hazards during machining of Ti-MMCs were not identified before.
- Tool wear mechanisms of CBN inserts, which could be considered the second alternative tool for machining this material, is not studied before.
- The statistical model for tool life estimation during machining of MMCs appears to be an effective predictive model, where considerable variability of tool wear data could exist.

However, very limited work has been done in this area. Furthermore, no model has been proposed capable of predicting different states of tool wear. In particular, estimating the second transition point accurately could reduce the costs associated with non-optimal tool replacement.

- No model has been proposed so far for estimating the remaining life of worn inserts. A few models exist for calculating the remaining life of inserts. But none of them use the tool wear value as the input of the model and are capable of estimating the remaining life of worn tool with different tool wear values.

Chapter 2 ARTICLE 1: TOOL WEAR MECHANISMS OF CBN INSERTS DURING TURNING OF TITANIUM METAL MATRIX COMPOSITES (TI-MMCS)

M. Aramesh, H. Attia, H. A. Kishawy, M. Balazinski, Submitted *to International Journal of Machine Tools and Manufacture*, 2015.

ABSTRACT

Tool wear mechanisms of CBN inserts during turning of titanium metal matrix composites (Ti-MMCs) including adhesion, abrasion, chemical interactions and their effects on the wear surface morphology were investigated. It was revealed that the workpiece material was the primary source of materials adhered to the tool surface. However, chemical reactions in addition to different adhesion and bonding mechanisms resulted in generation of distinct zones on the tool wear surfaces. Non-oxide elements with high metallic interlocking were found to be adhered to the tool wear surfaces inside the contact region, while the oxide contaminated, embrittled elements were just located outside the contact region. Embrittlement of the titanium alloy in the oxide contaminated areas resulted in generation of a discontinuity between the adhered materials. This discontinuity which was located at the border between the oxide and non-oxide components, appeared as a black zone on the worn surfaces. The entire material was surrounded by carbon and boron particles. The clustered material behind these particles appeared as a white zone on the worn surfaces. The mechanisms leading to this morphology were discussed for the first time, which has led to new insights in the identification of CBN tool wear mechanisms during machining of Ti-MMCs.

Key words:

CBN inserts; tool wear; Ti-MMCs; mapping

2.1 Introduction

Different tool materials such as polycrystalline diamond (PCD), cubic boron nitride (CBN), polycrystalline boron nitride (PCBN), chemical vapor deposition (CVD) diamond-coated, TiCN/TiN-coated carbide, triple-layer TiC/Al_2O_3/TiCN-coated carbide and uncoated carbide, have been tested for machining metal matrix composites (Davim, Pramanik, et al., 2008). By far, PCD tools appear to be the best choice for machining MMCs from researchers' point of view (Bhushan et al., 2010; Byrne et al., 2003; Davim & Astakhov, 2008; Heath, 2001). However, due to their high cost and high speed limitations (Monteiro et al., 2013), effort has been directed towards exploring other economical alternatives with similar productivity.

CBN inserts inherit superior characteristics, such as high hardness and ability to retain a sharp cutting edge, hence preserving the desired surface integrity. They also exhibit high melting point and low friction coefficient and show good chemical stability and wear resistance (Angseryd et al., 2011; Barry et al., 2001; H. M. Lin et al., 2008). Thus, they are proven to be viable tools for machining hard-to-cut materials such as metal matrix composites, high speed steels, titanium alloys, nickel-based alloys, die steels and white cast (Aouici et al., 2012; Hung et al., 1998).

In general CBN content varies from ~ 50 vol% CBN in "low content CBN" to ~ 80-90 vol% CBN in "high content CBN", depending on the desired application (Klimczyk et al., 2011). Direct or binder assisted sintering processes are used to consolidate the CBN inserts. Superior characteristics of CBN can be achieved through binder assisted sintering processes which also allow consolidating the PCBN in comparatively lower temperature and pressure comparing to the direct sintering methods (Monteiro et al., 2013). Different metallic elements like Al, Mg, Co and Ni as well as ceramic binders such as TiC, TiN and Al_2O_3 have been recommended for improving the sintering process (Bindal et al., 1991; Chiou et al., 2013).

Combination of different tool wear mechanisms have been reported during machining with CBN inserts. A chain of physical, chemical and thermo-mechanical phenomena is responsible for the occurrence of tool wear (Astakhov, 2013). Abrasion wear is reported as the dominant wear mechanism when machining at low cutting speeds, especially during cutting particle reinforced composites. Chemically-driven wear mechanisms, such as diffusion and oxidation wear are reported during machining at higher cutting speeds (Angseryd et al., 2011; Barry et al., 2001; H. M. Lin et al., 2008; Luo et al., 1999; Poulachon et al., 2001). Furthermore, at higher cutting

speeds chemical wear was detected in wider areas, attacking also beneath the worn surface (Angseryd et al., 2011). During machining P20 steel, Farhat (Farhat, 2003) identified diffusion wear as the main wear mechanism during machining at all speeds. He introduced the melt wear as the secondary wear mechanism at 1000 m/min cutting speed. Melt wear was described as the formation of low melting point Cr and Mn compounds with the insert material. Nose wear, excessive notching and chipping of the CBN cutting edge, in addition to the high diffusive wear, were also reported as predominant wear mechanisms, which is responsible for the reduction of the bond strength of the insert substrate (Ezugwu et al., 2005). In addition, reduction in the tool life with the increase of CBN content is observed (Ezugwu et al., 2005). Lin et al. (H. M. Lin et al., 2008) suggested the formation of a protective oxide layer, consisted of the workpiece material and its oxide compounds on the tool face during turning of high hardness alloy steels. This layer was suggested to work as a diffusion barrier and result in reduction of tool wear at moderate cutting speeds (H. M. Lin et al., 2008). Other wear mechanisms such as transformation from cubic structure (CBN) to softer hexagonal structure (HBN) and the consequent abrasion of the HBN were also reported as one of the mechanisms affecting the CBN tool life (Farhat, 2003).

Since there is a limited data about the tool wear mechanisms during machining Ti based MMCs, the aim of this study is to investigate the unique surface morphology of the worn surfaces during machining of Ti-MMCs via assessing the abundance and the distribution of different elements on the wear surfaces for determining the corresponding responsible tool wear mechanisms.

2.2 Experimental set up

In this study a cylindrical tube of 63.5 mm outer diameter made of Ti-6Al-4V alloy matrix reinforced with 10-12% volume fraction of TiC particles with irregular shapes and 10-20 μm size, is utilized. The machining tests were conducted on a Boehringer NG 200, CNC turning center. The CBN insert used in this study is a low content Seco tool (CBN 170), with TiC particles as well as SiC whiskers and Al_2O_3 ceramic binders. Presence of these binders enhances the toughness, and the wear and fracture resistance of the insert. However, high amount of Al_2O_3 binder in this insert results in a low thermal conductivity; around 40-50 W/mK. The insert is characterized by its very high hardness around 30 GPa.

Microstructural and elemental analyses were performed using JSM 7600 TFE Scanning Electron Microscopy (SEM) equipped with an Oxford Energy-Dispersive X-ray Spectroscopy (EDX). Primary backscattered electron (BSE) imaging was performed with SEM for investigating the microstructure. Material characterization were performed with both JSM 840 A and JSM 7600 TFE devices. EDS line scans and chemical mapping were performed with JSM 840 A EDS. A 20 kV accelerating voltage was used to record the peaks. The spatial resolution of the EDS is 1-5 μm^3 for low atomic numbers (Z) and 0.2 – 1 μm^3 for high Z, and the energy resolution is 132 eV. The EDS is efficiently capable of detecting elements heavier than Beryllium. JSM 7600 TFE device with EDS detector of Oxford X-max and an Oxford wave WDS with 5 crystals were also used to identify the weight percent of desired elements on the tool and the workpiece. The phase analyses were performed using Philips X'pert X-ray Diffraction (XRD), using theta/2theta motion.

Semi finishing tests were performed under relatively high cutting speeds in the range of 200-350 m/min, feed rate of 0.1 mm/rev and depth of cut of 0.15 mm. The rake angle was 8°. In order to investigate the effect of coolant on the CBN tool wear mechanisms, experiments are conducted under both through-coolant and dry conditions. TRIM™ VHP™ E210, a chemical emulsion concentrate, is used in this study as the coolant.

2.3 Methodology

A SEM investigation is performed on the entire worn surfaces of CBN tools to study their general morphology and microstructure. The focus of this study is to get more localized elemental information about the location, distribution and abundance of different elements present in the worn surfaces. To achieve this goal, chemical composition of the worn surface is investigated via EDS analysis, profiting from more localized techniques such as line scans and elemental mapping.

Three different zones are identified on the tool rake and flank surfaces, shown in Figure 2-1. These zones include a layer adhered to the insert face, a black zone grown around the margin of the adhered layer and a white zone surrounding the entire worn area. The composition of these different zones is explored and the tool wear mechanisms responsible for their generation are

studied.

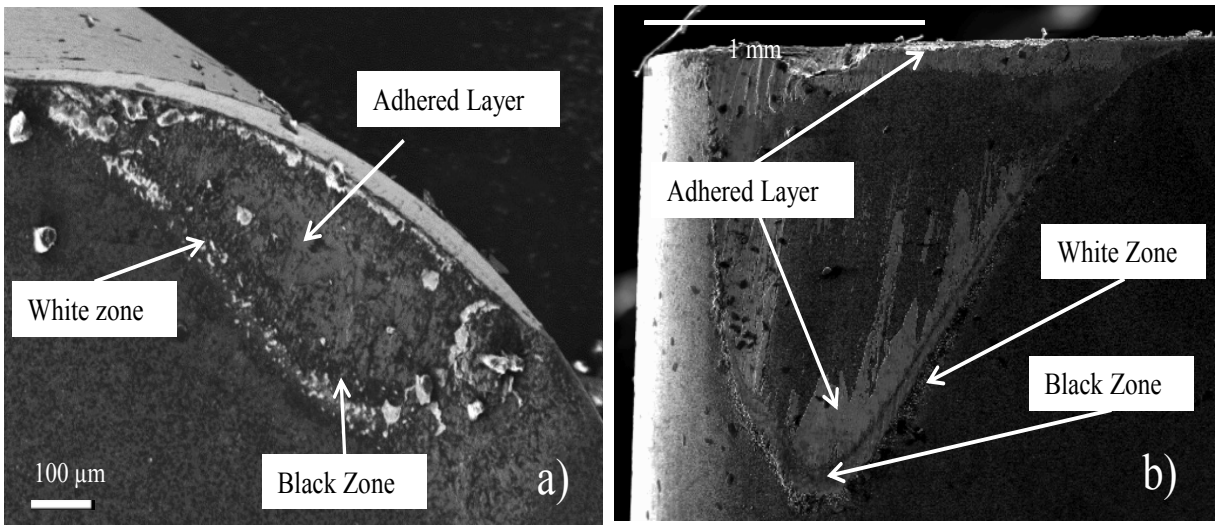

Figure 2-1: SEM image of the worn surface of a) CBN rake face b) CBN flank face under through-coolant turning with v=250 m/min, f=0.1 mm/rev and a_p= 0.15mm, machining time 55 second

Chemical reaction between the tool and the work-piece material is traced through phase identification via X-ray diffraction analysis (XRD) on the generated chips.

2.4 Results and discussion

2.4.1 Wet machining

2.4.1.1 Flank face

As a first step to define the different tool wear mechanisms of CBN, EDS analyses were performed on the entire tool flank wear surface to identify the key elements and their locations and distributions on the entire worn surfaces via elemental mapping.

Figure 2-2 shows the results obtained from the initial EDS analysis of the entire CBN tool flank wear area after a thorough-coolant turning with cutting speed of $250\ \mathrm{m/min}$, feed rate of $0.1\ \mathrm{mm/rev}$ and depth of cut of $0.15\ \mathrm{mm}$. Results revealed the presence of elements such as tungsten (W), calcium (Ca), silicon (Si), nitrogen (N), iron (Fe) and boron (B), which are typically constitutes of the tool material, as well as titanium (Ti), carbon (C), vanadium (V) and aluminum (Al), which mostly exist in the work-piece material. Al, Ti and C can also come from

the tool as they are the constituents of the tool material binders. Magnesium (Mg), which is also detected on the tool surface, may exist in small amounts in the insert. Depending on the type of the insert, Mg could be used as the catalyst for hexagonal boron nitride (HBN) to CBN transformation or added to the CBN insert as a sintering additive in the form of magnesium nitride or oxide (Bindal et al., 1991). Besides, magnesium is present in the titanium powder used in the production process of Ti-MMC. During a process known as Kroll process, reduction of titanium tetrachloride takes place by addition of magnesium metal to produce titanium metal (Abkowitz et al., 2011).

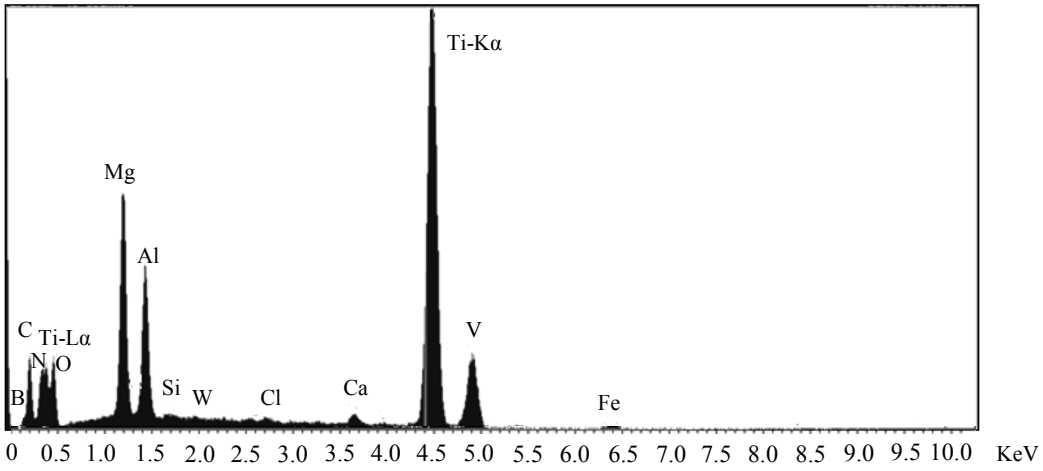

Figure 2-2: EDS result of the entire wear zone

In the coming section, elemental mapping of the defined key elements is performed to acquire their *distribution* on the worn surface. The SEM image of the flank wear surface is shown in Figure 2-3-a, for the test conducted at the conditions given in Figure 2-1. The corresponding maps of the key elements are presented in Figure 2-3-b to 2-3-h. Since the elements of W, Ca, Si and Fe which come from the base material of the tool are not significant, they are not considered as the key elements for the elemental map. It should be mentioned here that the distribution of different elements in the elemental mapping images could be distinguished from the brightness and color contrast of the images; higher element concentrations are displayed with brighter contrasts in the images.

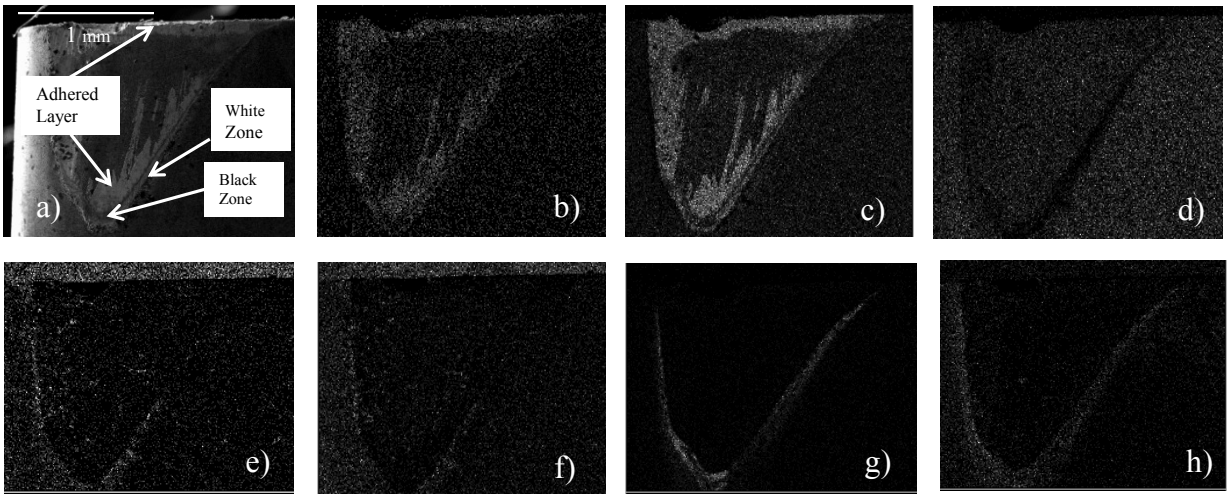

Figure 2-3: a) SEM of entire flank worn area, Elemental maps of b) Titanium (Ti-Kα), c) Vanadium, d) Aluminum, e) Carbon, f) Boron, g) Magnesium and h) Oxygen (for the conditions given in Figure 2-1)

A comparison between the SEM image of the worn surface (Figure 2-3-a) and the elemental maps shows that the *adhered layer* on the flank face (defined in Figure 2-1-b) consists mostly of titanium, vanadium and carbon (Figure 2-3-b, 2-3-c and 2-3-e), which mostly come from the workpiece material deposited on the tool surface. Comparison between Figure 2-3-a and 2-3-d suggest that except for a tiny zone around the adhered layer, Al is ubiquitous, which could be attributed to the high amount of aluminum in the workpiece material as well as in tool binder material, in the form of Al_2O_3. Considering the elemental maps of carbon and boron shown in Figure 2-3-e and 2-3-f, it can be seen that their concentration is considerably high around the adhered layer. Taking into account the oxygen map shown in Figure 2-3-h, an oxide layer is also formed around the adhered zone, adjacent to the Mg-rich region (Figure 2-3-g), where Mg is apparently agglomerated as a thin layer in the area between the black and white zones identified in Figure 2-1-b. The results suggest that in the vicinity of *black* and *white* zones, the magnesium, oxygen, carbon and boron contents are high. Detailed and magnified analyses of these zones will be presented in the upcoming sections.

In order to better investigate the morphology and composition of different elements around the adhered layer, closer views of the Figure 2-3-a are provided in Figure *2-4*. Assuming the black zone is the ultimate end of tool/workpiece contact region, the general morphology of the adhered layer is consistent with the literature (Grzesik, 2008). The *adhered layer* consists of a sticking

area near the cutting edge (region I in Figure *2-4*-a) and a sliding area which is located beyond the sticking area till the ultimate contact point between the workpiece and the tool (region II shown in Figure *2-4*-a and 2-4-b). However, the present results show that some material is also pushed outside the contact region (Region III in Figure *2-4*-a and 2-4-b).

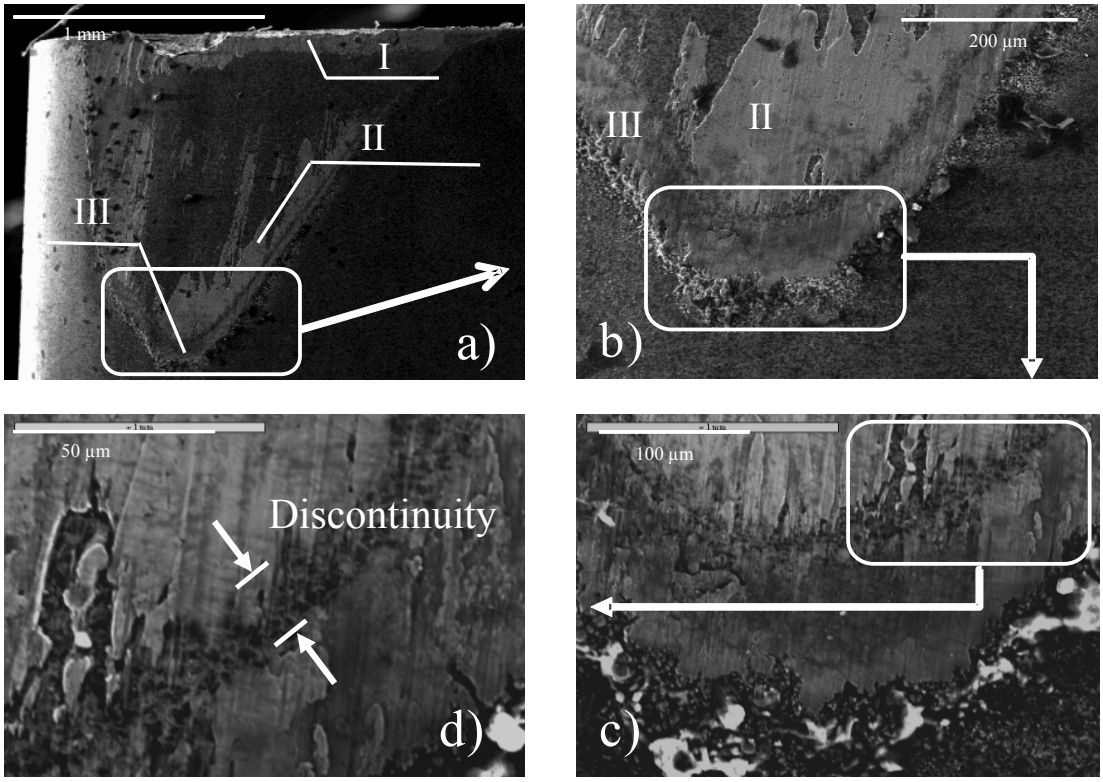

Figure 2-4: SEM images of increasing magnification (clockwise from a) of the CBN flank face showing the formation of a discontinuity between the adhered materials on the black zone (for the conditions given in Figure 2-1)

The magnified images of the outer region of the tool worn area show that the *black zone* is in fact a discontinuity within the adhered materials to the tool surface. Similar morphology was observed on the tool flank surface during machining with different cutting conditions (mentioned in section 2) and during wet and dry machining tests and after few seconds of machining till the end of tool life. This phenomenon was not studied before. Thus, line scan technique is further applied in order to investigate this fact and find the root causes.

Figure 2-5 shows an EDS line scan of Ti, V, Al, Mg and O performed across a line passing through the black zone (spot 1) and the white zone (spot 2).

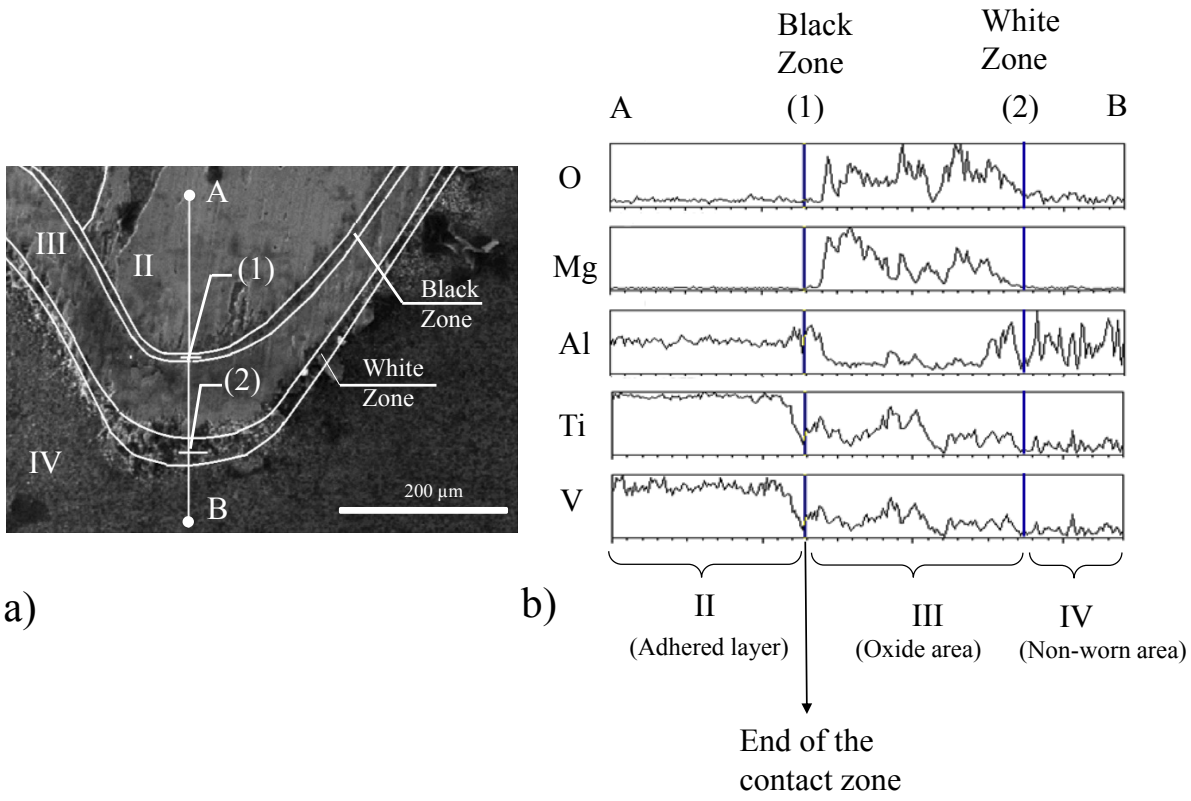

Figure 2-5: a) SEM image of the tool flank face b) EDS line scan of the tool flank face

Figure 2-5-b shows that the peak intensities of Ti and V vanish promptly at the black zone, confirming that there is a discontinuity in the adhered materials at this zone. It should be noted that since Al exists also in the tool material in a high amount, its peak intensity did not show a decrease at this zone. The results also clearly show that the peak intensities of Mg and O increase significantly in the area between spot (1) and spot (2) (referred to as oxide area in Figure 2-5-b), suggesting that the oxidation of Mg is the dominant oxidation mechanism during machining of Ti-MMCs. The overall lower peak intensities of Ti, Al and V in the oxide area could be also attributed to the masking effect of higher Mg and O in this area. Figure 2-5-b also suggests that the black zone could be considered as the boundary between the non-oxide and oxide components. At the end of this section, we will show that the results of different experiments revealed that the source of magnesium is the workpiece material; which is a left over from the titanium production process. Magnesium has a very high affinity to oxygen and formation of MgO. The elevated temperature generated during machining constantly results in the oxidation of magnesium outside the tool/chip contact region, where exposed to oxygen. In contrast with the

non-oxide products, which are adhered to the worn area via the high interlocking mechanism, MgO generated through the in-situ oxidation process will be frequently removed from the tool during the machining process. Thus, at the end of the machining process, MgO remains only at the periphery of the contact region. Magnesium oxide and magnesium hydroxide, $Mg(OH)_2$, which can also be generated during this process, could result in embrittlement of the titanium alloy. Generally, oxygen and hydrogen contamination in titanium-based alloys is known to result in their embrittlement, thereby reducing their mechanical properties and formation of porosities and inclusions within their structures, especially where they are exposed to any stress (Clark et al., 1983; Godfrey et al., 2000). It is worth mentioning here that several defects such as debonding and brittle fracture of the welded joints have been reported during friction stir welding of Ti-6Al-4V as a result of MgO contaminations (Mashinini, 2010). Titanium is also very resistance to alkaline media elements such as magnesium hydroxide, which could be attributed to excessive hydrogen uptake and resultant embrittlement at high temperatures. Thus the co-existence of Ti, V, and Al along with Mg and O, in the oxide area, suggests that embrittlement of workpiece titanium alloy may occur in this area. The black zone, which is the ultimate end of the contact zone, is the only zone which is simultaneously subjected to abrasion and oxidation mechanisms (Figure 2-6). Thus, as a result of tool abrasion, the contaminated adhered material is easily fractured and removed from the tool surface and leave behind a gap (also referred to as the discontinuity) on the tool face in this zone.

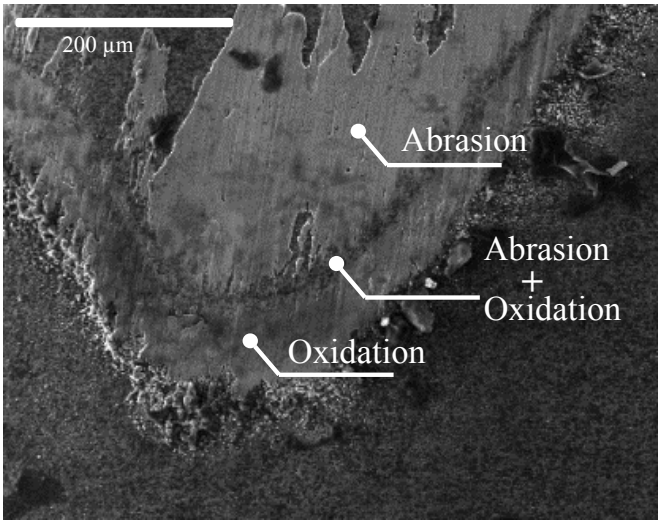

Figure 2-6: SEM image of the flank face showing the different affected areas: abrasion in the contact area, oxidation outside the contact area, and abrasion plus oxidation in between

Finally, it could be concluded from Figure 2-5 that the *white zone* acts as a boundary for the entire adhered materials on the tool. It is clearly seen in the Figure 2-5-b that the peak intensities of titanium and vanadium vanish after passing spot (2). As mentioned before, the existence of Al after the spot (2) could be attributed to the high amount of Al_2O_3 in the tool material.

As was shown by the elemental maps presented in Figure 2-3, the agglomeration of boron and carbon elements around the worn area was also observed on the flank face. In order clearly to address their relative distribution with respect to the other elements present in the outer regions of the worn areas, the corresponding maps of these elements are superimposed on the SEM image of the worn area. The superimposed maps of Mg, O, B and C are presented in dark blue, red, green and blue colors in Figure 2-7-a to 2-7-d, respectively.

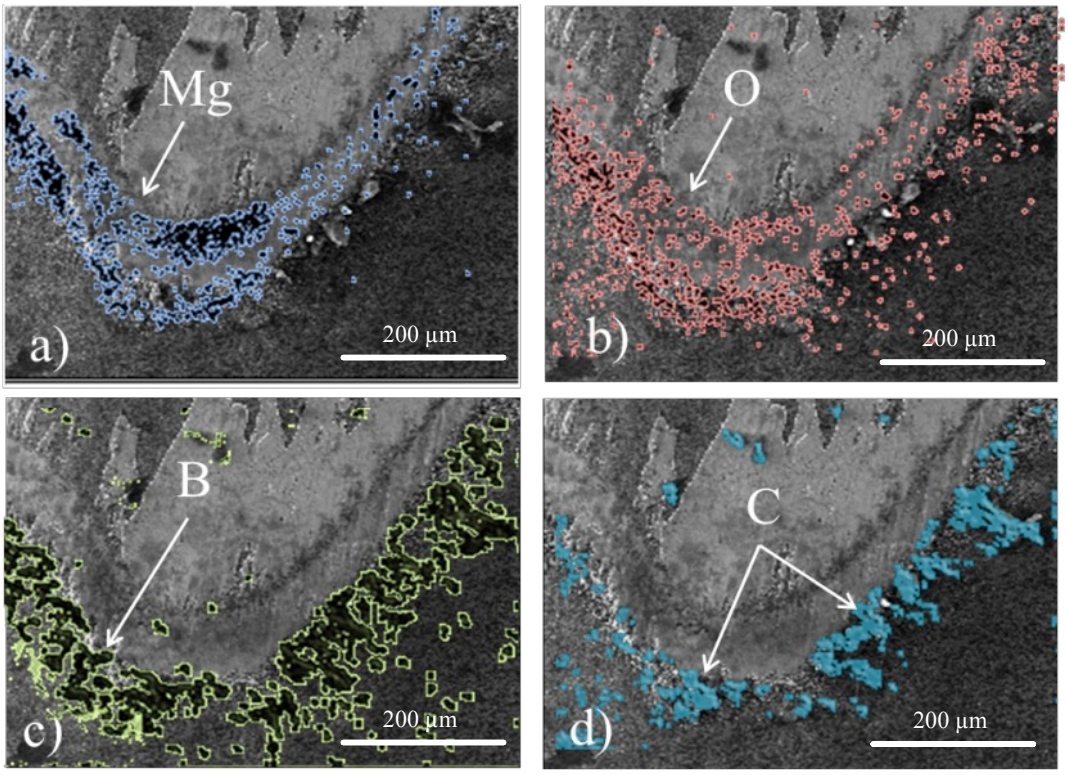

Figure 2-7: a) Elemental maps of a) Magnesium b) Oxygen, c) Boron and d) Carbon superimposed on the SEM image of tool flank worn area

Figure 2-7 shows that Mg and O rich zones are formed between the black and white zones, surrounded with areas rich in B and C.

The combination of high cutting speeds and the low thermal conductivity of these low content CBN inserts (around 40-50 W/mK) in addition to the very low thermal conductivity of the workpiece material (around 5.8 W/mK) results in generation of very high local temperature in the cutting zone. Excessive thermal and mechanical stresses result in the reduction of the interfacial debonding strength between CBN particles and the ceramic binders. Therefore, the boron particles could be pushed out in the direction of the cutting force and agglomerate in the border of the worn area.

Debonding of reinforcing particles from the workpiece matrix is a known phenomenon, which mostly happens during machining of MMCs. This phenomenon is considered as one of the most important challenges of machining of this class of materials. Once the bonding between the TiC particles and matrix breaks, they can be also pushed in the cutting direction and agglomerated around the worn regions. Thus, considering the location of boron- and carbon-rich areas on the tool face, generation of a distinct border for the adhered material on the worn area could be also explained. The agglomerated carbide and boron particles surrounding the flank worn area act as a barrier for the workpiece material adhered to the insert and could make a cluster of workpiece material in the border. This area appears as a white zone surrounding the worn area. This phenomenon was observed on the tool flank face under different cutting conditions. In addition, the white appearance of this zone could be also attributed to the TiC particles present in this area.

2.4.1.2 Rake face

Similar wear surface morphology to the flank face was observed on the rake face during wet machining with different cutting conditions. The three different zones were formed on the rake face. The elemental maps are presented in Figure 2-8. It can be observed that the elemental distributions in the different zones are similar to the flank face (Figure 2-3). Yet, noticing Figure 2-8-f, the agglomeration of boron particles was not observed around the adhered layer on the rake face.

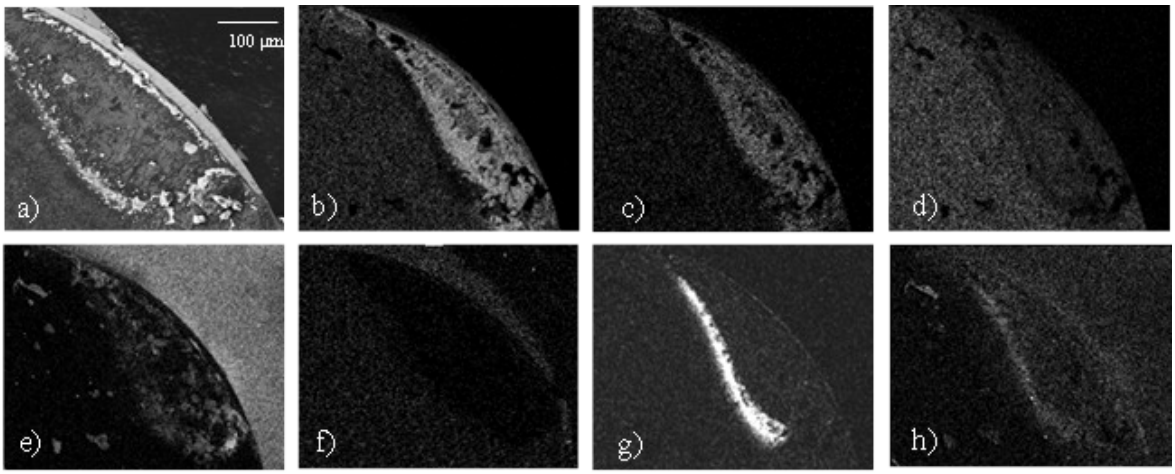

Figure 2-8: a) SEM of entire rake worn area, Elemental maps of b) Titanium (Ti-Kα), c) Vanadium, d) Aluminum, e) Carbon, f) Boron, g) Magnesium and h) Oxygen (for the conditions given in Figure 2-1)

2.4.2 Dry machining

The SEM image of the flank face and its corresponding oxygen and magnesium maps in dry machining with cutting speed of 300 m/min is presented in Figure 2-9-a to 2-9-c, respectively. The three different zones identified in Figure 2-1, are formed on the flank face during the dry machining. However, it can be observed that during dry machining, the oxide area is larger and is no more limited to the white zone.

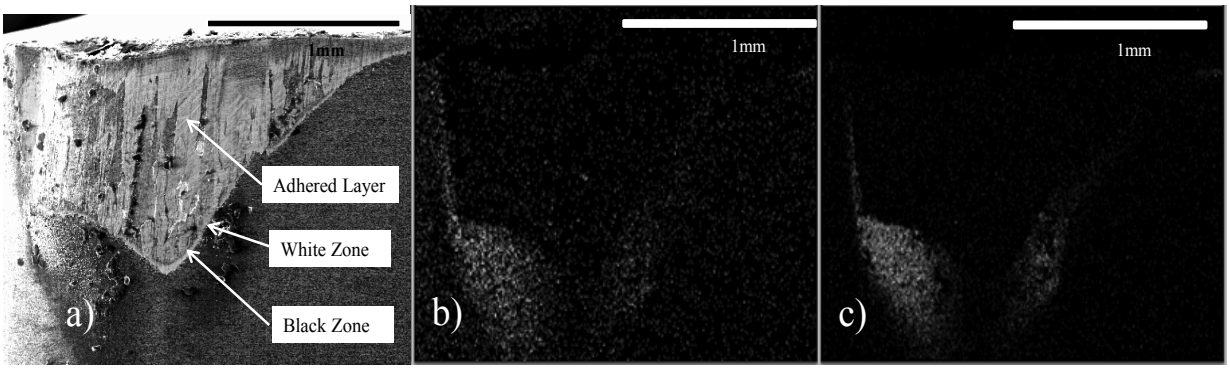

Figure 2-9: a) SEM image of the tool flank face after dry machining with v=300 m/min, f=0.1 mm/rev and a_p= 0.15mm, machining time 40 seconds, b) oxygen map, c) magnesium map

Regarding the rake face, as shown in Figure 2-10- b still the agglomeration of boron particles was not observed. TiC particles were also pushed away to the corners of the worn area (Figure 2-10-

e). Thus, such distinct black and white layers were not observed on the rake face during dry machining. As could be seen in Figure 2-10, the adhered material is just blocked behind the carbide particles in the corners of worn area. Also, similar to the flank face, during dry machining of Ti-MMCs the oxide area formed around the worn zone, is much larger comparing to the wet machining conditions.

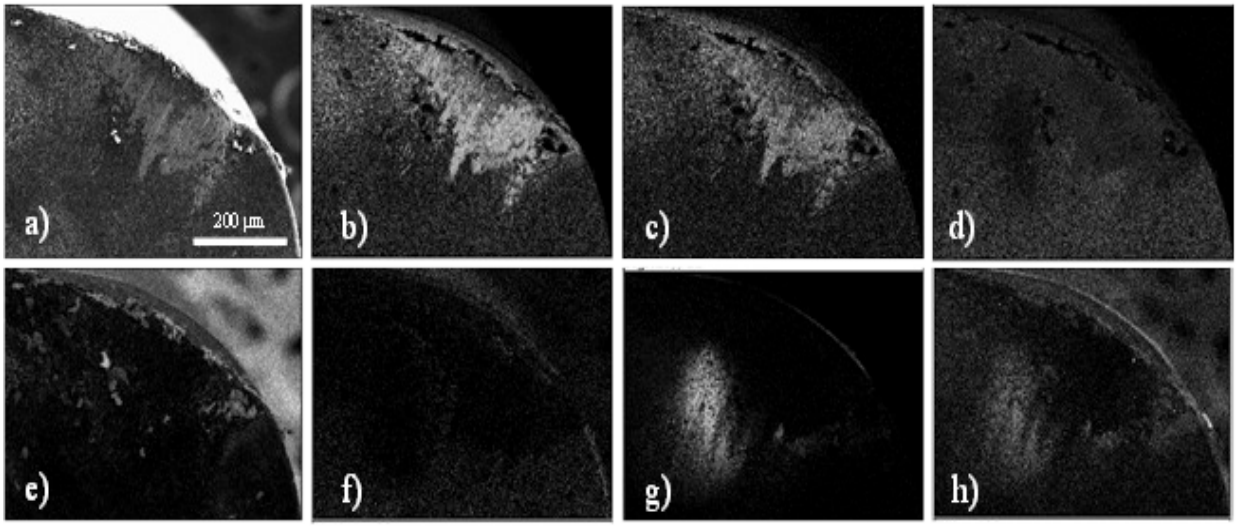

Figure 2-10: a) SEM image of the entire rake worn area, and elemental maps of b) Titanium (Ti-Kα), c) Vanadium, d) Aluminum, e) Carbon, f) Boron g) Magnesium and h) Oxygen, after dry machining with v=350 m/min, f=0.1 mm/rev and a_p= 0.15mm

Among different tool wear mechanisms of CBN inserts, transformation from cubic structure (CBN) to softer hexagonal structure (HBN) is also reported (H. M. Lin et al., 2008). In order to investigate if this phase transformation occurs during machining, the diffraction pattern of the HBN is analyzed. Results for the dry machining at $V = 350\ m/min$, $f = 0.1\ mm/rev$ and $a_p = 0.15\ mm$ are presented in Figure 2-11.

CBN pattern:

HBN pattern:

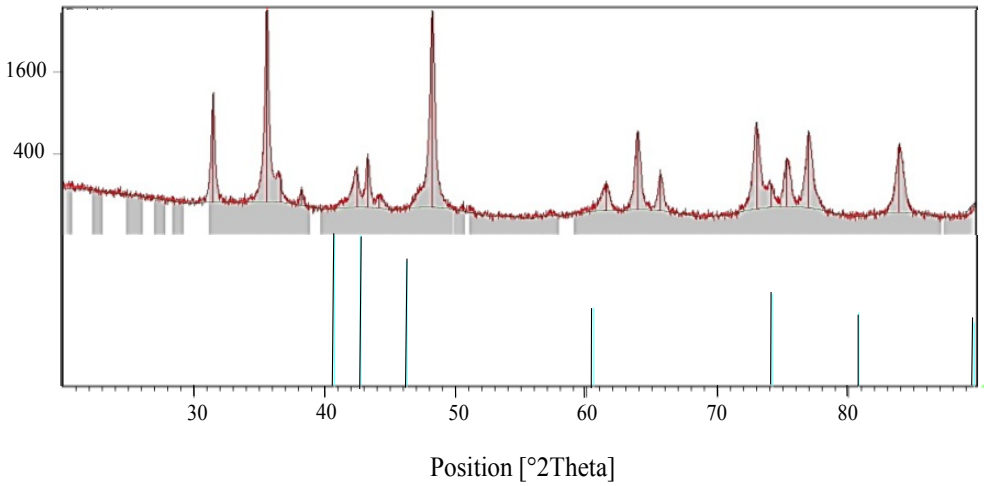

Figure 2-11: Comparison between the diffraction patterns of CBN after dry machining with HBN pattern (pdf no. 260773)

No compatibility between the CBN pattern and HBN is observed, suggesting no transformation occurred. Neither was this transformation observed in wet machining conditions.

Source of magnesium on the worn surfaces

Finally, in order to clearly address the source of magnesium found on the tool surface, experiments were performed with different inserts and workpiece materials.

The first group of experiments were performed with CBN insert on a workpiece made of 1080 steel, with no Mg content. Examination of the worn surfaces with EDS revealed no magnesium on the tool surfaces, instead a similar layer rich in Fe and O was found outside the contact region.

In addition, experiments were performed on the Ti-MMC workpiece material but this time with a carbide tool (SECO TH1000 coated carbide tool). A similar area rich in Mg and O was found surrounding the tool wear area. The results are presented in Figure 2-12.

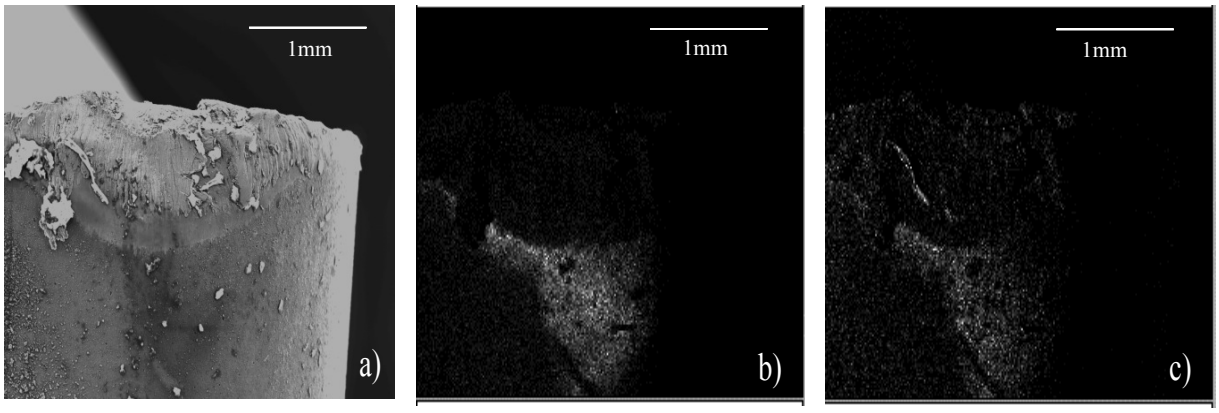

Figure 2-12: a) SEM of the flank face of a carbide insert (TH1000) after dry machining of Ti-MMC with v=80 m/min, f=0.1 mm/rev and a_p= 0.15mm, b) oxygen map, c) magnesium map

Furthermore, EDS and WDS analyses were performed on a new insert and the workpiece material. The results confirmed that there is no Mg in the CBN insert. The Mg was detected with EDS on the workpiece material with weight percent of < 0.1 %. WDS analysis also showed Mg in the material with 0.09 wt %.

The results suggest that the Mg found on the tool worn surface is originating from the workpiece material and it deposits on the tool surface during the machining process. The phase diagram of magnesium and titanium shows that Mg is barely soluble in titanium and at temperatures above 651 °C it is transformed to a liquid phase (Murray, 1986). Hence, during machining process magnesium could be removed from the workpiece material and adhere to the tool material. During machining Ti-6Al-4V alloy, a temperature of around 1000 K at low cutting speed of 75 m/min and higher temperatures of around 1400 K at moderate cutting speeds were reported (Bhaumik et al., 1995). A study in our research group estimated that a temperature up to 803 ^{o}C could be reached at the tool/chip interface, during machining of the same Ti-MMC material at cutting speed of 150 m/min with uncoated carbide tools (Bejjani, 2012). Mg is highly prone to oxidation at elevated temperatures. Hence, Mg agglomerated in the tool surface, is most likely to react with oxygen and form magnesium oxide at high temperatures. Although magnesium is present in the workpiece material in very small amounts, the oxidation mechanism is so great that severe ignition and flaming occurs during the dry machining of Ti-MMCs.

Fire hazard was mentioned as a significant issue during machining of Ti-MMCs (R. Bejjani et al., 2011). The responsible oxidation mechanism is reported for the first time in this paper, as well as

the effect on embrittlement of titanium alloys and thereby on the unique wear morphology. This phenomenon could also be responsible for the poor surface quality of the workpiece, which is considered as the main drawback of machining this class of materials. Since there is a limited data in this field, in the upcoming section a complementary study is performed to study other possible mechanisms of titanium embrittlement and the effect on the surface integrity.

2.4.3 Titanium embrittlement during machining of Ti-MMCs and the effect on the surface integrity

Different in-situ reaction products could alter the mechanical properties of titanium matrix and result in its embrittlement and generation of inclusion and defects. Therefore, close control of nitrogen, hydrogen and carbon contamination in titanium alloys is recommended (Godfrey et al., 2000). During manufacturing of Ti-6Al-4V, formation of in-situ hard needle like TiB is also reported to cause an increase in the flow stress, resulting in cavitation and embrittlement (Godfrey et al., 2000). Thus, an investigation is performed to study the formation of different in-situ products responsible for this phenomenon, using XRD analysis.

Titanium has a very high affinity to nitrogen. Its nitration which results in the formation of TiN is also among the most common reactions between Ti and CBN (Wenfeng et al., 2010). TiN is detected on the generated chips with the highest intensity compared to the other reaction products. TiN and TiC are significantly prone to react with CBN and form titanium boride. Formation of TiB, TiB_2 and Ti_3B_4 are highly possible as they inherit high negative Gibbs energy (W. F. Ding et al., 2006). In this study, formation of titanium boride in the generated chips was also confirmed through the XRD analysis. TiB had the highest intensity and perfect match followed by small amounts of TiB_2 and Ti_3B_4. The result of the XRD analysis for the dominant titanium boride of this study (TiB) is shown in Figure 2-13. One could see that the diffraction pattern of the generated chips matches perfectly the TiB pattern (eg. diffractions angles of 36°, 39°, 42°, 71°, 77°).

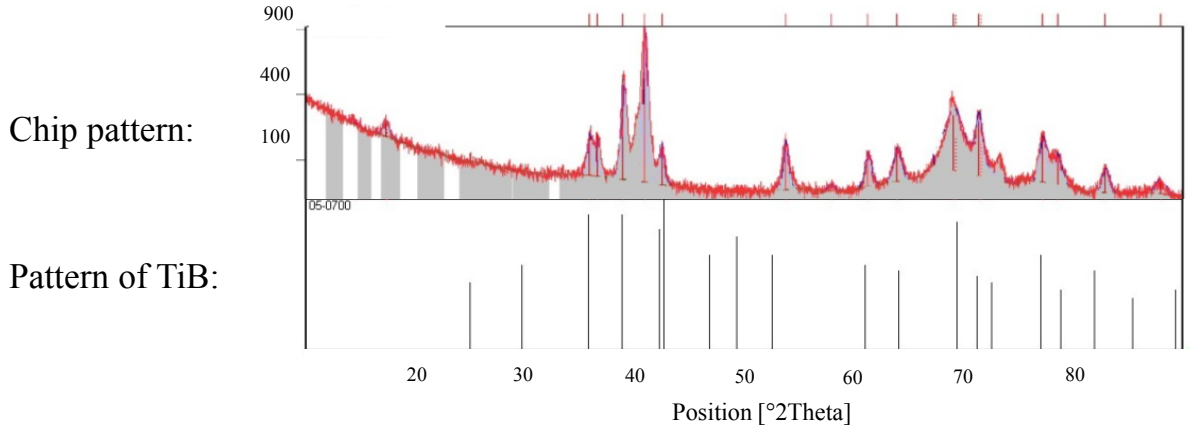

Figure 2-13: Comparison between the diffraction pattern of generated chips and the pattern of TiB (pdf no. 050700)

Preliminary results provided the evidence of oxidation on the surface of the workpiece. Figure 2-14-a shows the SEM image of the workpiece surface after dry machining at $V = 350\, m/min$, $f = 0.1\, mm/rev$ and $a_p = 0.15\, mm$. The oxygen line scan, shown in Figure 2-14-b, clearly reveals the presence of oxygen in the affected area shown in the SEM image.

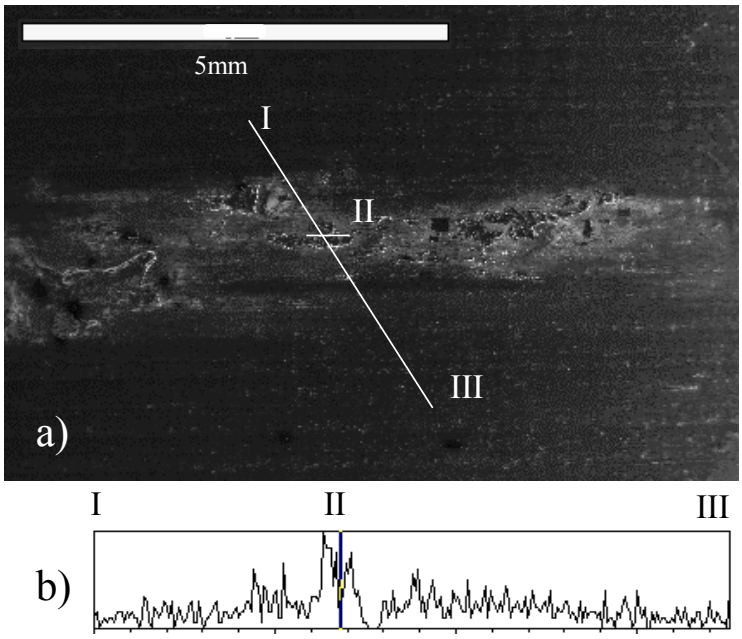

Figure 2-14: Generated machined surface

a) SEM image and b) oxygen line scan showing the severe oxidation on the machined surface

Higher magnification SEM images (presented in Figure 2-15) revealed brittle fracture, cavities and cracks in the affected area of the machined surface. The results suggest that titanium embrittlement due to the oxygen contamination could also occure on the machined surface which could significantly affect the surface quality of the parts. Thus, inert gas shielded conditions are recommended during machining Ti-MMCs in order to prevent any contamination.

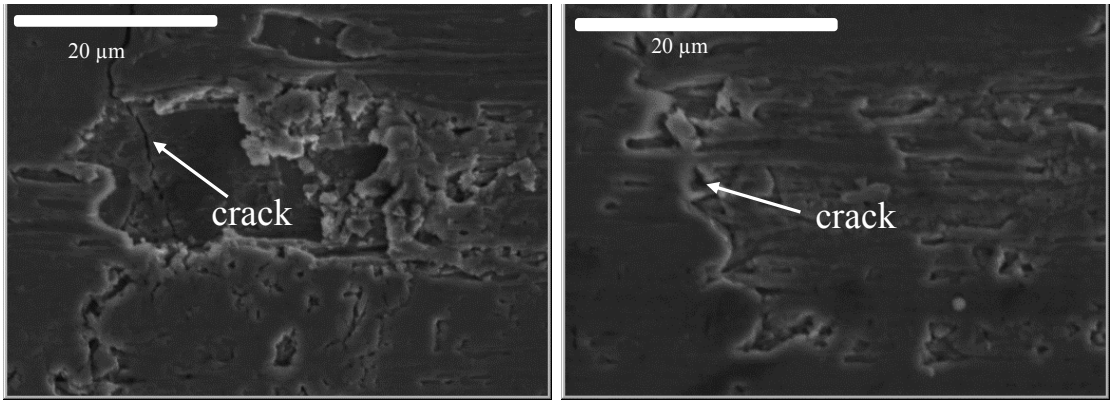

Figure 2-15: SEM image showing the fracture and crack initiation on the machined part

2.5 Conclusions

This study aimed at investigating the tool wear mechanisms of the CBN inserts during machining of Ti-MMCs. For the first time, the different mechanisms responsible for the embrittlement of titanium alloys during machining of Ti-MMCs and the effect on the unique wear surface morphology were studied.

Three different zones were identified on the CBN flank and rake surfaces during wet machining at relatively high cutting speeds: a *layer adhered* to the tool composed of work-piece materials such as Ti, Al and V adhered to the tool surface inside the contact region; *a black zone* on margin of the contact region, which found to be a discontinuity between the non-oxide components inside the contact zone and the oxide contaminated materials outside the contact zone; and *a white zone* surrounding the entire materials adhered to the tool. EDS and XRD analyses of the tool surfaces and generated chips revealed that MgO is a primary oxide product present on the tool surfaces. Contamination of the titanium matrix alloy with oxygen outside the contact region was found to result in its embrittlement and reduction in mechanical properties. Therefore, around the contact region, simultaneous abrasion and oxidation mechanisms resulted in the brittle

fracture and debonding of adhered materials from the tool. Thus, a distinct discontinuity was formed within the adhered materials to the tool, around the contact region. EDS analysis also confirmed that the entirety of the adhered materials was limited to the regions rich in C and B elements on the flank face, and C elements on the rake face. The clustered material behind these barriers appears as a white zone on the worn surfaces. The distinctive appearance of this zone could also be attributed to the TiC products around this zone. During the dry machining of Ti-MMCs the oxide area was bigger and was not limited to the white zone. On the other hand, such three distinct zones were not observed on the tool rake face during the dry machining conditions.

Traces of severe oxidation and brittle fracture were also detected on the machined surface, suggesting that the embrittlement of titanium alloy could also be considered as a root cause of the poor surface quality of the finished parts during machining of Ti-MMCs.

2.6 Acknowledgement

The authors acknowledge the Canadian Network for Research and Innovation in Machining Technology (CANRIMT) for their financial support, and the aerospace structures, materials and manufacturing laboratory of the National Research Council Canada (NRC) for its valuable contribution to this work. The authors also thank the Dynamet Technology Inc. for providing the Ti-MMC material, and Seco Tools for supplying the inserts.

2.7 References

Abkowitz, S., & Fisher, H. (2011). Breakthrough claimed for titanium PM. *Metal Powder Report, 66*(6), 16-21.

Angseryd, J., & Andrén, H. O. (2011). An in-depth investigation of the cutting speed impact on the degraded microstructure of worn PCBN cutting tools. *Wear, 271*(9–10), 2610-2618. doi: http://dx.doi.org/10.1016/j.wear.2010.11.059

Aouici, H., Yallese, M. A., Chaoui, K., Mabrouki, T., & Rigal, J.-F. (2012). Analysis of surface roughness and cutting force components in hard turning with CBN tool: Prediction model and cutting conditions optimization. *Measurement, 45*(3), 344-353. doi: 10.1016/j.measurement.2011.11.011

Astakhov, V. P. (2013). Tribology of Cutting Tools Tribology in Manufacturing Technology. In J. P. Davim (Ed.), (pp. 1-66): Springer Berlin Heidelberg.

Barry, J., & Byrne, G. (2001). Cutting tool wear in the machining of hardened steels. Part II: Cubic boron nitride cutting tool wear. *Wear, 247*(2), 152-160. doi: 10.1016/s0043-1648(00)00528-7

Bejjani, R. (2012). *Mashinability and modeling of cutting mechanism for titanium metal matrix composites.* Doctarate degree dissertation, Polytechnique Montreal.

Bejjani, R., M. Balazinski, B. Shi, H. Attia, H. Kishawy. (2011). Machinability and chip formation of Titanium Metal Matrix Composites (Ti-MMCs). *Int. J. of Advanced Manufacturing Systems, IJAMS, 13*(1).

Bhaumik, S. K., Divakar, C., & Singh, A. K. (1995). Machining Ti-6Al-4V alloy with a WBN-CBN composite tool. *Materials & Design, 16*(4), 221-226. doi: http://dx.doi.org/10.1016/0261-3069(95)00044-5

Bhushan, R. K., Kumar, S., & Das, S. (2010). Effect of machining parameters on surface roughness and tool wear for 7075 Al alloy SiC composite. *International Journal of Advanced Manufacturing Technology, 50*(Compendex), 459-469.

Bindal, M. M., Singhal, S. K., Singh, B. P., Nayar, R. K., Chopra, R., & Dhar, A. (1991). Synthesis of cubic boron nitride using magnesium as the catalyst. *Journal of Crystal Growth, 112*(2-3), 386-401. doi: 10.1016/0022-0248(91)90314-u

Byrne, G., Dornfeld, D., & Denkena, B. (2003). Advancing Cutting Technology. *CIRP Annals - Manufacturing Technology, 52*(2), 483-507. doi: Doi: 10.1016/s0007-8506(07)60200-5

Chiou, S.-Y., Ou, S.-F., Jang, Y.-G., & Ou, K.-L. (2013). Research on CBN/TiC composites Part1: Effects of the CBN content and sintering process on the hardness and transverse rupture strength. *Ceramics International, 39*(6), 7205-7210. doi: http://dx.doi.org/10.1016/j.ceramint.2013.02.066

Clark, R. K., & Unnam, J. (1983). Residual mechanical properties of Ti-6Al-4V after simulated Space Shuttle reentry. *NASA Technical Memorandum*.

Davim, J. P., & Astakhov, V. P. (2008). Tools (Geometry and Material) and Tool Wear *Machining* (pp. 29-57): Springer London.

Davim, J. P., Pramanik, A., Arsecularatne, J. A., & Zhang, L. C. (2008). Machining of Particulate-Reinforced Metal Matrix Composites *Machining* (pp. 127-166): Springer London.

Ding, W. F., Xu, J. H., Fu, Y. C., Xiao, B., Su, H. H., & Xu, H. J. (2006). Interfacial reaction between cubic boron nitride and Ti during active brazing. *Journal of Materials Engineering and Performance, 15*(3), 365-369. doi: 10.1361/105994906x108747

Ezugwu, E. O., Da Silva, R. B., Bonney, J., & Machado, A. R. (2005). Evaluation of the performance of CBN tools when turning Ti-6Al-4V alloy with high pressure coolant supplies. *International Journal of Machine Tools & Manufacture, 45*(9), 1009-1014. doi: 10.1016/j.ijmachtools.2004.11.027

Farhat, Z. N. (2003). Wear mechanism of CBN cutting tool during high-speed machining of mold steel. *Materials Science & Engineering A (Structural Materials: Properties, Microstructure and Processing), A361*(1-2), 100-110. doi: 10.1016/s0921-5093(03)00503-3

Godfrey, T. M. T., Wisbey, A., Goodwin, P. S., Bagnall, K., & Ward-Close, C. M. (2000). Microstructure and tensile properties of mechanically alloyed Ti–6A1–4V with boron additions. *Materials Science and Engineering: A, 282*(1–2), 240-250. doi: http://dx.doi.org/10.1016/S0921-5093(99)00699-1

Grzesik, W. (2008). *Advanced machining processes of metallic materials: theory, modelling and applications*: Elsevier.

Heath, P. J. (2001). Developments in applications of PCD tooling. *Journal of Materials Processing Technology, 116*(Compendex), 31-38.

Hung, N. P., Venkatesh, V. C., & Loh, N. L. (1998). Cutting tools for metal matrix composites. *Key Engineering Materials, 138-140*(Compendex), 289-325.

Klimczyk, P., Figiel, P., Petrusha, I., & Olszyna, A. (2011). Cubic boron nitride based composites for cutting applications. *Journal of Achievements in Materials and Manufacturing Engineering, 44*(2), 198-204.

Lin, H. M., Liao, Y. S., & Wei, C. C. (2008). Wear behavior in turning high hardness alloy steel by CBN tool. *Wear, 264*(7-8), 679-684. doi: 10.1016/j.wear.2007.06.006

Luo, S. Y., Liao, Y. S., & Tsai, Y. Y. (1999). Wear characteristics in turning high hardness alloy steel by ceramic and CBN tools. *Journal of Materials Processing Technology, 88*(1–3), 114-121. doi: http://dx.doi.org/10.1016/S0924-0136(98)00376-8

Mashinini, P. M. (2010). *Process window for Friction Stir Welding of 3 mm Titanium (Ti-6Al-4V)*. Research dissertation, Nelson Mandela Metropolitan University.

Monteiro, S. N., Skury, A. L. D., de Azevedo, M. G., & Bobrovnitchii, G. S. (2013). Cubic boron nitride competing with diamond as a superhard engineering material–an overview. *Journal of Materials Research and Technology, 2*(1), 68-74.

Murray, J. (1986). The Mg− Ti (Magnesium-Titanium) system. *Bulletin of Alloy Phase Diagrams, 7*(3), 245-248.

Poulachon, G., Moisan, A., & Jawahir, I. S. (2001). Tool-wear mechanisms in hard turning with polycrystalline cubic boron nitride tools. *Wear, 250*(1–12), 576-586. doi: 10.1016/s0043-1648(01)00609-3

Wenfeng, D., Jiuhua, X., Zhenzhen, C., Honghua, S., & Yucan, F. (2010). Effects of Heating Temperature on Interfacial Microstructure and Compressive Strength of Brazed CBIN-AlN Composite Abrasive Grits. *Journal of Wuhan University of Technology - Materials Science Edition, 25*(6), 952-956.

Chapter 3 ARTICLE 2: SURVIVAL LIFE ANALYSIS OF THE CUTTING TOOLS DURING TURNING TITANIUM METAL MATRIX COMPOSITES (TI-MMCS)

M. Aramesh, Y. Shaban, M. Balazinski, H. Attia, H. A. Kishawy, and S. Yacout, *Procedia CIRP,* vol. 14, pp. 605-609, 2014.

ABSTRACT

Metal matrix composites (MMCs), as a new generation of materials; have proven to be viable materials in various industrial fields such as biomedical and aerospace. In order to achieve a valuable modification in various properties of materials, metallic matrices are reinforced with additional phases based on the chemical and/or physical properties required in the in-service operating conditions. The presence of the reinforcements in MMCs improves the physical, mechanical and thermal properties of the composite; however it induces significant issues in the domain of machining, such as high tool wear and inferior surface finish. The interaction between the tool and abrasive hard reinforcing particles induces complex deformation behaviour in the MMC structure. Sever tool wear is technically the most important drawback of machining MMCs.

In this study a statistical model is developed to estimate the mean residual life (MRL) of the cutting tool during machining Ti-MMCs. Initial wear, steady wear and rapid wear regions in the tool wear curve are regarded as the different states in the statistical model. Hence, the valuable information regarding the estimated total time spent in each state, called the sojourn time, and the transition times between the states are obtained from the model.

In this paper the standard cutting conditions, based on the recommendation of the tool supplier, are adopted. Based on a Weibull model, the reliability and hazard functions are obtained and are utilized in order to calculate the MRL and the sojourn times.

3.1 Introduction

Metal matrix composites (MMCs) inherit such a combination of desirable characteristics which has brought them up as the prime candidate materials in various industries. However, hard and abrasive nature of the reinforcing particles in MMCs, are the potential detriments to the severe

tool wear and surface roughness occurring during machining of this class of materials (S. Kannan et al., 2006; Songmene et al., 1999). This emphasizes the importance of developing a statistical model, in which the progressive states of tool wear from an initial point to the failure state is represented. Recognizing the probabilistic nature of cutting tool life, different researches have been conducted to assess the cutting tool reliability. Devor et al. studied the random nature of the cutting tool life (DeVor et al., 1977), while several studies were perform to represent the tool life with different probability distributions (Hitomi et al., 1978; J. G. Wager et al., 1971). Mazzuchi et al (Mazzuchi et al., 1989) presented the proportional hazard model (PHM) for modeling the machine tool failure. The model described the effect of aging and also machining environment on the tool life. Tail et al (Tail et al., 2010) investigated the cutting tool reliability under different cutting speeds using PHM. Benkedjouh et al (Benkedjouh et al., 2013) used a method based on the support vector regression to obtain the remaining useful life of cutting inserts.

As shown previously, reliability analyses have always been of interest in order to assess the cutting tool reliability and to acquire information about tool failure time. Considering the typical tool wear curve shown in Figure 3-1, tool wear process consists of three distinct states. The initial state, with very high wear rate known as rapid wear zone, a steady state with almost constant tool wear rate followed by a very rapid wear rate state.

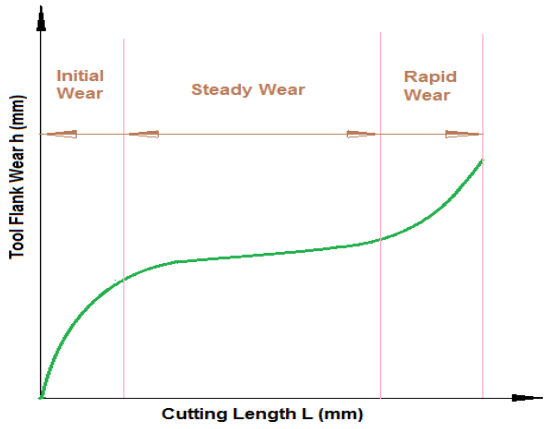

Figure 3-1: The tool wear curve

During many machining operations, it is preferable to replace the cutting tool before entering the third state in order to prevent any probable damage to the high quality products. This is the case especially during machining MMCs in which the sojourn time in the rapid wear zone is very short.

Since there is a lack of knowledge in this area, an attempt is made in this study to obtain the transition time between different wear states and to find the sojourn time of the cutting insert in each state. Hence, at each desired point, the remaining time to each transition state in addition to the mean residual life until failure can be obtained. The data is a useful piece of information which could be further implemented in different machining models.

In this study the standard fixed cutting conditions are utilized, based on the recommendation of the tool supplier.

3.2 Experiment set up

A cylindrical bar of Ti-6Al-4V alloy matrix reinforced with 10-12% volume fraction of TiC ceramic particles is used in this study.

Dry machining tests were conducted on a 6-axis Boehringer NG 200, CNC turning center. TiSiN-TiAlN nano-laminate PVD coated grades (Seco TH1000 coated carbide grades) were utilized for this study. A total of six inserts is used for this study.

The experiment set up is shown in Figure 3-2.

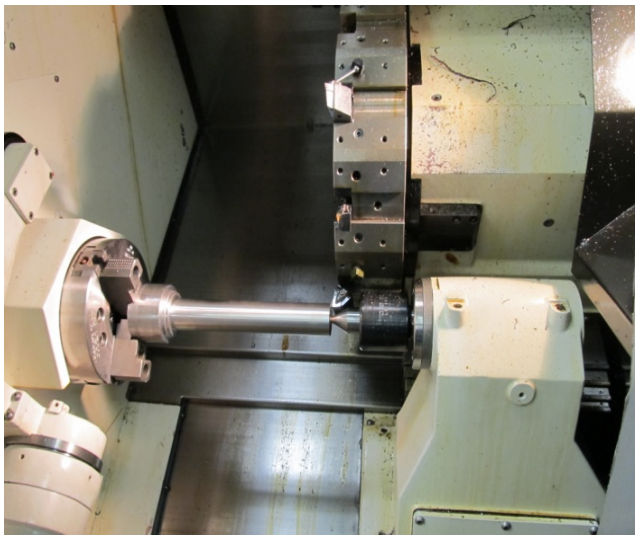

Figure 3-2: The experiment set up

The experiments are performed under constant cutting conditions based on the supplier's recommendations. The values assigned for each cutting parameter are listed in Table 3-1.

Table 3-1: Cutting parameters

Insert / Parameters	TH1000
Cutting Speed (m/min)	60
Feed Rate (mm/rev)	0.15
Depth of Cut (mm)	0.20

After each experimental run, the tool maximum flank wear length (VB_{Bmax}) wear was measured using an Olympus SZ-X12 microscope.

3.3 Methodology

For each insert, sequential turning tests were conducted. VB_{Bmax} was measured after each step. This is to insure that the tool life curve is constructed with adequate accuracy for each insert, and that the failure criterion is reached for each tool. An approximate number of ten measurements for each insert are taken until the maximum tool flank wear threshold is reached. The same procedure is replicated six times for different inserts.

After obtaining the tool wear curves for each insert, time to failure for each insert is calculated by interpolating between the lower and upper measurements values from the experiments.

Since the goal of this study is to obtain the information about the transition time between different wear states, each state on the tool wear curve is first analyzed as a separate case. Hence, a failure criterion is assigned separately for each zone; namely, potential, critical and functional failures.

In this study we have assigned initial, steady and rapid wear zones to states 1 to 3, respectively. Thus, the mean value of VB_{Bmax} for six inserts, corresponding to the transition point from state 1 to state 2 is considered as the potential criterion. While the corresponding value for state 2 to 3 transition is considered as the critical failure criterion.

Considering the tool wear curves for different inserts, the maximum flank wear length, VB_{Bmax}, equal to 0.075 and 0.09 mm are considered as the potential and critical failure criteria for the first and second tool wear states, respectively.

A maximum value of tool flank wear equal to 0.2 mm was defined as the functional failure limit.

In this study, Weibull distributions with two parameters (β, η), representing the survival functions were developed based on the experimental times to failure (TTF) for the six inserts and for each state separately.

The probability density function corresponding to the Weibull distribution is represented by the following equation:

$$f(t) = {}^{\beta}/_{\eta}\ ({}^{t}/_{\eta})^{\beta-1} exp\left[-({}^{t}/_{\eta})^{\beta}\right] \quad \beta, \eta > 0; t \geq 0 \tag{3-1}$$

where β is the shape parameter and η is the scale parameter.

The corresponding reliability function is obtained from the following relation:

$$R(t) = exp\left[-({}^{t}/_{\eta})^{\beta}\right] \tag{3-2}$$

The mean time to failure (MTTF) was obtained by the following equation:

$$MTTF = \eta\, \Gamma(1 + {}^{1}/_{\beta}) \tag{3-3}$$

Mean residual life (MRL) at the observation moment t_r for each state (i, i=1, 2, 3) is calculated by the following equation:

$$MRL(t_r) = \frac{\int_{t_r}^{\infty} t f_i(t) dt}{R_i(t)} - t_r \tag{3-4}$$

The mean residual life function is an informative function, which is of interest mostly in reliability and medical fields. It can be obtained from the model`s distribution function and provides us with the expected remaining survival life of a subject, given that the subject has survived up to the observation point, t_r (Cook et al., 2007).

Thus, for our case, the time to the tool potential failure (i=1), critical failure (i=2) and functional failure (i=3), given that for each case the insert has survived till time t_r, can be obtained from equation (3-5).

$$E[T_i - t_r | T_i > t_r] \quad (3\text{-}5)$$

3.4 Results and discussion

As discussed before, reliability analysis is performed on each state separately by considering a separate limit for the flank wear VB_{Bmax} for each state. As a first step, the tool wear curves for the six different inserts are depicted. Figure 3-3 shows the results for the six inserts.

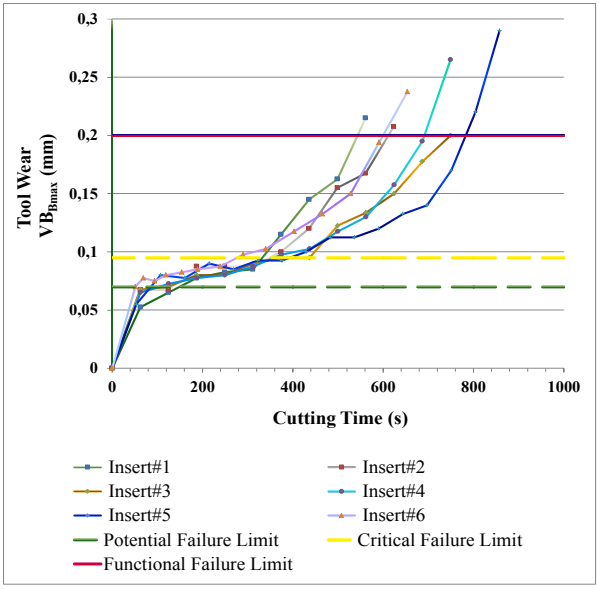

Figure 3-3: Tool wear curve for 6 inserts

The time to failure for each state was obtained from the experiments separately and are summarized in Table 3-2.

Table 3-2: Time to failure for different states

Insert #	*Time to Potential Failure (First state) [s]*	*Time to Critical Failure (Second state)[s]*	*Time to Functional Failure (Third state) [s]*
1	174,4631	321,926	542,9719
2	147,9821	324,0029	611,6142
3	155,9612	311,992	749,1702
4	156,1351	327,8836	691,1465

5	149,2257	304,4203	782,7383
6	94,0907	252,1631	599,5416

3.4.1 Fitting the reliability model

Based on the experimental results given in Figure 3-3 and Table 3-2, and after calculating the Weibull distribution parameters, the reliability and hazard functions, and the MTTF for each state are obtained. This was carried out using the software Mathematica.

The Weibull distribution parameters and MTTF for each state are presented in Table 3-3.

Table 3-3: Weibull distribution parameters and MTTF for each case

State	***Shape function***	***Scale function***	***MTTF [s]***
1	8,44	155,75	146,96
2	19,86	317,11	308,70
3	8,8	700,83	663,96

3.4.2 Transition time between states

In some cases, like the case under consideration in this study, the prediction time to the next event is of interest. This prediction time could be vital when significant cost is associated with the events. Having the probability model for a current event, the prediction for the next events could be calculated, based on the event history up to that point (Cook et al., 2007).

Considering the transition from one state to another as the desired event, the time to the next event from the current event could be calculated based on the event history for each state, knowing the reliability function and MTTF associated with each state.

Thus, the transition time to state two could be calculated taking to account the reliability distribution for state one. Therefore, the expected time to reach the transition point from state one to state two for a given time (t_r), is obtained through calculating the mean residual life to the potential failure (T_l) for the observation point, given that the system has survived up to the time t_r. One could find the related equation below:

$$E[T_1 - t_r | T_1 > t_r] = \frac{\int_{t_r}^{\infty} t f_1(t) dt}{R_1(t)} - t_r \quad (3\text{-}6)$$

Similarly, the expected time to change from state two to state three is calculated from the reliability model for state 2, given the survival up to t_r. The corresponding relation is presented as follows:

$$E[T_2 - t_r | T_2 > t_r] = \frac{\int_{t_r}^{\infty} t f_2(t) dt}{R_2(t)} - t_r \quad (3\text{-}7)$$

The same methodology is applied to calculate the residual time for the third state:

$$E[T_3 - t_r | T_3 > t_r] = \frac{\int_{t_r}^{\infty} t f_3(t) dt}{R_3(t)} - t_r \quad (3\text{-}8)$$

For example suppose that the observation time is at 50 seconds, then the transition time to state two and state three could be calculated from equations 3-6 and 3-7, respectively, while the transition times for final failure could be obtained from equation 3-8. The results are presented in Table 3-4.

Table 3-4: time to different transition points from t_r=50s

Time to first transition point [s]	***Time to Second transition point [s]***	***Time to third transition point [s]***
97.05	258.65	612.98

3.4.3 Sojourn time

If the total time spent in each state is of interest, then it can be calculated, taking into account the mean residual life for each insert.

Accordingly, the duration of sojourns in state one can be obtained from the mean residual life to potential failure for state one, given that the observation time is equal to zero. The related equation is presented below:

$$Sojourn\ time_1 = \frac{\int_0^{\infty} t f_1(t) dt}{R_1(0)} \quad (3\text{-}9)$$

The sojourn time for the second state can calculated from the mean residual life corresponding to state two, conditional on the observation point fixed on the $MTTF_1$:

$$Sojourn\ time\ _2 = \frac{\int_{MTTF_1}^{\infty} tf_2(t)dt}{R_2(MTTF_1)} - MTTF_1 \quad (3\text{-}10)$$

Finally for the third state, the sojourn time was calculated through equation 3-11, by taking into account that the observation point was considered as $MTTF_2$.

$$Sojourn\ time_3\ = \frac{\int_{MTTF_2}^{\infty} tf_3(t)dt}{R_3(MTTF_2)} - MTTF_2 \quad (3\text{-}11)$$

The estimated results for the sojourn time in each state are presented in Table 3-5. In order to assess the validity of the results, the sojourn times calculated directly from the experiments are also presented.

Table 3-5: Sojourn time obtained from the statistical model and the experiment results

State	***Sojourn time from model [s]***	***Experimental sojourn times [s]***	***Percent Error***
1	147.0526	146.3096	0.50 %
2	161.6938	160.7550	0.58 %
3	354.5592	355.7991	0.35 %

As can be seen in Table 3-5, the statistical results are in excellent agreement with the results obtained directly from the experiments.

3.5 Conclusions

Statistical model was developed to estimate the progressive tool life of the cutting inserts during turning Ti-MMCs.

Different regions on the tool life curve are regarded as different states in the model. Reliability distribution is developed for each state separately and the related MTTF is calculated for each state based on the TTF driven from the machining tests. The mean time to transition from each state to another, in addition to the total time spent in each zone, is predicted from the model, conditional on the given history.

Thus, the mean residual life to failure for each state was utilized to predict the time to transition to the next state. The Sojourn time for each state was also obtained from the mean residual life to failure each state, given that the observation time is equal to zero for state one and equal to $MTTF_1$ and $MTTF_2$ for second and third state, respectively. Addition of cutting conditions as the covariates to the model, and calculation of useful residual life of the inserts under different cutting conditions are considered as the future work.

3.6 Acknowledgement

The authors thank the Dynamet Technology Inc. for providing the Ti-MMC material, and Seco Tools for supplying the inserts. The authors acknowledge the NSERC-Canadian Network for Research and Innovation in Machining Technology (CANRIMT) for their financial support, and Manufacturing Laboratory of the National Research Council Canada (NRC) for its valuable contribution to this work.

3.7 References

Benkedjouh, T., Medjaher, K., Zerhouni, N., & Rechak, S. (2013). Health assessment and life prediction of cutting tools based on support vector regression. 1-11. doi: 10.1007/s10845-013-0774-6

Cook, R. J., & Lawless, J. F. (2007). *The statistical analysis of recurrent events*: Springer.

Devor, R. E., Anderson, D. L., & Zdeblick, W. J. (1977). Tool life variation and its influence on the development of tool life models. *Journal of Engineering for Industry, Transactions of the ASME, 99 Ser B*(3), 578-584.

Hitomi, K., Nakamura, N., & Inoue, S. (1978). reliability analysis of cutting tools (78 - WA/PROD-9).

Kannan, S., Kishawy, H. A., & Balazinski, M. (2006). Flank Wear Progression During Machining Metal Matrix Composites. *Journal of Manufacturing Science and Engineering, 128*(3), 787-791. doi: 10.1115/1.2164508

Mazzuchi, T. A., & Soyer, R. (1989). Assessment of machine tool reliability using a proportional hazards model. *Naval Research Logistics, 36*(6), 765-777.

Songmene, V., & Balazinski, M. (1999). Machinability of graphitic metal matrix composites as a function of reinforcing particles. *CIRP Annals - Manufacturing Technology, 48*(Compendex), 77-80.

Tail, M., Yacout, S., & Balazinski, M. (2010). Replacement time of a cutting tool subject to variable speed. *Proceedings of the Institution of Mechanical Engineers, Part B (Journal of Engineering Manufacture), 224*(B3), 373-383. doi: 10.1243/09544054jem1693

Wager, J. G., M.M. Barash. (1971). Study for distribution of the life of HSS tools. *ASME, J. Eng. Ind., 73*, 295-299.

Chapter 4 ARTICLE 3: SURVIVAL LIFE ANALYSIS APPLIED TO TOOL LIFE ESTIMATION WITH VARIABLE CUTTING CONDITIONS WHEN MACHINING TITANIUM METAL MATRIX COMPOSITES (TI-MMCS)

M. Aramesh, Y. Shaban, S. Yacout, M. H. Attia, H. A. Kishawy, M. Balazinski, *Acepted, to be published in Machining Science and Technology,* 2015.

ABSTRACT

A survival analysis methodology is employed through a novel approach to model the progressive states of tool wear under different cutting conditions during machining of titanium metal matrix composites (Ti-MMCs). A proportional hazards model (PHM) with a Weilbull baseline is developed to estimate the reliability and hazard functions of the cutting inserts. A proper criterion is assigned to each state of tool wear and used to calculate the tool life at the end of each state. Accounting for the machining time and different stages of tool wear, in addition to the effect of cutting parameters, an accurate model is proposed. Investigating the results obtained for different states, it was shown that the evolution of the time-dependent phenomena, such as different tool wear mechanisms, throughout the whole machining process were also reflected in the model. The accuracy and reliability of the predicted tool lives were experimentally validated. The results showed that the model gives very good estimates of tool life and the critical points at which change of states take place.

Keywords: Tool life prediction, survival analysis, proportional hazards model, titanium metal matrix composites (Ti-MMCs)

4.1 Introduction

Costs are incurred by inaccurate estimation of tool life. Overestimation of tool life may cause in-service failures, such as scrapped parts, sub-optimal surface quality, or machine tool damage. On the other side, underestimation of tool life, may affect the overall productivity indices due to excess machine downtime associated with unnecessarily frequent tool replacements, as well as the cost of consumables. This is even more critical when machining difficult-to-machine

materials (Salonitis et al., 2014). Titanium metal matrix composites (Ti-MMCs) fall in this category due to the hard and abrasive nature of their reinforcing particles which induce severe tool wear and premature tool failure (S Kannan et al., 2006).

The first attempt for direct estimation of the tool life goes back to around hundred years ago when Taylor (Taylor, 1906) presented his first model. This empirical model is still widely applied in various machining studies. However, the results are reported to be reliable for specific tool workpiece combinations in a narrow range of cutting speeds (Marksberry et al., 2008). The accuracy of the model for different tool materials rather than steels and high-speed steels is still questionable (Davim & Astakhov, 2008; Mamalis et al., 2002).

Owning to the recognition of the correlation between the cutting forces and the progressive tool wear (Ravindra et al., 1993), different analytical models were proposed for indirect tool life estimations based on force monitoring methodologies (Braun et al., 1999; S. Das et al., 1996; Huang et al., 2007; Lee et al., 1998; Sikdar et al., 2002). Similarly, different studies have been also performed by correlating different signals including tool temperature, vibration, surface finish, power signals and optical measurements of tool wear (Dimla Snr, 2000). Although success was claimed in these studies, disregarding the random nature of the tool wear may adversely affect the precision of these models (Martin, 1994). Various factors such as differences in the physical and mechanical properties of different batches of workpiece and tool materials, could result in considerable variability of the tool wear data. This is even more pronounced during machining of composite materials, where non-homogenous distribution of the reinforcement particles can cause significant variations even within one batch of workpiece material. Thus, for this class of materials, developing a model based on the theory of probability is imperative. The probabilistic nature of the cutting tool life was studied by DeVor et al. (DeVor et al., 1977). Different distributions including normal, lognormal and Weibull were proposed for modeling the tool life data (Hitomi et al., 1978; Negishi, 1976; J. G. Wager et al., 1971; K.-S. Wang et al., 2001). Klim et al. (Klim et al., 1996) developed a reliability model to study the effect of feed rate variation on the tool life. Lin (Lin, 2008) performed a reliability analysis on the cutting tools and assessed the reliability curve variation under different cutting speeds. Rodriguez et al. (Patiño Rodriguez et al., 2010) developped a strategy for tool replacement in turning and milling operations based on reliability analysis.

Proportional hazards model (PHM), which proved to be an effective tool for survival analysis, has been proposed by Mazzuchi (Mazzuchi et al., 1989) for tool reliability assessment. The advantage of this model is that it not only accounts for the time and aging process, but also for the effect of the process variables. These variables, which are usually referred to as covariates, describe the conditions of usage (Tail et al., 2010). In machining, the cutting conditions; mainly, the cutting speed and feed rate, are regarded as the covariates. Ding et al. (Feng et al., 2011) used PH model for tool reliability assessment using tool vibration signal feature extraction. Liu et al. (Liu et al., 1996) implemented PHM for developing a general formula for tool reliability calculation under variable cutting conditions, assuming constant parameter values of hazard function during a cutting process. Tail et al. predicted the time to replacement of cutting tools based on the fixed reliability and hazard threshold criteria using PHM (Tail et al., 2010).

Typical tool wear curve demonstrates three states of tool wear, namely, initial, steady, and rapid wear zones. Estimates of between-states transition times are considered as important machining data, due to their impact on the entire machining process. The second transition time is especially crucial since tool wears out drastically during the third tool wear state (Astakhov, 2006). Generally, the tool wear associated with this point is called the permissible tool wear VB_{BC}, which is often regarded as the tool life criterion due to its critical effect on the machining process. Hence, an accurate estimation of this point is necessary in order to prevent detrimental effects on the workpiece and the machine tool by entering the rapid wear region. Furthermore, this will contribute to the process productivity by operating at full capacity. It has been reported that only 38% of the time the cutting tools are performed at their full capacity. The economic impact of such sub-optimal utilization of cutting inserts are estimated to be as high as $10 billion per year on the US industry alone (Umbrello et al., 2004b).

Although the third state of tool wear is avoided for practical applications, it is of interest for fundamental and academic studies. Many researchers prefer to enter this stage of tool wear intentionally for better understanding of different mechanisms behind the microstructural evolution and generation of machining induced residual stresses.

A new study in our research group has confirmed the significant influence of the initial wear state on the entire tool wear propagation and tool life while machining of hard-to machine materials such as Ti-MMCs. Employing the data about the first transition time and initial cutting

conditions, Xuan-Troung (Xuan-Troung, 2014) established a methodology to model the wear propagation over time, using the chaos theory.

So far, no conclusive model capable of predicting all the progressive states of tool wear has been introduced. In this study a PHM with a Weibull baseline is developed to estimate the progressive states of tool wear under different cutting conditions. Although semi-finishing tests were conducted in this study for model validation, the same approach could be applied for roughing and finishing operations.

4.2 Experiment set up

A cylindrical bar of Ti-6Al-4V alloy matrix reinforced with 10-12% volume fraction of TiC particles was used as the workpiece material for this study. Dry machining tests were conducted on a 5-axis Boehringer NG 200 CNC turning center. TH1000 coated carbide inserts; TiSiN-TiAlN nano-laminate PVD (Physical Vapor Deposition) coated grade, with nose radius of 0.8 mm were utilized for the turning tests. During each test, tool wear was measured using an Olympus SZ-X12 microscope.

4.3 Methodology

A survival analysis is performed in this study in order to estimate the progressive states of tool wear under different cutting parameters during machining of Ti-MMCs. In general, survival analysis is a statistical technique for data analysis where modeling the time to an event is of interest. The model provides the relationship between the explanatory variables (or covariates) and the survival time before occurrence of the desired event. Depending on the purpose of the study the explanatory variables and events are defined (Kleinbaum et al., 1996). In this study, cutting speed and feed rate are considered as the covariates, and reaching the end of each wear state is defined as the event of interest. Significant changes in the tool wear *rate* indicate the position of the transition time between the states. The values of the maximum wear corresponding to the first and second transition times are considered as the wear state criteria. Every state of tool wear is analyzed as an individual case, using its own criterion $VB_{Bmax,i}$, i =1 to 3. Generally, the first and second criteria were found to be in the range of 0.05 - 0.1 mm and 0.15-1.00 mm, respectively, depending on the type of the operation (Astakhov, 2006). The third criterion is arbitrarily selected for predicting the time required to reach $VB_{Bmax,3}$ for given cutting

conditions. In this study, $VB_{Bmax,3}$ =0.2 mm was selected. The experimental and statistical procedures, required to estimate the time elapsed to reach each criterion are discussed in the upcoming sections.

Since flank wear is the dominant wear mechanism during machining of MMCs (H. A. Kishawy et al., 2005), the criterion used to quantify the wear states was the maximum flank wear length $VB_{Bmax,i}$. However, based on the desired application, any other criterion such as crater wear could be selected.

4.3.1 Experimental Procedure

Experiments were conducted under different cutting speeds and feed rates, while the depth of cut was kept constant at a level of 0.2 mm for the present semi-finishing turning tests. The cutting conditions were selected based on the recommendations of the tool supplier. Table 4-1 provides the values assigned to each level; low, center and high.

Table 4-1: Cutting independent variables and their values

	Levels		
Parameters	**Low**	**Center**	**High**
Cutting Speed (m/min)	40	60	80
Feed rate (mm/rev)	0.15	0.25	0.35

The design of experiments for this study is based on a 2^2 design with an additional center point. Experiments are performed randomly in order to avoid experimental bias. Experimental run parameters are presented in Table 4-2.

Table 4-2: Cutting parameters for each experimental run

Parameter / Experimental Run	**Number of Replications**	**Cutting speed (m/min)**	**Feed Rate (mm/ rev)**	**Depth of Cut (mm)**
1	5	40	0.15	0.2
2	5	80	0.15	0.2
3	6	40	0.35	0.2
4	6	80	0.35	0.2
5	6	60	0.25	0.2

The first two runs were conducted using 5 identical inserts in 5 different replications. After the preliminary analysis, another replicate was added to the next runs to improve the accuracy of the model. For each insert, an approximate number of 8 sequential tests were conducted until the maximum pre-defined tool flank wear length in the third state ($VB_{Bmax,3}$ = 0.2) was reached. For each experimental run, time to the first and second transition points, in addition to the time to the end of the third state ($VB_{Bmax,3}$) were calculated for each replication. This has been done, by interpolating between the lower and upper values of tool wear, measured for each insert. The results for the fourth run in Table 4-2 are presented as an example in Table 4-3.

Table 4-3: Time the transition point in addition to the total time to the end of the third state for the fourth run (V=80 m/min, f=0.35 mm/rev, a_p=0.2 mm)

Insert #	Time to the first transition point (s)	Time to the second transition point (s)	Total tool time to the end of the third state (s)
1	30	97.5	121
2	14	68	87.5
3	52.5	109	135
4	37.5	120	135
5	30	101	121

4.3.2 Statistical procedure

The survival function, also known as the reliability function, *R(t),* and the hazard function, *h(t),* are considered as the fundamental data for any survival analysis. Survival function is defined as the probability of surviving at least to time t. The hazard function provides "the instantaneous potential per unit time for [an] event to occur, given that the individual has survived up to time t" (Kleinbaum et al., 1996). Proportional Hazards Model (PHM) is a common model for the survival data analysis. The model is the product of two terms expressed in Equation 4-1. The first term, $h_0(t)$, is called the baseline hazard function, which is a function of time t, reflecting the aging phenomenon. The second exponential term takes into account the model covariates, Z_i with weight factors of γ_i (Kleinbaum et al., 1996):

$$h(t;Z) = h_0(t)\, e^{\sum_1^m \gamma_i Z_i} \quad ; m \equiv \text{number of covariates} \tag{4-1}$$

In this research, the parametric Weibull model is used as the baseline function for the proportional hazards model. The probability density function for the Weibull distribution is represented in equation 4-2 (Kleinbaum et al., 1996):

$$f(t) = \frac{\beta}{\eta}\left(\frac{t}{\eta}\right)^{(\beta-1)} \exp\left[-\left(\frac{t}{\eta}\right)^{\beta}\right] \quad \beta, \eta > 0; t \geq 0 \tag{4-2}$$

Where β is the shape parameter and η is the scale parameter.

The reliability function is expressed as follows:

$$R(t) = \int_t^{\infty} f(t)\, dt \tag{4-3}$$

Hence, the reliability function for Weibull distribution is presented as below:

$$\mathrm{R(t)} = \exp\left[-\left(\frac{t}{\eta}\right)^{\beta}\right] \tag{4-4}$$

Using Equations 4-2 and 4-4, the baseline hazard function (h_0) in Equation 4-1 is calculated as below:

$$h_0(t) = \frac{f(t)}{R(t)} \tag{4-5}$$

Thus, the Weibull baseline hazard function is presented as:

$$h_0(t) = (\beta/\eta)\,(t/\eta)^{\beta-1} \tag{4-6}$$

Substitution of equation 4-6 into equation 4-1 yields:

$$h(t;Z) = (\beta/\eta)(t/\eta)^{\beta-1} e^{\sum_1^m \gamma_i Z_i} \tag{4-7}$$

The conditional survival function for the PHM is calculated using equation 4-7:

$$R(t;\, Z) = exp\left[-\int_0^t h(t;Z)\, dt\right] = e^{-(\frac{t}{\eta})^{\beta} e^{\gamma_1 Z_1 + \gamma_2 Z_2}} \tag{4-8}$$

For this study cutting speed and feed rate are considered as the covariates of the model. It should be mentioned that values of cutting speed and feed rate were normalized in order to obtain a stable convergence of the weight factors. Thus, the normalized Z value is calculated such that the

corresponding value for the center point equals to zero. The related equations are presented below:

$$Z_1 = \frac{V - V_m}{\frac{(V_{max} - V_{min})}{2}} \quad (4\text{-}9)$$

$$Z_2 = \frac{f - f_m}{\frac{(f_{max} - f_{min})}{2}} \quad (4\text{-}10)$$

The model parameters ($\beta, \eta, \gamma_1, \gamma_2$) are calculated through the maximum likelihood algorithm (Banjevic et al., 2001). In this study, the PHM parameters are computed using Exakt software.

Tool Life formulation

Once the Proportional Hazards Model (PHM) is developed, the remaining time to each criterion can be obtained through calculating the Mean Residual Life (*MRL*) function, also called expected remaining life $e(T)$. In general, this function will provide us with the expected remaining survival life of a subject from any observation point, given that the subject has survived up to that observation point (Cook et al., 2007). Without considering the effect of covariates, the remaining life of a subject to time *T*, from the given time t_r, can be calculated as follows:

$$MRL\ (t_r) = \mathrm{e}(t_r) = E[\mathrm{T} - t_r | \mathrm{T} > t_r] = \frac{\int_{tr}^{\infty} t\, f(t) dt}{R(t_r)} - t_r \quad (4\text{-}11)$$

Accounting for the effect of covariates of our study, the mean residual life of inserts to the criterion i, where i=1,2 and 3, at any observation moment, t_r, can be calculated as follows:

$$MRL\ (t_r; \mathrm{Z}) = \frac{\int_{tr}^{\infty} t f_i(t,Z) dt}{R_i(t_r, Z)} - t_r \quad (4\text{-}12)$$

Since the goal of this study is to obtain the total sojourn time until the desired event, one should calculate the mean residual life for the insert, given that the observation time is equal to zero. Thus the formula for the total tool life spent in each state is presented below:

$$\text{Total tool life} = \frac{\int_{0}^{\infty} t\, f_i(t,Z) dt}{R_i(0, \mathrm{Z})} \quad (4\text{-}13)$$

It should be mentioned that the sojourn time spent in each state can also be calculated using equation 4-12 (Aramesh et al., 2014).

4.4 Results and discussions

The tool wear curves were obtained for all the experimental runs.

As an example, tool wear curves for the different replications of Run 4 are shown in Figure 4-1.

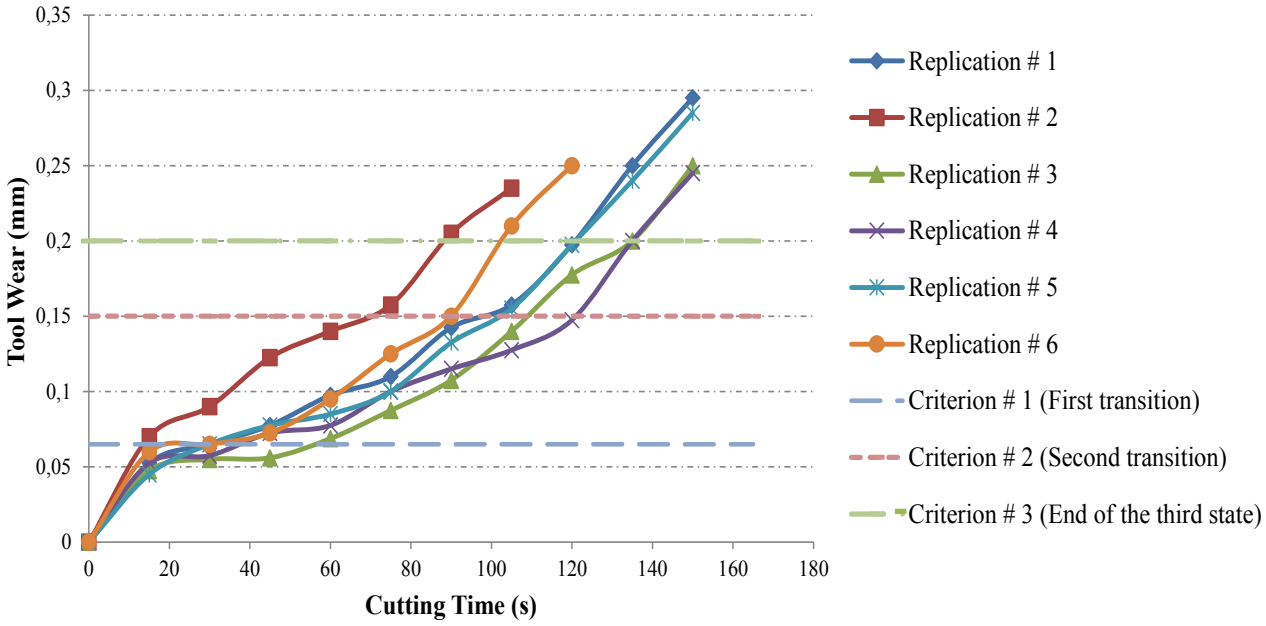

Figure 4-1: Tool life curves for v=80 m/min, f=0.35 mm/rev and a_p= 0.2 mm

The evolutions of the tool wear rates (curve slopes) were inspected for each replication of each run. The tool wear values associated with the greatest changes in the wear rates were chosen as the first and second state criteria, which were found to be 0.065 ± 0.012 mm and 0.15 ± 0.015 mm, respectively, for all tested cutting conditions.

Figure 4-2 presents an example, showing the criteria for the three different replications of Run # 4.

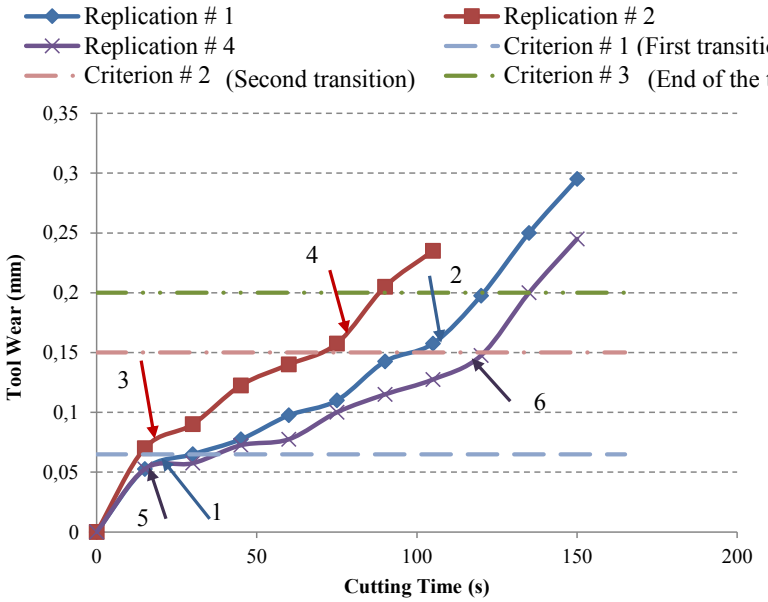

Point	Slope Change	Tool Wear
# 1	70 % Decrease	0.06 mm
# 2	167 % Increase	0.16 mm
# 3	71 % Decrease	0.071 mm
# 4	125 % Increase	0.16 mm
# 5	85 % Decrease	0.053 mm
# 6	162 % Increase	0.1465 mm

Figure 4-2: Points 1, 3 and 5 correspond to the greatest decrease in slope along the tool wear curves, indicating the first transition points; Points 2, 4 and 6 correspond to the greatest slope increase, indicating the second transition points for replications # 1, #2 and #4 respectively. The corresponding tool wear values are presented in the attached table.

The PHM parameters regarding each criterion, assigned for the different tool wear states, are computed separately and are presented in Table 4-4.

Table 4-4: Parameters of the PH model corresponding to each criterion

Parameter / Criterion	β	η	γ_1	γ_2
Criterion # 3 (third state)	7.749	536.853	8.19	2.343
Criterion # 2 (second state)	6.994	446.5	6.957	2.229
Criterion # 1 (first state)	2.847	122.4	2.005	1.11

4.4.1 The total time to reach the end of the third state

Implementing the PHM parameters associated with criterion # 3 ($i=3$) for the last state, the related hazard and reliability functions are calculated as follows:

$$h_3(t;Z) = \left(\frac{7.749}{536.853}\right)\left(\frac{t}{536.853}\right)^{6.749} e^{8.19\,Z_1 + 2.343\,Z_2} \quad (4\text{-}14)$$

$$R_3(t;Z) = e^{-\left(\frac{t}{536.853}\right)^{7.749} e^{8.19\,Z_1 + 2.343\,Z_2}} \quad (4\text{-}15)$$

Considering the PH model, the hazard function $h(t;Z)$ presented by equation 4-1 for the center point of the designed experiments will be reduced to the Weibull baseline hazard function. This is due to the normalized covariates being equal to zero at this point. Thus, the reliability functions calculated from the two models are expected to agree with each other at this point. The Weibull reliability function for the center point (Run # 5) is presented below:

$$R_{Weibull}(t) = e^{-\left(\frac{t}{535.8017}\right)^{9.693}} \quad (4\text{-}16)$$

As the first step to validate the model, the reliability functions versus machining time for the Weibull and PH models for the center point are superimposed in Figure 4-3.

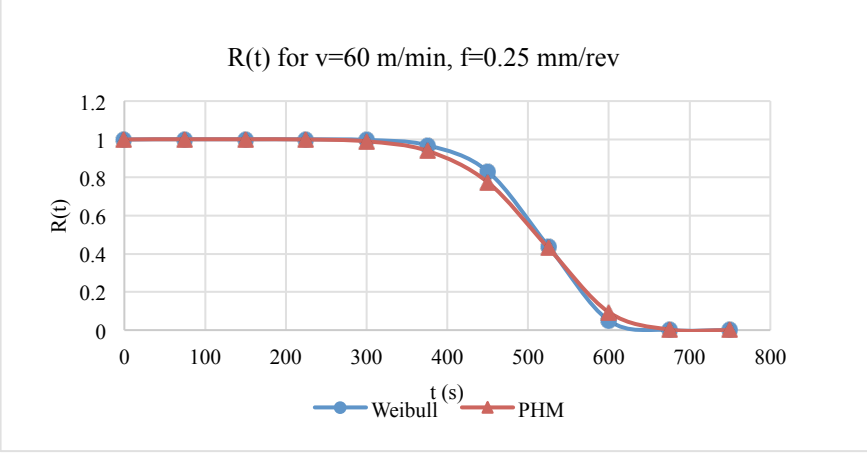

Figure 4-3: Reliability functions for v=60 m/min and f=0.25 mm/rev obtained from the Weibull model vs PHM

The results show that the two models are in a very good agreement with each other. The same trend was observed for all the selected experimental runs, as demonstrated in Figure 4-4 for v=80 m/min and f=0.15 and a_p= 0.2 mm.

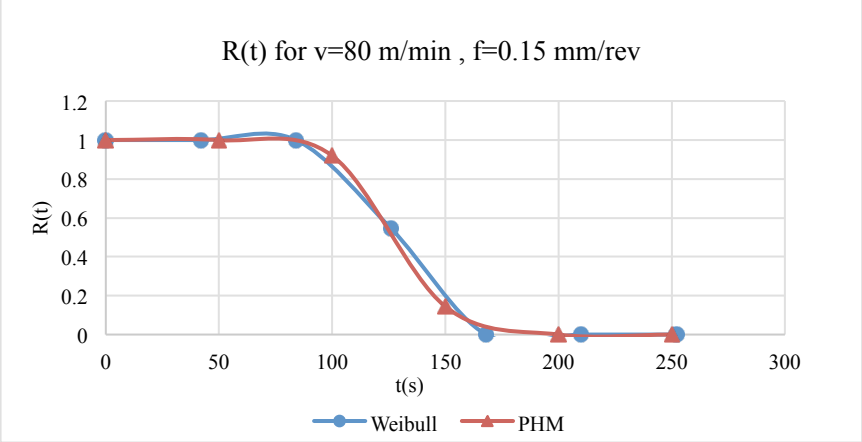

Figure 4-4: Reliability functions for v=80 m/min and f=0.15 mm/rev from the Weibull model vs PHM

Using the related hazard and reliability functions presented by equations 4-14 and 4-15, the final tool life, for any combination of cutting conditions within the defined range for this study, could be calculated using equation 4-13 for *i=3*. The corresponding equation is presented as follows:

$$\text{Total time to the end of the third state} = \frac{\int_0^\infty t\, f_3(t;Z)dt}{R_3(0;Z)} \qquad (4\text{-}17)$$

Tool lives of the defined cutting conditions (Run 1-5) were estimated from the model and compared with the experimental results. The difference between the predicted and mean measured tool lives for all experimental runs were found to be <8%, with 95% confidence interval, as shown in Figure 4-5.

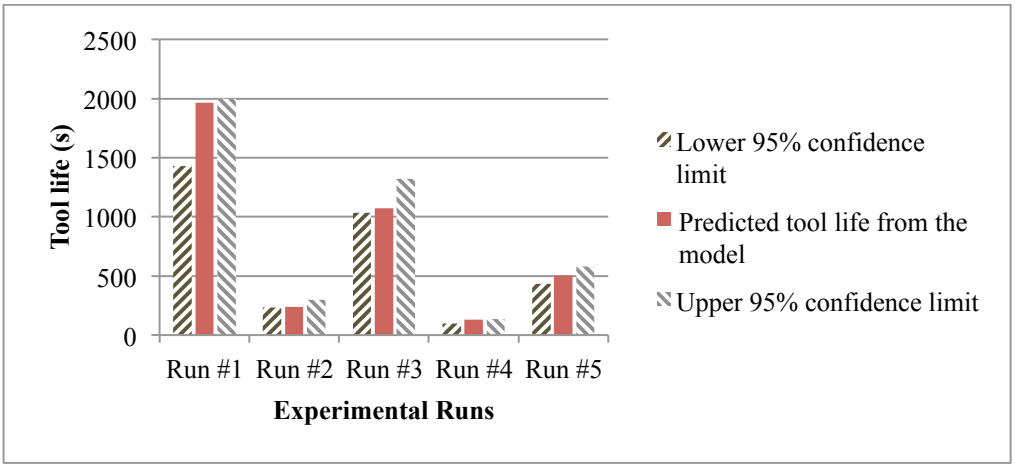

Figure 4-5: For each run of Table 4-2, the center bar of each run shows the estimated tool life calculated from the model. The 95% confidence limits are shown to each side of each center bar

As mentioned before, the model is capable of predicting the tool life under any combination of cutting conditions in the defined range. Thus, in order to validate the predictive performance of the model at different cutting conditions, an extra series of experiments were designed. The cutting conditions assigned for the validation runs are presented in Table 4-5.

Table 4-5: Designed experimental runs for the model validation

Parameter / Experimental	Number of Replications	Cutting speed (m/min)	Feed Rate (mm/ rev)	Depth of Cut (mm)
6	2	50	0.2	0.2
7	2	70	0.2	0.2
8	2	50	0.3	0.2
9	2	70	0.3	0.2

Two replications are conducted for each experimental run. Tool lives for the designed validation runs (Table 4-5) are calculated with the model and compared with the average value obtained from the experiments. The results, presented in Table 4-6, confirm that the model is highly efficient in predicting the tool life at any desired combination of cutting conditions, showing less than 9% error with the experimental results.

Table 4-6: Estimated total time to the end of the third state calculated from the model vs the average value obtained from the experiments for the validation runs

Experimental Run #	*Estimated total time from model [s]*	*Average time from the experiments [s]*	*Absolute Percent Error*
6	1000	1080	7.4
7	347	376	7.7
8	739	809	8.6
9	257	248	3.6

4.4.2 Between-state transition times

Following the same procedure presented in the previous section, the hazard and reliability functions for the second state are calculated as below:

$$h_2(t;Z) = \left(\frac{6.994}{446.5}\right)\left(\frac{t}{446.5}\right)^{5.994} e^{6.957\,Z_1 + 2.229\,Z_2} \quad (4\text{-}18)$$

$$R_2(t;Z) = e^{-\left(\frac{t}{446.5}\right)^{6.994} e^{6.957\,Z_1 + 2.229\,Z_2}} \quad (4\text{-}19)$$

Thus, the time to transition from state 2 to 3 can be calculated as below:

$$\text{Time to transition from state 2 to state 3} = \frac{\int_0^\infty t\, f_2(t;Z)dt}{R_2(0;\mathrm{Z})} \quad (4\text{-}20)$$

In order to validate the results of the model for estimating the transition times between the 2nd and 3rd states, they are calculated from the model for the validation runs (Run 6-9 presented in Table 4-5) and compared with the mean value obtained from the experiments. The results are presented in Table 4-7. As can be seen the results of the model are in an excellent agreement with the experimental results with less than 7 % error.

Table 4-7: Estimated transition times from state 2 to 3 calculated from the model vs the average values obtained from experiments for the validation runs

Experimental Run #	***Estimated transition time from model [s]***	***Average time from the experiments [s]***	***Absolute Percent Error***
6	805	842	4.3
7	298	320	6.8
8	586	600	5.3
9	217	220	1.36

The same procedure is performed to find the 1st to 2nd state transition times. One could find the hazard and reliability functions, as well as the related tool life formula for the first state in equations 4-21 to 4-23 respectively:

$$h_1(t;Z) = \left(\frac{2.847}{122.4}\right)\left(\frac{t}{122.4}\right)^{1.847} e^{2.005\,Z_1 + 1.11\,Z_2} \quad (4\text{-}21)$$

$$R_1(t;Z) = e^{-\left(\frac{t}{122.4}\right)^{2.847} e^{2.005\,Z_1 + 1.11\,Z_2}} \quad (4\text{-}22)$$

$$\text{Transition time from state 1 to state 2} = \frac{\int_0^\infty t\, f_1(t;Z)dt}{R_1(0;\mathrm{Z})} \quad (4\text{-}23)$$

The results for this transition time are also validated using the data from validation experimental runs. The validation results are presented in Table 4-8. It is shown that the model gives a good estimate for the first transition time with average of 16% error from the experimental data. Since the duration of the first state is very short, adding more measurements in this state could yield to higher accuracy of the results.

Table 4-8: Estimated transition times from state 1 to 2 calculated from the model vs the average values obtained from experiments for the validation runs

Experimental Run #	***Estimated transition time from model [s]***	***Average time from the experiments [s]***	***Absolute Percent Error***
6	188	173	8.6
7	93	78	19
8	127	158	19
9	63	75	16

As mentioned before, a 2^2 design with a center point with at least 5 replications of each run (total number of 28 sequential tests) were used in this study. Analysing the same data without the center point and with only 3 replications (total number of 12 sequential tests) gave around 10% additional error.

Finally, three-dimensional plots of estimated tool lives till the end of each wear state for different cutting conditions are presented in Figure 4-6 to Figure 4-8. The provided plots could be very useful in process planning and optimization of cutting parameters.

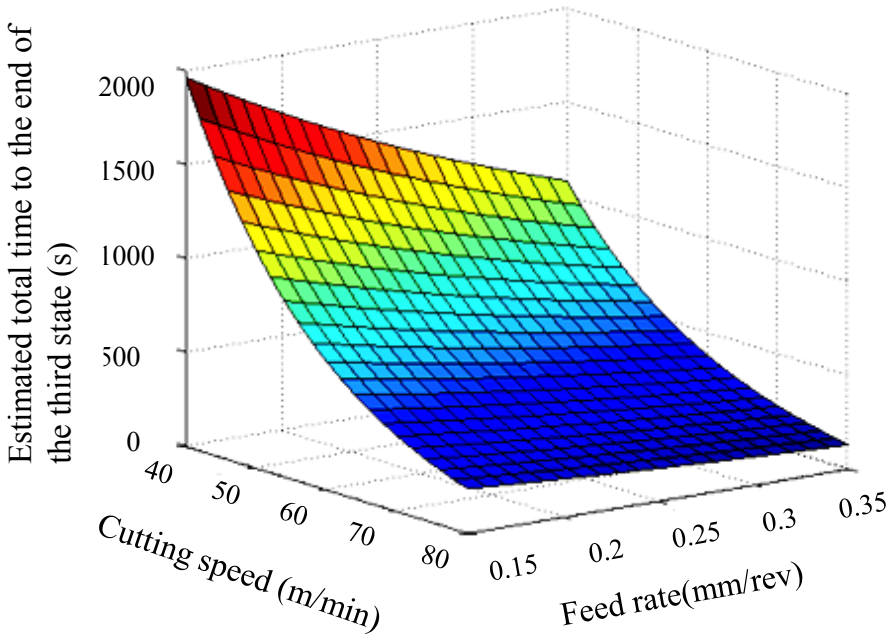

Figure 4-6: 3D plot of estimated total time to the end of the third state for different cutting speeds and feed rates

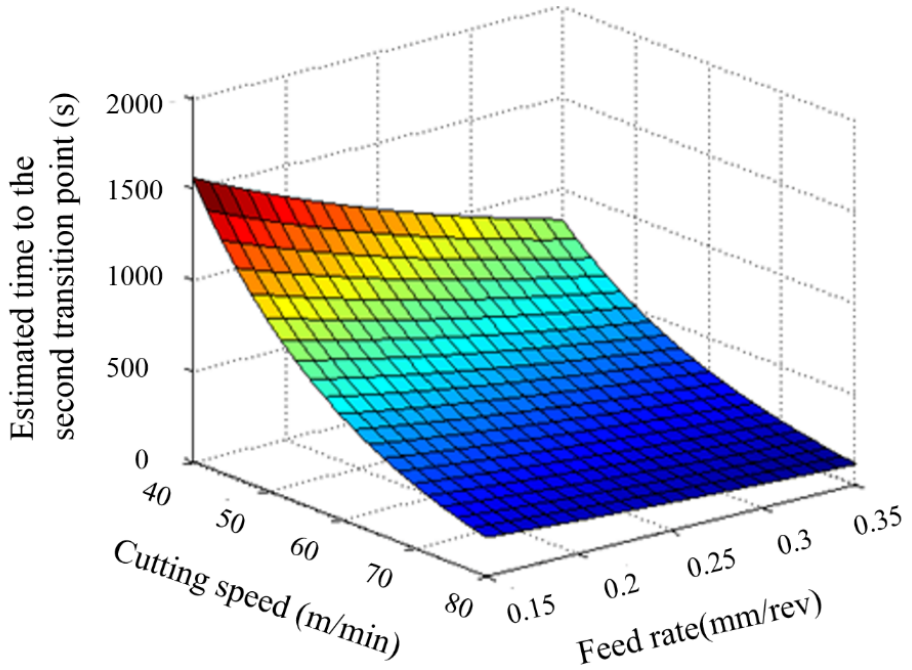

Figure 4-7: 3D plot of estimated time to the second transition point for different cutting speeds and feed rates

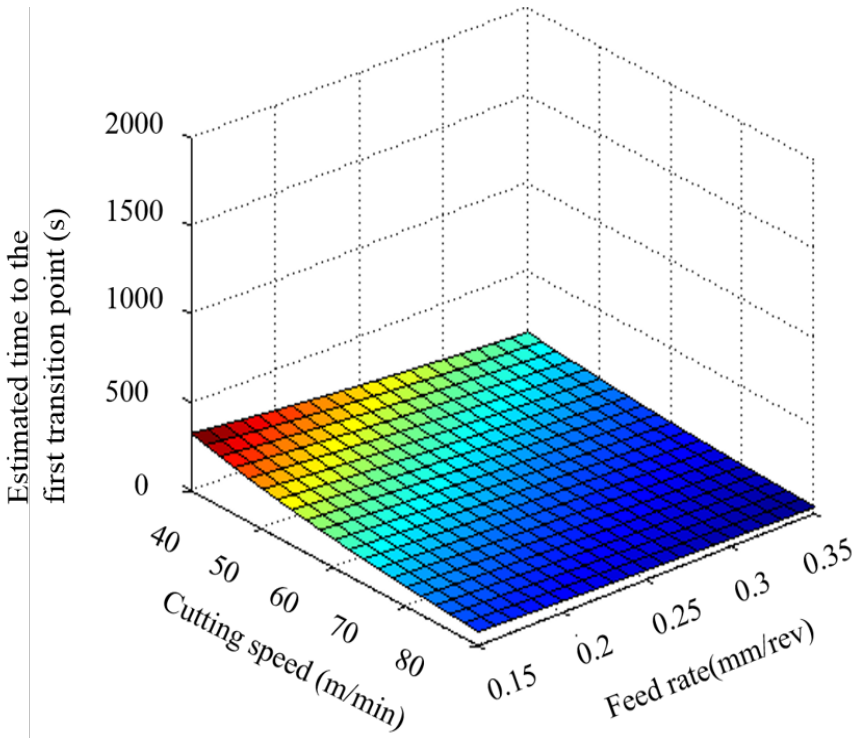

Figure 4-8: 3D plot of estimated time to the first transition point for different cutting speeds and feed rates

As shown above, a generalized function was separately developed for each state and was used to calculate the time elapsed to the end of each state. It was further observed that the covariate weight factors of cutting speed and feed rate (γ_1 and γ_2 presented in Table 4-4) follow an ascending pattern from state 1 to state 3, suggesting that the contribution of cutting speed and feed rate on the tool wear increased during the cutting process. Furthermore, the results showed that the ratio of cutting speed contribution over the feed rate was the least ($\gamma_1 / \gamma_2 \approx 1.8$) for the first state of tool wear and was gradually increased to around 3.5 for the third state.

The carbide tools used in this study, show the typical evolution of tool wear from temperature-independent mechanisms in the beginning of machining to temperature-dependent ones at the end of the process (Knight et al., 2005; Milton Clayton Shaw, 1984). At the first state of tool wear, the dominant wear mechanisms are mechanical, such as tool edge deformation, chipping, etc., which are considered as temperature-independent mechanisms. Furthermore, the cutting tool is very sharp and the contact area between the tool and workpiece is very small. The result is very high contact stresses. Therefore, tool wear rate is very high in this region, and less dependent on the cutting speed. As the cutting advances and the contact area increases (at the first transition

point), the wear rate drops considerably and the second state begins. In this state temperature-dependent mechanisms such as diffusion and other chemical mechanisms are further involved. As the temperature rises, the second transition point is reached and material softening occurs, resulting in the increase of tool wear rate (Milton Clayton Shaw, 1984). Since in this state, the dominant wear mechanisms are all temperature-dependent, cutting speed becomes increasingly more important than feed rate.

4.5 Conclusions

A new approach based on a proportional hazards model (PHM) with a Weibull baseline is developed in order to estimate all the progressive states of tool wear under different cutting conditions during turning of Ti-MMCs. Employing the PHM as the predictive model for tool life estimation, the effects of aging and cutting parameters are taken into consideration. In the machining process, the effect of machining time is not limited to the cumulative tool wear over time. As the machining process advances, evolution of different temperature-dependent wear mechanisms at each state of tool wear significantly affects the kinetics of the wear process. In this study, each state of the tool wear process is analyzed as an individual case, possessing its own proper criteria. An adjusted function is derived and used for calculating each between-states transition time. Thus, the evolution of different phenomena occurring at each state is also reflected in the model. Accounting for all these factors, accurate results were obtained from the model. The results of the model were validated using experimental data from different cutting conditions within the defined range. The measured and predicted tool lives are in excellent agreement.

4.6 Acknowledgement

The authors would like to thank Canadian Network for Research and Innovation in Machining Technology (CANRIMT) for their financial support, the Dynamet Technology Inc. for providing us with the workpiece material, and Seco Tools for supplying the cutting inserts. The Aerospace Structures, Materials and Manufacturing Laboratory of the National Research Council Canada (NRC) is acknowledged for its valuable contribution, support and the use of its equipment.

4.7 References

Aramesh, M., Shaban, Y., Balazinski, M., Attia, H., Kishawy, H. A., & Yacout, S. (2014). Survival Life Analysis of the Cutting Tools During Turning Titanium Metal Matrix Composites (Ti-MMCs). *Procedia CIRP, 14*(0), 605-609.

Astakhov, V. P. (2006). *Tribology of Metal Cutting*: Elsevier.

Banjevic, D., Jardine, A. K. S., Makis, V., & Ennis, M. (2001). A control-limit policy and software for condition-based maintenance optimization. *INFOR, 39*(1), 32-50.

Braun, W. J., Miller, M. H., & Schultze, J. F. (1999). The development of machine-tool force reconstruction for wear identification. Paper presented at the *Proceedings of the 17th International Modal Analysis Conference*.

Cook, R. J., & Lawless, J. F. (2007). *The statistical analysis of recurrent events*: Springer.

Das, S., Chattopadhyay, A., & Murthy, A. (1996). Force parameters for on-line tool wear estimation: a neural network approach. *Neural networks, 9*(9), 1639-1645.

Davim, J. P., & Astakhov, V. P. (2008). Tools (Geometry and Material) and Tool Wear *Machining* (pp. 29-57): Springer London.

Devor, R. E., Anderson, D. L., & Zdeblick, W. J. (1977). Tool life variation and its influence on the development of tool life models. *Journal of Engineering for Industry, Transactions of the ASME, 99 Ser B*(3), 578-584.

Dimla Snr, D. E. (2000). Sensor signals for tool-wear monitoring in metal cutting operations—a review of methods. *International Journal of Machine Tools and Manufacture, 40*(8), 1073-1098. doi: http://dx.doi.org/10.1016/S0890-6955(99)00122-4

Feng, D., Lijuan, Z., & Zhengjia, H. (2011). On-line monitoring for cutting tool wear reliability analysis. Paper presented at the *2011 9th World Congress on Intelligent Control and Automation (WCICA 2011), 21-25 June 2011*, Piscataway, NJ, USA.

Hitomi, K., Nakamura, N., & Inoue, S. (1978). reliability analysis of cutting tools (78 - WA/PROD-9).

Huang, S., Tan, K., Wong, Y., De Silva, C., Goh, H., & Tan, W. (2007). Tool wear detection and fault diagnosis based on cutting force monitoring. *International Journal of Machine Tools and Manufacture, 47*(3), 444-451.

Kannan, S., Balazinski, M., & Kishawy, H. (2006). Flank wear progression during machining metal matrix composites. *Journal of Manufacturing Science and Engineering, 128*(3), 787-791.

Kishawy, H. A., Kannan, S., & Balazinski, M. (2005). Analytical modeling of tool wear progression during turning particulate reinforced metal matrix composites. *CIRP Annals - Manufacturing Technology, 54*(Compendex), 55-58.

Kleinbaum, D. G., & Klein, M. (1996). *Survival analysis*: Springer.

Klim, Z., Ennajimi, E., Balazinski, M., & Fortin, C. (1996). Cutting tool reliability analysis for variable feed milling of 17-4PH stainless steel. *Wear, 195*(1-2), 206-213. doi: 10.1016/0043-1648(95)06863-5

Knight, W. A., & Boothroyd, G. (2005). *Fundamentals of metal machining and machine tools* (Vol. 69): CRC Press.

Lee, J., Kim, D., & Lee, S. (1998). Statistical analysis of cutting force ratios for flank-wear monitoring. *Journal of Materials Processing Technology, 74*(1), 104-114.

Lin, W. (2008). The reliability analysis of cutting tools in the HSM processes. *Archives of Materials Science and Engineering, 30*(2), 97-100.

Liu, H., & Makis, V. (1996). Cutting-tool reliability assessment in variable machining conditions. *IEEE Transactions on Reliability, 45*(4), 573-581. doi: 10.1109/24.556580

Mamalis, A., Kundrak, J., & Horvath, M. (2002). Wear and tool life of CBN cutting tools. *The International Journal of Advanced Manufacturing Technology, 20*(7), 475-479.

Marksberry, P., & Jawahir, I. (2008). A comprehensive tool-wear/tool-life performance model in the evaluation of NDM (near dry machining) for sustainable manufacturing. *International Journal of Machine Tools and Manufacture, 48*(7), 878-886.

Martin, K. (1994). A review by discussion of condition monitoring and fault diagnosis in machine tools. *International Journal of Machine Tools and Manufacture, 34*(4), 527-551.

Mazzuchi, T. A., & Soyer, R. (1989). Assessment of machine tool reliability using a proportional hazards model. *Naval Research Logistics, 36*(6), 765-777.

Negishi, H., K. Aoki. (1976). Investigations on reliability of carbide cutting tools. *Precis Machining, 42*(6), 578-589.

Patiño Rodriguez, C. E., & Francisco Martha de Souza, G. (2010). Reliability concepts applied to cutting tool change time. *Reliability Engineering & System Safety, 95*(8), 866-873. doi: http://dx.doi.org/10.1016/j.ress.2010.03.005

Ravindra, H., Srinivasa, Y., & Krishnamurthy, R. (1993). Modelling of tool wear based on cutting forces in turning. *Wear, 169*(1), 25-32.

Salonitis, K., & Kolios, A. (2014). Reliability assessment of cutting tool life based on surrogate approximation methods. *International Journal of Advanced Manufacturing Technology, 71*(5-8), 1197-1208. doi: 10.1007/s00170-013-5560-2

Shaw, M. C. (1984). *Metal cutting principles*: Clarendon press Oxford.

Sikdar, S. K., & Chen, M. (2002). Relationship between tool flank wear area and component forces in single point turning. *Journal of Materials Processing Technology, 128*(1), 210-215.

Tail, M., Yacout, S., & Balazinski, M. (2010). Replacement time of a cutting tool subject to variable speed. *Proceedings of the Institution of Mechanical Engineers, Part B (Journal of Engineering Manufacture), 224*(B3), 373-383. doi: 10.1243/09544054jem1693

Taylor, F. W. (1907). On the art of cutting metals. Paper presented at the *Annual meeting in New York*.

Umbrello, D., Hua, J., & Shivpuri, R. (2004). Hardness-based flow stress and fracture models for numerical simulation of hard machining AISI 52100 bearing steel. *Materials Science and Engineering: A, 374*(1–2), 90-100. doi: http://dx.doi.org/10.1016/j.msea.2004.01.012

Wager, J. G., & Barash, M. M. (1971). Study of the Distribution of the Life of HSS Tools. *Journal of Manufacturing Science and Engineering, 93*(4), 1044-1050. doi: 10.1115/1.3428041

Wang, K.-S., Lin, W.-S., & Hsu, F.-S. (2001). A new approach for determining the reliability of a cutting tool. *The International Journal of Advanced Manufacturing Technology, 17*(10), 705-709.

Xuan-Troung, D., R. Mayer, M. Balazinski. (2014, November 14-20, 2014). Chaotic Tool wear during machining of titanium metal matrix composites (TiMMCs). Paper presented at the *2014 ASME International Mechanical Engineering Congress and Exposition*, Montreal, Canada.

Chapter 5 ARTICLE 4: ESTIMATING THE REMAINING USEFUL TOOL LIFE OF WORN TOOLS UNDER DIFFERENT CUTTING CONDITIONS: A SURVIVAL LIFE ANALYSIS DURING TURNING OF TITANIUM METAL MATRIX COMPOSITES (TI-MMCS)

M. Aramesh, H. Attia, H. A. Kishawy, M. Balazinski *submitted to the CIRP Journal of Manufacturing Science and Technology,* 2015.

ABSTRACT

Utilizing the full tool life capacity of cutting tools has always been a concern, due to the considerable costs associated with suboptimal replacement of tools. Reliable reuse of worn inserts could significantly reduce machining costs. This study aims at estimating the remaining useful life of worn cutting inserts under multiple cutting conditions during turning of Ti-MMCs, using the actual tool wear value of the worn tool as the input data. A proportional hazards model with a Weibull baseline is developed. Maximum flank wear length at the transition point between the second and third state of tool wear is chosen as the failure criteria. Tool wear, cutting speed and feed rate are considered as the covariates of the model. The reliability and hazard functions are calculated from the model and are utilized to obtain the mean residual life of inserts under different cutting conditions and tool wear levels. The accuracy of the model is validated using experimental data. The results confirmed the validity and reliability of the model.

5.1 Introduction

Significant costs are associated with inaccurate estimations of tool lives. It has been reported that in the USA, only 38% of the time tools are utilized up to their full capacity, which has been estimated to have an impact up to $ 10 billion per year on the US industry alone (Jawahir et al., 2007; Umbrello et al., 2004a). This necessitates the development of reliable methodologies for tool life estimation. Safe and reliable reuse of worn tools could also contribute significantly to cost reduction and productivity increase. Thus, it is highly economical to establish methodologies for estimating the remaining useful life of worn inserts.

Different mathematical and experimental models have been proposed for tool life estimation. Majority of the proposed models were developed based on the force monitoring methodologies, benefiting from the correlation between the cutting forces and tool wear (Bhattacharyya et al., 2007). Moreover, numerous studies have been performed using other machining data such as workpiece dimension, surface roughness, tool temperature, vibration, acoustic emission, texture features of the machined images, cutting power and machining induced stresses (Bonifacio et al., 1994; Cuppini et al., 1990; de Agustina et al., 2014; Dimla Snr, 2000; Gadelmawla et al., 2014; Liang et al., 1989; Mathew, 1989; Wanigarathne et al., 2005; Wong et al., 2004; Zhou et al., 1995).

After the recognition of the probabilistic nature of the tool were by DeVor (DeVor et al., 1977), several models were proposed for evaluating the reliability of cutting inserts (Hitomi et al., 1978; Klim et al., 1996; Negishi, 1976; Patiño Rodriguez et al., 2010). Since these models were developed based on the theory of probability, they account for errors originated from the non-homogeneities of the tool and work-piece materials. This could be an important advantage for modeling the tool life when machining particle reinforced composites, for which the distribution of reinforcing particles is responsible for considerable variability of the tool wear data.Proportional hazards model (PHM), which is mostly used in medical applications, has been introduced by Mazzuchi (Mazzuchi et al., 1989) in machining and has been used for reliability assessment of cutting inserts and developing methodologies for tool replacement (Feng et al., 2011; Liu et al., 1996; Tail et al., 2010). Aramesh et al. (Aramesh et al., 2015), used a PHM to estimate the total tool life in addition to the transition times between different states of tool wear, under variable cutting conditions. The advantage of this model over other statistical models is that it could account for effect of the aging and cumulative tool wear, in addition to the effect of cutting conditions. Furthermore, different variables including controllable variables (such as cutting conditions in machining) and monitoring variables (such as tool wear and surface roughness) could be added to the model.

Very limited work has been done to calculate the remaining life of inserts (Ao et al., 2010; Baruah et al., 2005; Gokulachandran et al., 2012; Karandikar et al., 2013; Wang et al., 2012). However, to the best of our knowledge, so far no model has been introduced implementing the tool wear itself as a variable in the model in addition to the cutting conditions, thereby being able to predict the remaining life of *worn* inserts based on the current tool wear value. Employing a

PHM in this study, tool wear was considered as the monitoring variable in addition to the controllable variables, cutting speed and feed rate. Thus, the valuable information about the remaining useful life of worn inserts under any untested cutting conditions and tool wear levels were obtained. This could be considered as the significant practical advantage of this model over the previous models, since it is capable of estimating the remaining life of any used tool, regardless of its usage history, with a simple tool wear measurement.

5.2 Experiment set up

A Cylindrical bar of Ti-6Al-4V alloy matrix reinforced with 10-12% volume fraction of TiC particles were used as the work-piece material for this study. Dry machining tests were conducted on a 5-axis Boehringer NG 200 CNC turning center. TH1000 coated carbide inserts; TiSiN-TiAlN nano-laminate PVD (Physical Vapor Deposition) coated grade, with nose radius of 0.8 mm were utilized for the turning tests. During each test, tool wear was measured using an Olympus SZ-X12 microscope. The maximum flank wear length (VB_{Bmax}) was selected as the tool life criterion. Microstructural and elemental analyses were performed using JSM 7600 TFE Scanning Electron Microscopy (SEM) equipped with an Oxford Energy-Dispersive X-ray Spectroscopy (EDX). Primary backscattered electron (BSE) imaging was performed with SEM for investigating the microstructure.

5.3 Methodology

Survival analysis is a statistical technique for modeling the time till the occurrence of an event (s) of interests (eg. a pre-defined VB_{Bmax} in machining), and to find the relationship of this time to different variables of a study (eg. cutting conditions in machining). Depending on the purpose of the study, the event, and covariates of the study should be defined. Usually, for the engineering purposes, the event is defined as the failure (Kleinbaum et al., 1996). After defining the failure criterion and covariates of the study, sequential machining tests should be performed based on the design of experiments, and continued till the defined failure criterion is reached. The collected experimental data will be used to establish the specific data layout necessary for the development of the survival model. The data consists of important information such as the time to the desired event (survival time) and the event status (failure status in our case) at any observation (Kleinbaum et al., 1996). In section 5.3.1, the experimental procedure required to

establish the data layout for the proportional hazards model (PHM), used in this study, is explained. Once the required data is collected, the parameters of the proportional hazards model (PHM) will be estimated, using EXAKT software. Reliability, hazard functions will be obtained and used to calculate the mean residual life of inserts till failure, using Mean Residual Life (MRL) function. The required statistical procedure is explained in section 5.3.2. At the end, the results from the model were validated with the experimental results. The experimental and statistical results are presented in section 5.4. The sequential steps required for the development of PH model are presented in Figure 5-1. The complete procedure for tool life estimation of *new* tools (without considering the tool wear as a covariate) under different cutting conditions is explained in our previous work (Aramesh et al., 2015).

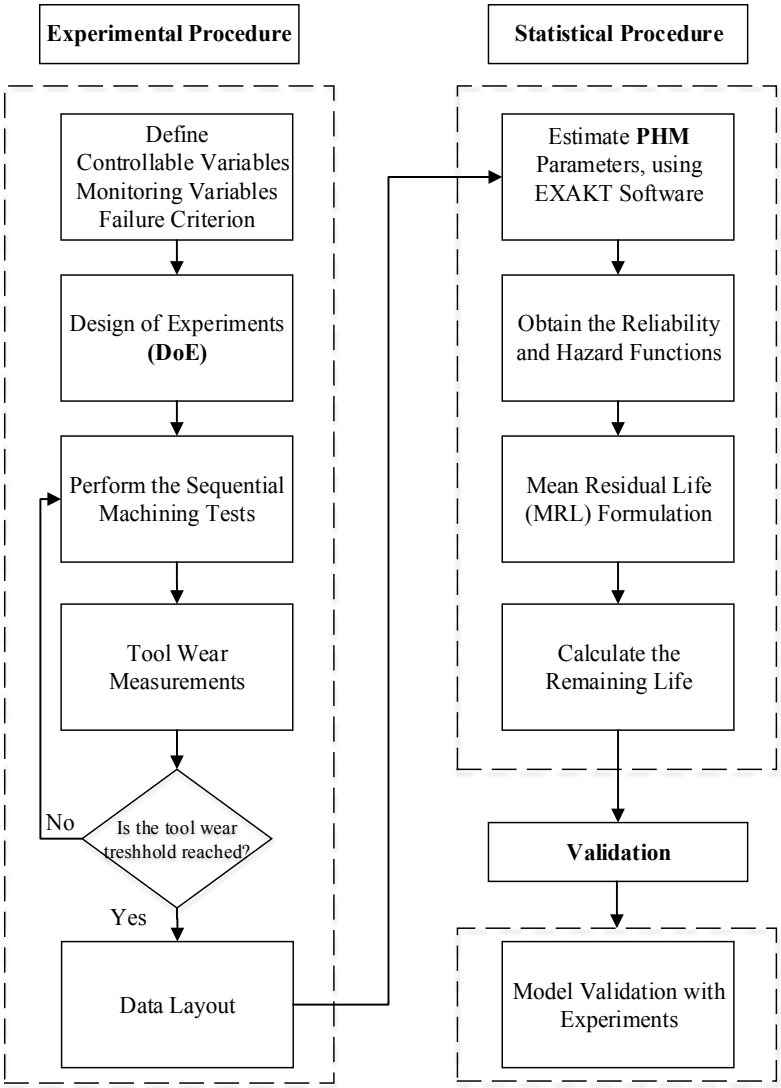

Figure 5-1: Sequence of steps required for calculating the remaining tool life via PHM

5.3.1 Experimental procedure

For the machining processes, the failure is usually defined, in terms of the permissible maximum tool wear. The tool wear curve demonstrates three states; initial, steady and rapid states of tool wear. Severe vibration, temperature and cutting forces are induced at the third (rapid) state. Thus, during any machining process it is highly recommended not to enter this state. The tool wear associated with the transition between the second and third state is often regarded as the tool life criterion (Astakhov, 2006). This criterion, which is also called the permissible tool wear VB_{BC}, is adopted for this study, based on the experimental results.

Variables (also called covariates) of the study could be classified as controllable and uncontrollable (monitoring) ones. Controllable covariates are those that can be controlled during a process such as cutting speed, feed rate and depth of cut in machining. Monitoring or uncontrollable covariates mostly change in response to the controllable ones and are monitored during a process. They have influence on the process but cannot be adjusted during a process, such as surface roughness and tool wear in machining process. In this study, cutting speed and feed rate are considered as the controllable covariates of the study, and tool wear is considered as the monitoring covariate.

The design of experiments consists of a 2^2 design enhanced with an additional center point. The cutting conditions are selected based on the recommendations of the tool supplier. The corresponding experimental runs are presented in Table 5-1. Minimum of 5 replications were performed for each run, using a new tool. It should be mentioned that the experiments were performed randomly in order to avoid experimental bias.

Table 5-1: Cutting parameters for each experimental run

Run # \ Cutting Parameter	Number of Replications	Cutting Speed (m/min)	Feed Rate (mm/ rev)	Depth of Cut (mm)
1	5	40	0.15	0.2
2	5	80	0.15	0.2
3	6	40	0.35	0.2
4	6	80	0.35	0.2
5	6	60	0.25	0.2

In this study, VB_{Bmax} equal to 0.15 was found to be the best approximation for the second transition point (failure criterion) for all the cutting conditions, as will be seen in section 5.4. Five arbitrary levels are assigned to the monitoring covariate of this study, tool wear. Maximum tool flank wear length (VB_{Bmax}) equal to 0, 0.08, 0.1, 0.12, 0.14 mm are chosen as the different levels.

For each insert, an approximate number of 8 sequential turning tests (observation) were performed till the maximum pre-defined tool flank wear length threshold (VB_{Bmax}=0.15) was reached. The tool wear is measured after each observation. After performing all the experiments and collecting all the data, the specific data layout for the survival analysis, should be prepared. The basic layout is shown Table 5-2, where each raw corresponds to a single observation, for which *i* corresponds to the run number, and *n* represents the replication number.

Table 5-2: Basic data layout for the survival analysis (Kleinbaum et al., 1996)

	Survival Time	*Failure Status*	*Variables (Covariates)*		
Tool ID # (Run-Replication)	t	δ	X_1 *(Cutting Speed)*	X_2 *(Feed Rate)*	$X3$ *(Tool Wear)*
i-1	*0*	*B*	X_1	X_2	X_3
i-2	t_1	*IN*	X_1	X_2	X_3
.	.	.	.	.	.
.	.	.	.	.	.
i-n	t_m	*F*	X_1	X_2	X_3

Information regarding the survival time and failure status are provided in the second and third columns. The failure status of each observation was identified in the data layout, using the following terminology: B-event, which stands for the *beginning* of the observation; IN-event, which stands for the *inspection* process, meaning that failure has not occurred yet; and F-event, which indicates the occurrence of the *failure* event at m^{th} observation. The corresponding survival time (the time to the event) for each event is given in the second column.

5.3.2 Statistical Procedure

Proportional Hazards Model (PHM), which is a common model for survival data analysis, is developed based on the fact that the failure rate of the desired random variable (time to failure) is dependent on *time*, which reflects the aging phenomenon, in addition to *covariates* which describe the operating environment (Kleinbaum et al., 1996; Mazzuchi et al., 1989).

The survival function R(t), and the hazard function, h (t), are considered as the fundamental quantitative functions for any survival analysis. The survival function is defined as the probability of surviving at least to time t, and the hazard function provides the instantaneous potential per unit time for occurrence of an event, knowing that the individual has survived up to time t (Kleinbaum et al., 1996).

The hazard function which is given in Equation 5-1, is expressed as a product of two terms: the baseline failure rate, $h_0(t)$, which is only a function of time; and the second part, $e^{\sum_1^m \gamma_i Z_i}$, which is a positive function of model covariates Z_i with weight factors of γ_i.

$$h(t;Z) = h_0(t)\, e^{\sum_1^m \gamma_i Z_i} \qquad m \equiv \text{number of covariates} \tag{5-1}$$

Different parametric models such as Weibull, lognormal and normal distributions could be used in the baseline function for modeling the tool life data. In this study, Weibull distribution is chosen due to its flexibility, thus adjustability for different aging scenarios (Hitomi et al., 1978; Mazzuchi et al., 1989; Negishi, 1976; J. G. Wager et al., 1971; K.-S. Wang et al., 2001). The Weibull baseline hazard function is presented as (Kleinbaum et al., 1996):

$$h_0(t) = (\beta/\eta)\,(t/\eta)^{\beta-1} \qquad \beta, \eta > 0; t \geq 0 \tag{5-2}$$

Where β is the shape parameter and η is the scale parameter.

Replacing the corresponding Weibull hazard function from equation 5-2, equation 5-1 is reduced to:

$$h(t;Z) = (\beta/\eta)(t/\eta)^{\beta-1} e^{\sum_1^m \gamma_i Z_i} \tag{5-3}$$

There is a direct relationship between the hazard and reliability functions. The conditional survival function for the PHM could be calculated using the following equation:

$$R(t;\ Z) = \ exp\left[-\int_0^t h(t;Z)\ dt\right] = \ e^{-(\frac{t}{\eta})^{\beta} e^{\gamma_1 Z_1+\gamma_2 Z_2+\gamma_3 Z_3}} \quad (5\text{-}4)$$

The failure density function $f(t;\ Z)$ is presented in equation 5-5. This function describes the failure behaviour over time; and will be used for the calculation of residual life.

$$f(t;Z) = \frac{-dR(t;\ Z)}{dt} = \ \frac{\beta}{\eta}\ \left(\frac{t}{\eta}\right)^{(\beta-1)}\ e^{-(\frac{t}{\eta})^{\beta} e^{\gamma_1 Z_1+\gamma_2 Z_2+\gamma_3 Z_3}} \quad (5\text{-}5)$$

The covariates are labelled as Z_1, Z_2 and Z_3 representing cutting speed, feed rate and tool wear respectively. The values of the covariates are normalized in order to obtain a stable convergence of the weight factors. The normalized Z values is calculated such that the corresponding value for a new tool at the center point equals to zero. The related equations are presented below:

$$Z_1 = \frac{V-V_m}{\frac{(V_{max}-V_{min})}{2}} \quad (5\text{-}6)$$

$$Z_2 = \frac{f-f_m}{\frac{(f_{max}-f_{min})}{2}} \quad (5\text{-}7)$$

$$Z_3 = \frac{W}{0.15} \quad (5\text{-}8)$$

Exakt software (Jardine et al., 1997), a computer package developed for conducting the survival analysis, is used in this study for calculating the parameters of the PH model (β,η,γ_1,γ_2,γ_3).

After developing the PH model, the last step is to calculate the remaining tool life. Mean Residual Life (MRL) function, also called expected remaining life $e(T)$, could provide us with the required information.

Given that an object has survived up to an observation point, the remaining survival life of the object from that observation point can be obtained, using MRL function (Cook et al., 2007). Considering the effect of covariates, the general formula for calculating the remaining life of a subject to a failure time t, from an arbitrary fixed given time t_r is:

$$MRL\ (t_r;Z) = \mathrm{e}(t_r;\mathrm{Z}) = \frac{\int_{t_r}^{\infty} t\ f(t;Z)dt}{R(t_r;Z)} - t_r \quad (5\text{-}9)$$

Since the total sojourn time from the beginning till failure is of interest, the observation point, t_r, is set equal to zero.

The probability density function $f(t; Z)$ and reliability function $R(t; Z)$ are calculated using equations 5-4 and 5-5 respectively.

5.4 Results and discussions

In order to define the value of VB_{Bmax} at the transition point between the second and third states of tool wear, the evolutions of tool wear rates were inspected for all the different replications performed at different cutting conditions. The tool wear values associated with the second greatest changes in the wear rate were obtained for all the experimental runs. It was found that the location of this point does not change considerably in terms of tool wear. The corresponding value of VB_{Bmax} was found equal to 0.15± 0.015 mm for almost all the conditions tested. As an example, the results for the four different conditions are presented in Figure 5-2.

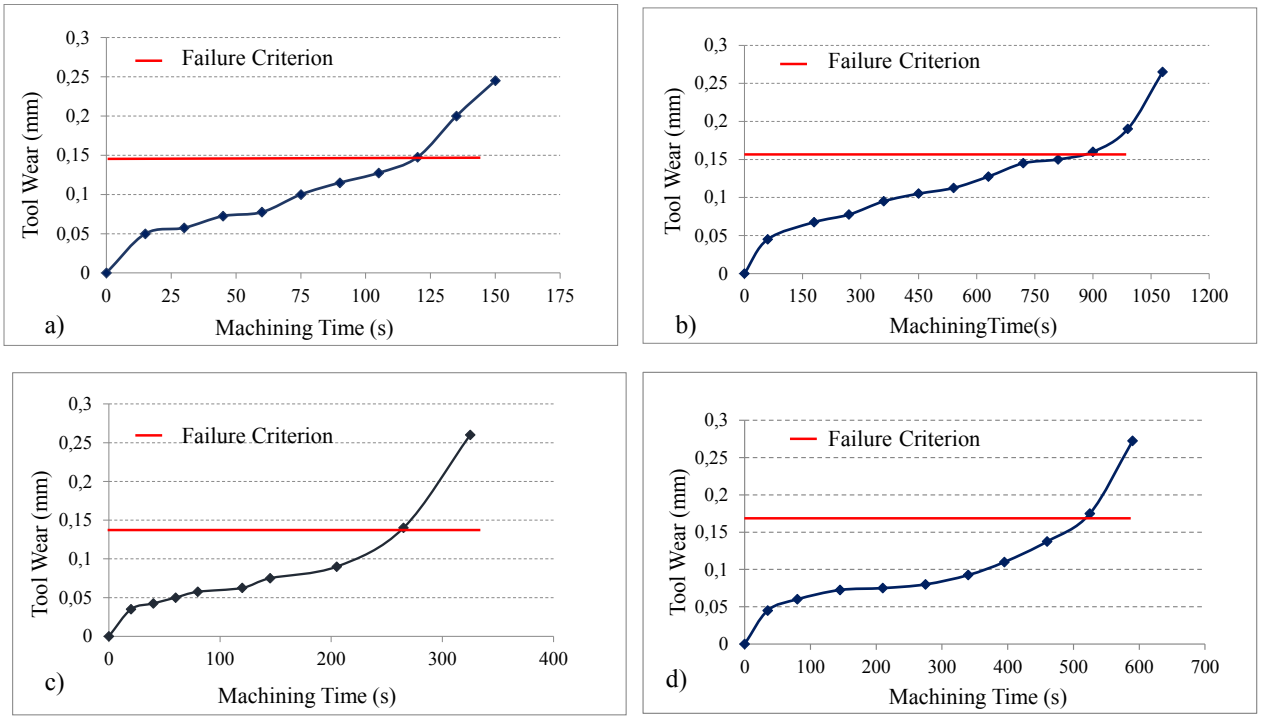

Figure 5-2: Tool wear curves and defined failure criterion for the cutting conditions:
a) V=80 m/min, f= 0.35 mm/rev, a_p= 0.2 mm; b) V=40 m/min, f= 0.35 mm/rev, a_p= 0.2 mm
c) V=80 m/min, f= 0.15 mm/rev, a_p= 0.2 mm; d) V=60 m/min, f= 0.25 mm/rev, a_p= 0.2 mm

It is worth mentioning that almost the same value of VB_{Bmax} was obtained for the second transition point during the roughing operation (V = 60 m/min, f = 1.5 mm/rev and a_p = 1.5 mm).

The tests were performed in our group (Xuan-Troung, 2014) on the same material with a coated carbide tool.

Typically, the VB_{Bmax} at the second transition point is found in the range of 0.15-1.00 mm depending on the machining operation type (Astakhov, 2013). The results of this study showed that this transition occurs at the lower limit of this range during machining of Ti-MMCs and the tool is worn out extremely fast after reaching this point. As an example, during roughing operation with cutting speed of 60 m/min, the tool was worn out up to VB_{Bmax} equal to 0.4 after just 20 seconds of machining beyond this point (Xuan-Troung, 2014).

At the second state of machining, in addition to the mechanical wear mechanisms, temperature-dependant mechanisms such as oxidation and diffusion are involved and progressed till the tool fails at the third state. Above the second transition point, material softening also occurs which results in further increase of the tool wear rate (Milton Clayton Shaw, 1984).

Titanium alloy matrix of the workpiece material inherits very low thermal conductivity around 5.8 W/m.K. Thus, extremely high local temperature is generated very fast in a very small area around the cutting edge. During machining of Ti-6Al-4V alloy, a temperature of around 1000 K at cutting speed of 75 m/min and temperatures of around 1400 K at higher cutting speeds were reported (Bhaumik et al., 1995).

High contact temperatures are known to result in high tool wear rates during the machining operation (Odelros, 2012). Temperature dependent wear mechanisms will be involved very fast even at low tool wear values. Figure 5-3-a, shows a SEM image of the tool flank wear ($VB_{Bmax}\approx0.15$mm). The corresponding oxygen map is presented in Figure 5-3-b. It can be seen this relatively low tool wear level, sever oxidation has occurred.

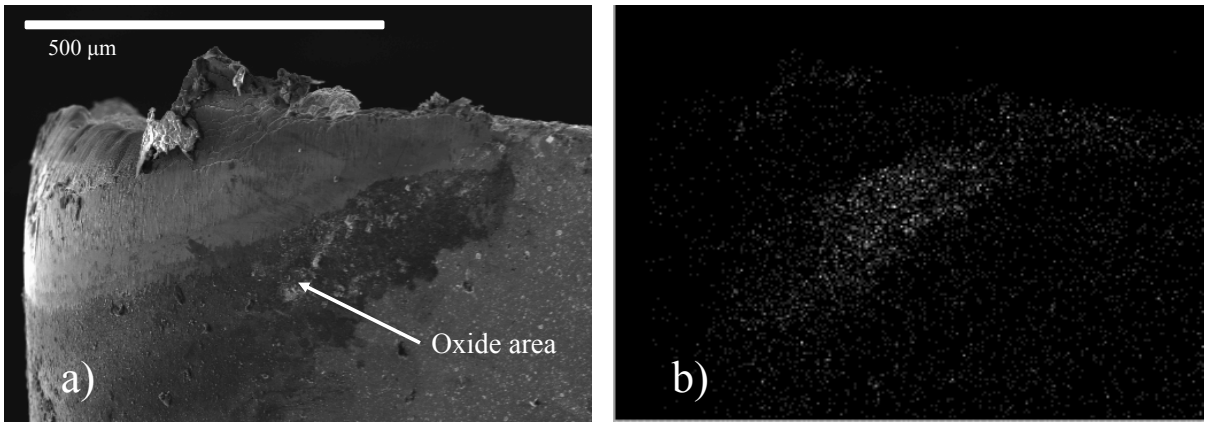

Figure 5-3: a) SEM image of the tool flank face after machining of Ti-MMCs at V= 80 m/min, f= 0.15, a_p= 0.2, with carbide tool (Seco TH1000); b) Corresponding oxygen map

Furthermore, once the strength of material is reduced at elevated temperatures, debonding of the reinforcing particles from the workpiece could also occur and result in high the abrasion wear. Holes and scratches on the tool flank surface as a result of the tool/particles interactions are shown in Figure 5-4.

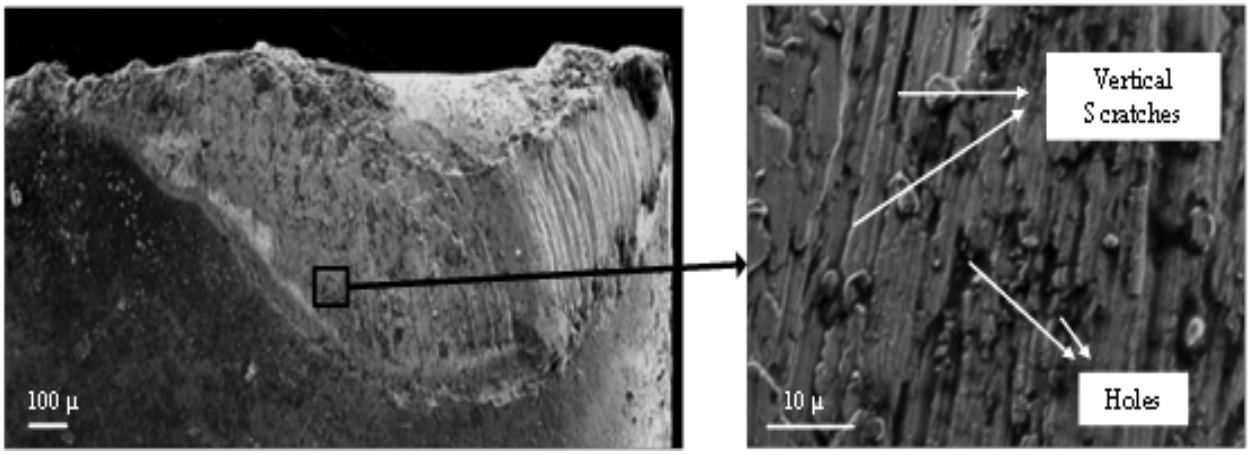

Figure 5-4: SEM image of the tool flank face, showing the holes and vertical scratches as the result of two body and three body abrasion wear mechanisms occurred during machining of Ti-MMCs at V= 60 m/min, f= 0.15, a_p= 0.2, with carbide tool (Seco TH1000)

Therefore, for this class of material it is very crucial not to pass this limit in order to avoid severe detriments to the tool and workpiece material. This further necessitates the development of a

reliable model capable of predicting this point under different cutting conditions especially for the worn tools.

The results of the machining tests for run #4 (Table 5-1) are presented in Figure 5-5.

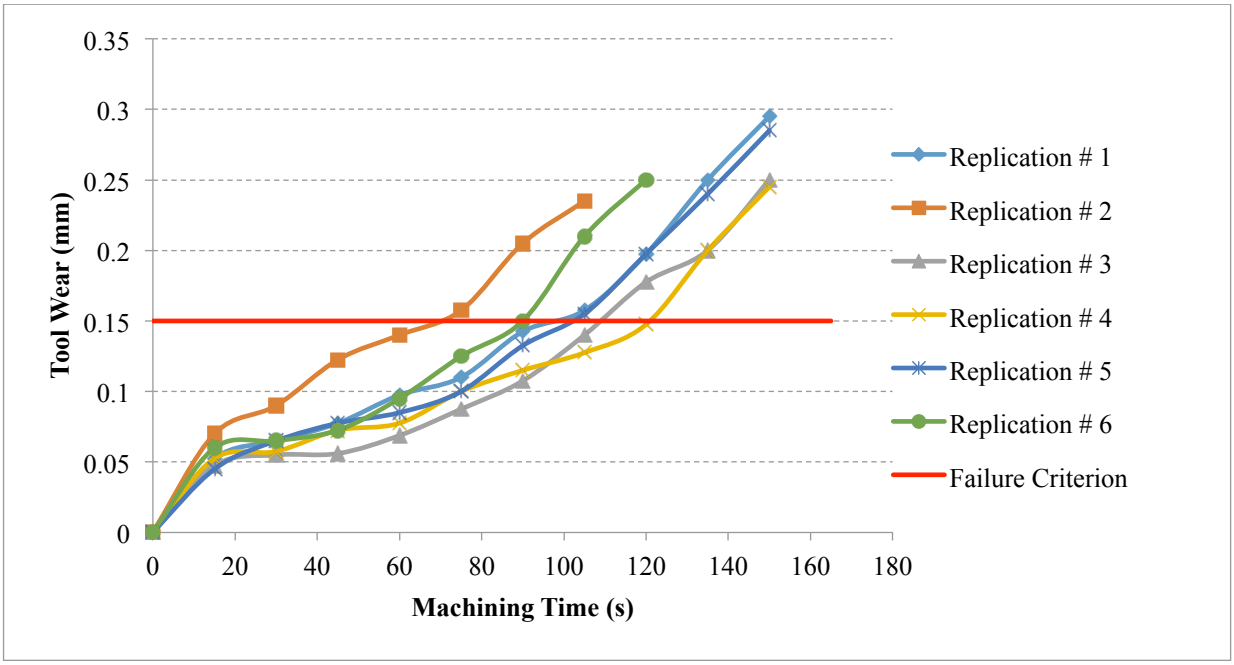

Figure 5-5: Tool life curve for different replications of Run # 4

As mentioned before, the last step of the experimental procedure is to construct the basic data layout for the PH model. As shown in Table 5-2, tool wear is not included as a variable in the design of experiments. Instead a stratagem is proposed in order to generate the related data for the data layout from the results of the existing design, without the need to add it as a separate variable in the design. Thus, almost equal data were generated while the number of experimental runs was almost reduced to half compared to the same design including the tool wear as a variable. As an example, the stratagem to produce the data layout for the run #4 is explained in this section.

The cutting time at different tool were levels in addition to the final time to failure (cutting time at VB_{Bmax}=0.15), were calculated for each replication, using the linear interpolation method. As an example, the related values for the first replication of run#4 are shown in Figure 5-6.

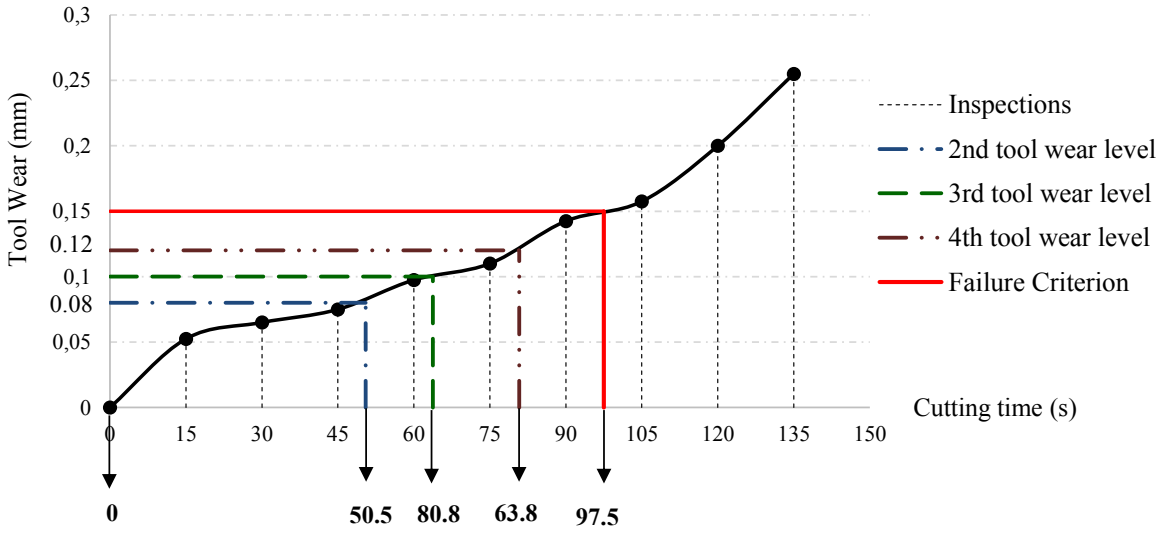

Figure 5-6: Calculated tool lives associated with different tool wear levels in addition to the time to failure, for the 1st replication of Run #4

The *failure status* at each observation in addition to the *survival time* were obtained, following the terminology explained section 5.3.1.

The B-event for the *new tool* always coincides with the cutting time equal to zero, followed by the inspection events at different observations to the final failure event (at tool wear equal to 0.15 mm).

The event statuses for the different observations for the first replication of Run # 4 at the first level of tool wear (new tool), are shown in Figure 5-7-a The survival times are equal to the observation times.

To obtain the data for the second tool wear level, the B-event should be shifted to the time associates with the tool wear (VB_{Bmax}) equal to 0.08 mm (50.5 s in this case). This has been shown in Figure 5-7-b. Therefore, the survival time to the inspections (IN-events) and final survival time to failure (F-event) should be calculated with regard to the new B-event. As an example, the survival time for the first inspection will be 60 -50.5=9.5 s in this case.

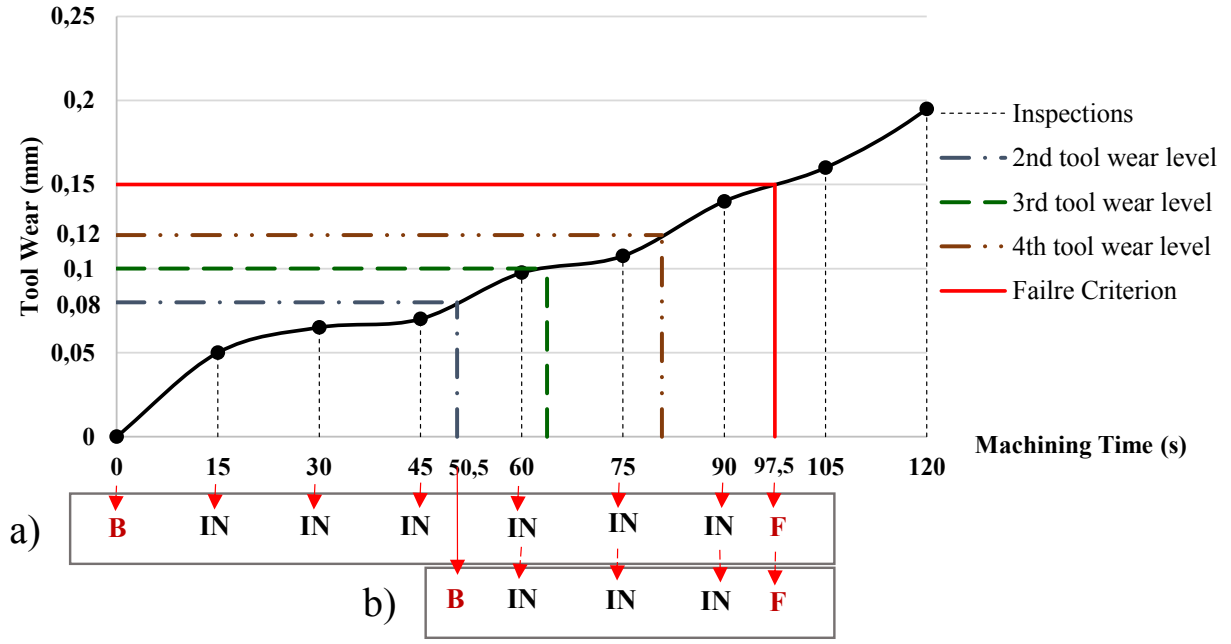

Figure 5-7: Event status for different observations of the Run #4 at the first level of tool wear 7-b) Event status for different observations of the Run #4 at the second level of tool wear

The same procedure was performed for all the other conditions (different levels of cutting conditions and tool wear) for all the experimental runs, in order to obtain the complete experimental data layout. The parameters of the PHM model developed for this data layout are calculated using EXAKT software and are presented in Table 5-3.

Table 5-3: Parameters of the PH model

Parameter	β	η	γ_1	γ_2	γ_3
Estimated value	2.858	483.1	3.378	0.841	5.047

Substituting the PH parameters in equations 5-3, to 5-5, the related hazard, reliability and probability density functions of this study were calculated. The remaining useful tool life till failure of any used tool with any tool wear and at any desired cutting condition could be calculated via inputting the calculated reliability and its corresponding probability density function in equation 5-9.

The model is capable of predicting the remaining life of inserts at any desired cutting conditions and at any desired tool wears level. In order to visualize the results in a 3-D plot, the remaining

life versus cutting speed and feed rate is plotted separately for four different arbitrary tool wear levels. The results are shown in Figure 5-8:

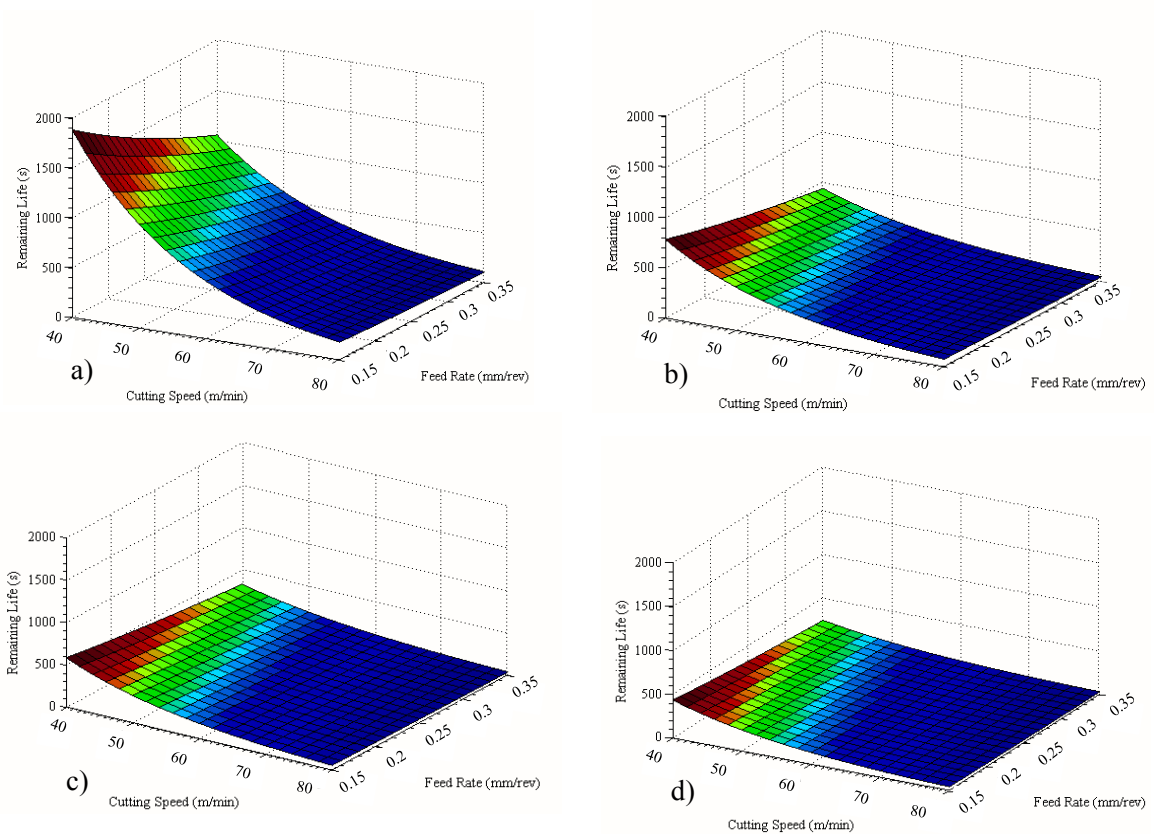

Figure 5-8: Remaining tool life versus cutting conditions calculated for cutting inserts with: VB_{Bmax}=0; b) VB_{Bmax}=0.075; VB_{Bmax}=0.1; VB_{Bmax}=0.125

In Figure 5-8-a, the tool wear level is set as zero. Thus, the remaining life till failure for a new tool at any desired combination of cutting speed and feed could be estimated using this plot.

As another example, suppose that have a worn tool with the tool wear of VB_{Bmax} equal to 0.075 mm. Figure 5-8-b provides the information regarding the remaining life of this worn insert under different cutting conditions. This could be considered as a valuable data for tool planning and optimization.

In order to validate the predictive performance of the model, a series of experimental tests were designed, consisting of four different experimental runs with arbitrary cutting conditions (Table 5-4). Three replications are conducted for each experimental run.

Table 5-4: Experimental runs for the model validation

Cutting Parameter / Run#	Number of Replications	Cutting Speed (m/min)	Feed Rate (mm/ rev)	Depth of Cut (mm)
6	3	50	0.2	0.2
7	3	70	0.2	0.2
8	3	50	0.3	0.2
9	3	70	0.3	0.2

For each experimental run, the estimated remaining useful life calculated from the model for the range of tool wear between 0 and 0.14 were compared with the results of the experiments. The results are shown in Figure 5-9.

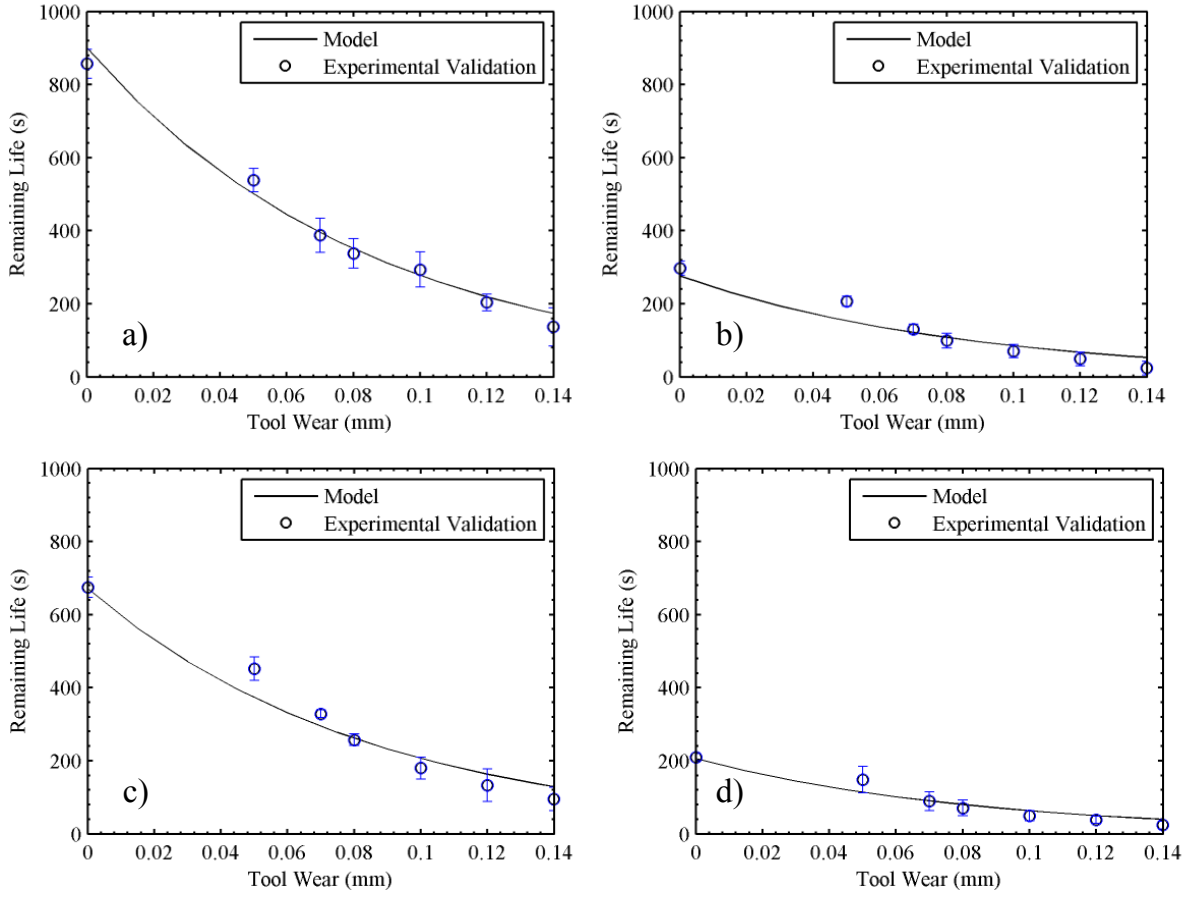

Figure 5-9: Estimated remaining tool life calculated from the model vs the data obtained from the experiments for the validations runs 6 (a) to run 9 (d)

Considering the results for different experimental runs at different tool wear levels shown in Figure 5-9, it can be seen that the results of the model are consistent with the results of the experiments for new and used tools. Almost all the estimated tool lives lie within the calculated 95% confidence interval range obtained from the experiments.

This model could be considered as a very useful and applicable tool for estimating the remaining life of inserts. Minimum number of four machining runs (with only the extreme cutting speeds and feed rates) and with 3 replications are required to establish the model.

Unlike the other models presented before, the real amount of tool wear is used as the input of the model. Thus, only a simple tool wear measurement is requires to find the remaining life of the insert under any desired cutting condition. The method could be applied for any machining operation using its own data.

5.5 Conclusions

A survival analysis is performed in order to estimate the remaining useful life of worn inserts, using a proportional hazards model (PHM). The first substantial advantage of using this model for tool life estimation is that the model accounts for the effect of aging, in addition to the effect of cutting parameters, significantly increasing the accuracy of the results. The second principal advantage is that different uncontrollable variables such as tool wear itself can contribute to the model. Benefitting from these advantages, an accurate model is proposed to estimate the remaining useful life of new and used inserts under different cutting conditions, using the tool wear and cutting conditions as the input data. Therefore, merely by having the amount of tool wear of the worn tool, the remaining useful life under any desired cutting condition could be estimated. The accuracy of the estimated results was tested using validation experiments, showing a very good agreement.

5.6 Acknowledgement

The authors would like to thank Canadian Network for Research and Innovation in Machining Technology (CANRIMT) for their financial support, the Dynamet Technology Inc. for providing us with the material workpieces, and Seco Tools for supplying the cutting inserts. The aerospace structures, material and manufacturing laboratory of National Research Council Canada (NRC) is

acknowledged for its valuable contributions and support. The authors would also acknowledge Professor S. Yacout for providing us with EXAKT software and her contribution in this study.

5.7 References

Ao, Y., & Qiao, G. (2010). Prognostics for drilling process with wavelet packet decomposition. *The International Journal of Advanced Manufacturing Technology, 50*(1-4), 47-52.

Aramesh, M., Y. Shaban, S. Yacout, M. H. Attia, Kishawy, H. A., & M.Balazinski. (2015). Survival life analysis applied to tool life estimation with variable cutting conditions when machining titanium metal matrix composites (Ti-MMCs). *Machining Science and Technology, in press*.

Aramesh, M., Y. Shaban, S. Yacout, M. H. Attia, H. A. Kishawy, M. Balazinski, . (2015). Survival life analysis applied to tool life estimation with variable cutting conditions when machining titanium metal matrix composites (Ti-MMCs). *Machining Science and Technology, in press*.

Astakhov, V. P. (2006). *Tribology of Metal Cutting*: Elsevier.

Astakhov, V. P. (2013). Tribology of Cutting Tools, *Tribology in Manufacturing Technology*. J. P. Davim (Ed.), (pp. 1-66): Springer Berlin Heidelberg.

Baruah, P., & Chinnam, R. B. (2005). HMMs for diagnostics and prognostics in machining processes. *International Journal of Production Research, 43*(6), 1275-1293.

Bhattacharyya, P., Sengupta, D., & Mukhopadhyay, S. (2007). Cutting force-based real-time estimation of tool wear in face milling using a combination of signal processing techniques. *Mechanical Systems and Signal Processing, 21*(6), 2665-2683.

Bhaumik, S. K., Divakar, C., & Singh, A. K. (1995). Machining Ti-6Al-4V alloy with a WBN-CBN composite tool. *Materials & Design, 16*(4), 221-226. doi: http://dx.doi.org/10.1016/0261-3069(95)00044-5

Bonifacio, M., & Diniz, A. (1994). Correlating tool wear, tool life, surface roughness and tool vibration in finish turning with coated carbide tools. *Wear, 173*(1), 137-144.

Cook, R. J., & Lawless, J. F. (2007). *The statistical analysis of recurrent events*: Springer.

Cuppini, D., D'Errico, G., & Rutelli, G. (1990). Tool wear monitoring based on cutting power measurement. *Wear, 139*(2), 303-311. doi: http://dx.doi.org/10.1016/0043-1648(90)90052-C

de Agustina, B., Rubio, E. M., & Sebastian, M. A. (2014). Surface roughness model based on force sensors for the prediction of the tool wear. *Sensors (Switzerland), 14*(4), 6393-6408. doi: 10.3390/s140406393

Devor, R. E., Anderson, D. L., & Zdeblick, W. J. (1977). Tool life variation and its influence on the development of tool life models. *Journal of Engineering for Industry, Transactions of the ASME, 99 Ser B*(3), 578-584.

Dimla Snr, D. E. (2000). Sensor signals for tool-wear monitoring in metal cutting operations—a review of methods. *International Journal of Machine Tools and Manufacture, 40*(8), 1073-1098. doi: http://dx.doi.org/10.1016/S0890-6955(99)00122-4

Feng, D., Lijuan, Z., & Zhengjia, H. (2011). *On-line monitoring for cutting tool wear reliability analysis.* Paper presented at the 2011 9th World Congress on Intelligent Control and Automation (WCICA 2011), 21-25 June 2011, Piscataway, NJ, USA.

Gadelmawla, E. S., Al-Mufadi, F. A., & Al-Aboodi, A. S. (2014). Calculation of the machining time of cutting tools from captured images of machined parts using image texture features. *Proceedings of the Institution of Mechanical Engineers, Part B: Journal of Engineering Manufacture, 228*(2), 203-214. doi: 10.1177/0954405413481291

Gokulachandran, J., & Mohandas, K. (2012). Predicting remaining useful life of cutting tools with regression and ANN analysis. *International Journal of Productivity and Quality Management, 9*(4), 502-518. doi: 10.1504/IJPQM.2012.047195

Hitomi, K., Nakamura, N., & Inoue, S. (1978). reliability analysis of cutting tools (78 - WA/PROD-9).

Jardine, A., Banjevic, D., & Makis, V. (1997). Optimal replacement policy and the structure of software for condition-based maintenance. *Journal of Quality in Maintenance Engineering, 3*(2), 109-119.

Jawahir, I., & Wang, X. (2007). Development of hybrid predictive models and optimization techniques for machining operations. *Journal of Materials Processing Technology, 185*(1), 46-59.

Karandikar, J., McLeay, T., Turner, S., & Schmitz, T. (2013). *Remaining useful tool life predictions using Bayesian inference.* Paper presented at the ASME 2013 International Manufacturing Science and Engineering Conference collocated with the 41st North American Manufacturing Research Conference.

Kleinbaum, D. G., & Klein, M. (1996). *Survival analysis*: Springer.

Klim, Z., Ennajimi, E., Balazinski, M., & Fortin, C. (1996). Cutting tool reliability analysis for variable feed milling of 17-4PH stainless steel. *Wear, 195*(1-2), 206-213. doi: 10.1016/0043-1648(95)06863-5

Liang, S., & Dornfeld, D. (1989). Tool wear detection using time series analysis of acoustic emission. *Journal of Manufacturing Science and Engineering, 111*(3), 199-205.

Liu, H., & Makis, V. (1996). Cutting-tool reliability assessment in variable machining conditions. *IEEE Transactions on Reliability, 45*(4), 573-581. doi: 10.1109/24.556580

Mathew, P. (1989). Use of predicted cutting temperatures in determining tool performance. *International Journal of Machine Tools and Manufacture, 29*(4), 481-497.

Mazzuchi, T. A., & Soyer, R. (1989). Assessment of machine tool reliability using a proportional hazards model. *Naval Research Logistics, 36*(6), 765-777.

Negishi, H., K. Aoki. (1976). Investigations on reliability of carbide cutting tools. *Precis Machining, 42*(6), 578-589.

Odelros, S. (2012). Tool wear in titanium machining.

Patiño Rodriguez, C. E., & Francisco Martha de Souza, G. (2010). Reliability concepts applied to cutting tool change time. *Reliability Engineering & System Safety, 95*(8), 866-873. doi: http://dx.doi.org/10.1016/j.ress.2010.03.005

Shaw, M. C. (1984). *Metal cutting principles*: Clarendon press Oxford.

Tail, M., Yacout, S., & Balazinski, M. (2010). Replacement time of a cutting tool subject to variable speed. *Proceedings of the Institution of Mechanical Engineers, Part B (Journal of Engineering Manufacture), 224*(B3), 373-383. doi: 10.1243/09544054jem1693

Umbrello, D., Hua, J., & Shivpuri, R. (2004). Hardness-based flow stress and fracture models for numerical simulation of hard machining AISI 52100 bearing steel. *Materials Science and Engineering: A, 374*(1), 90-100.

Wager, J. G., & Barash, M. M. (1971). Study of the Distribution of the Life of HSS Tools. *Journal of Manufacturing Science and Engineering, 93*(4), 1044-1050. doi: 10.1115/1.3428041

Wang, K.-S., Lin, W.-S., & Hsu, F.-S. (2001). A new approach for determining the reliability of a cutting tool. *The International Journal of Advanced Manufacturing Technology, 17*(10), 705-709.

Wang, M., & Wang, J. (2012). CHMM for tool condition monitoring and remaining useful life prediction. *The International Journal of Advanced Manufacturing Technology, 59*(5-8), 463-471. doi: 10.1007/s00170-011-3536-7

Wanigarathne, P., Kardekar, A., Dillon, O., Poulachon, G., & Jawahir, I. (2005). Progressive tool-wear in machining with coated grooved tools and its correlation with cutting temperature. *Wear, 259*(7), 1215-1224.

Wong, T., Kim, W., & Kwon, P. (2004). Experimental support for a model-based prediction of tool wear. *Wear, 257*(7–8), 790-798. doi: http://dx.doi.org/10.1016/j.wear.2004.03.010

Xuan-Troung, D., R. Mayer, M. Balazinski. (2014, November 14-20, 2014). *Chaotic Tool wear during machining of titanium metal matrix composites (TiMMCs).* Paper presented at the 2014 ASME International Mechanical Engineering Congress and Exposition, Montreal, Canada.

Zhou, J., Andersson, M., & Ståhl, J.-E. (1995). A system for monitoring cutting tool spontaneous failure based on stress estimation. *Journal of materials processing technology, 48*(1), 231-237.

Chapter 6 ARTICLE 5: META-MODELING OPTIMIZATION OF THE CUTTING PROCESS DURING TURNING TITANIUM METAL MATRIX COMPOSITES (TI-MMCS)

M. Aramesh, B. Shi, A. O. Nassef, H. Attia, M. Balazinski, and H. A. Kishawy, *Procedia CIRP, vol. 8, pp. 576-581, 2013.*

ABSTRACT

The outstanding characteristics of titanium metal matrix composites (Ti-MMCs) have brought them up as promising materials in different industries, such as aerospace and biomedical. They exhibit high mechanical and physical properties, in addition to their low weight, high stiffness and high wear resistance. The presence of the ceramic reinforcements in a metallic matrix further contributes to these preferable properties. However, the high abrasive nature of the ceramic particles limits greatly the machinability of this class of material, as they induce significant tool wear and poor surface finish. In this study an attempt is made to find the optimum cutting conditions in terms of minimizing the tool wear and surface roughness during machining Ti-MMCs. Meta-modeling optimization in performed to achieve the goal.

In this study the three independent parameters under consideration are the cutting speed, feed rate and the depth of cut. The response parameters are the surface roughness and the tool wear rate. The independent parameters are divided into a set of levels at which the experiments are conducted. At each experimental condition the two response parameters are measured. Kriging meta-modeling technique is used to fit a model to the response parameters in the multi-dimensional space. These models are used, in turn, within a multi-objective optimization algorithm to find the optimum cutting condition space. The above-mentioned algorithm is based on an evolutionary multi-objective search technique known as SPEA (Strength Pareto Evolutionary Algorithm).

6.1 Introduction

Metal matrix composites, as a new generation of materials, are aimed at advancing various industrial sectors such as aerospace and biomedical. Titanium MMCs, possessing the advantages of both Titanium and Ti-C particles, exhibit outstanding combination of preferable properties, such as high mechanical and physical properties, increased strength, low weight, high stiffness, high wear resistance and high elastic modulus at the same time. Despite all the favorable properties mentioned above, these materials suffer from poor machinability due to the presence of extremely abrasive reinforcements. Although these MMCs are manufactured as near-net-shape, they require finish machining. The interaction between the tool and abrasive hard reinforcing particles of the workpiece induces severe machining issues. Hence the most important drawbacks of machining MMCs can be listed as severe tool wear and poor surface finish. This in turn leads to high cost and low productivity (Davim, Pramanik, et al., 2008).

Surface quality is one significant concern of machinability, which has been the case of consideration for many years. The selection of optimum cutting parameters in order to achieve the required surface quality has always been a challenge. Cutting conditions, tool characteristics and the workpiece material are among the most important factors affecting the surface roughness. Tool- particle interaction during machining of MMCs significantly influences the quality of the machined surface due to the generation of voids and cavities as a result of particle fracture and/or debonding. This interaction is mainly affected by the variation of the feed, and the effect is reported to be greater than that of cutting speed and volume fraction of particles in machining MMCs (Bhushan et al., 2010). Besides, contradictory effects of feed on the surface roughness have been observed during machining MMCs which requires further examination (Pramanik et al., 2008). Cutting speed also has a significant effect on the surface roughness. Better surface finish has been reported during machining MMCs with higher cutting speeds due to the facilitated removal of the hard reinforcement particles (Bhushan et al., 2010).

Tool life and tool wear tests are considered as one of the most commonly used criteria for evaluating the machinability, which will reveal the performance of the tool as well as the evaluation of the workpiece material (W. H. Cubberly, 1989). Cutting conditions and the size of particle reinforcements as well as volume fraction of particles are the main factors influencing the tool life during machining MMCs. Cutting speed has the major influence on the tool wear.

Flank wear is reported as the dominant wear mode, while two-body and three-body abrasive wear are reported to be the main wear mechanisms during machining MMCs (Karthikeyan et al., 2001; H. A. Kishawy et al., 2005; Li et al., 2001).

Two-body abrasion wear takes place when the reinforcing particles abrade the cutting tool material while they are tightly confined in the matrix material. Scratches parallel with the cutting direction are generated on the flank face through this mechanism. Three-body abrasion wear occurs when the debonded particles from the ductile matrix roll between the tool and the matrix, leaving behind some holes and grooves on the tool flank face (H. A. Kishawy et al., 2005).

This study aims at using a multi-objective algorithm to detect the optimum cutting conditions. The optimization results in achieving the lowest surface roughness and tool wear while maintaining the highest productivity.

6.2 Experiment set up

A 25.4 mm diameter bar of Ti-6Al-4V alloy matrix reinforced with 10-12% volume fraction of TiC ceramic particles is utilized in this study. Dry machining tests were conducted on a 6-axis Boehringer NG 200, CNC turning center, equipped with a Kistler dynamometer model 9121 for force measurement. TH1000 coated carbide inserts (TiSiN-TiAlN nano-laminate PVD coated grades) with nose radius of 0.8 mm were used. The experiment set up is shown in Figure 6-1.

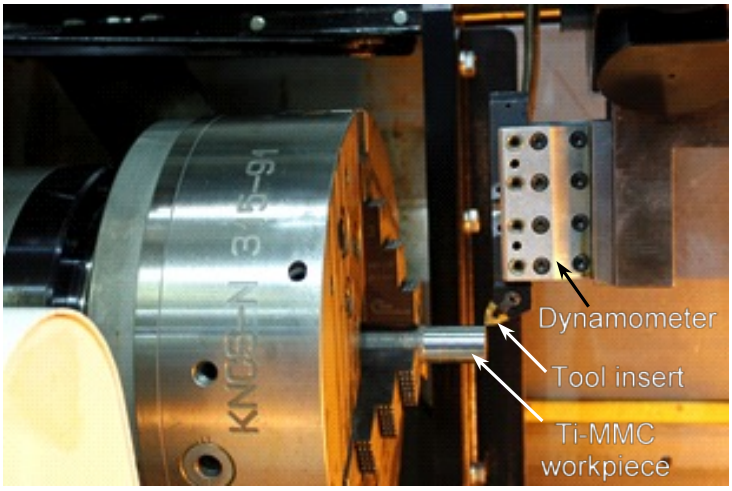

Figure 6-1: The experiment set up

The experiment matrix used in this study is based on a 3 factors and 3 level full factorial design. Cutting speed, feed rate, and depth of cut are selected as the independent parameters. Their values used in this experimental investigation are shown in Table 6-1.

Table 6-1: Cutting parameters and their levels

	Levels		
Factors	Low	Center	High
Cutting Speed (m/min)	80	100	120
Feed rate (mm/rev)	0.1	0.15	0.2
Depth of Cut (mm)	0.8	1	1.2

During each experimental run, surface roughness and tool wear were measured using a Taylor Hobson Precision Form Talysurf Series S4C profilometer and an Olympus SZ-X12 microscope, respectively. The average surface roughness (R_a) is taken as the surface quality criterion. The measurements were repeated three times and their average value is used. The maximum flank wear length (VB_{Bmax}) is selected as the tool wear index. Material removal rate (MRR) is calculated for each run and the normalized rate of tool wear, with respect to MRR, is considered as the basis for comparison in this analysis. This allows reducing the number of variables and comparing tool wear obtained under different cutting conditions of speed, feed and depth of cut. In other words, the combined effect of these parameters that are embedded in the MRR is accounted for.

6.3 Methodology

Surface quality, tool wear and productivity are the crucial aspects of machining processes. The sought-for optimum cutting conditions should be corresponding to the best surface quality, least tool wear and highest productivity. Since these are competing objectives, there is no unique combination of cutting conditions that would correspond to the optimal conditions at the same time. For example, the cutting conditions that reflect the highest productivity or the lowest surface roughness will not necessarily produce the best tool life.

For better understanding of the trade-off between competing objectives, Figure 6-2 shows the contours of two arbitrary functions (e.g. surface roughness and tool wear) drawn for two design variables x_1 and x_2 (e.g., cutting speed and feed). The blue lines represent the desired lower values for either function. Point 1 reflects the best combination of [x_1 and x_2] for one function, while Point 2 is the best point for the second function. The solid line connecting these two points represents a set of combinations of x_1 and x_2 that are better than any other combinations in the design space. This line is known as the trade-off line in the space of design variables.

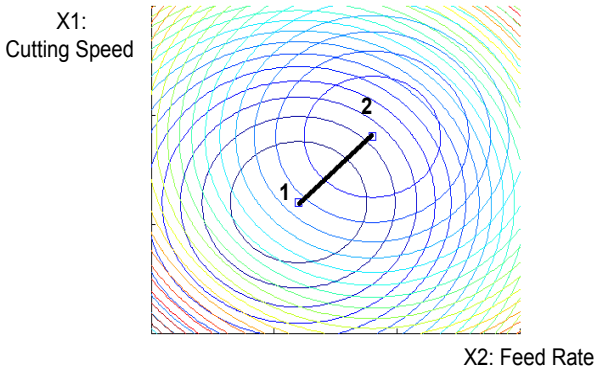

Figure 6-2: An example showing the trade-off line

In the present paper, the design variables are the cutting conditions (cutting speed, feed rate and depth of cut), while the objective functions are the surface quality, tool wear and productivity.

By normalizing tool wear with respect to MMR, this reduces the problem to optimizing two objective functions only. The paper presents an algorithm, which spreads a population of points along the trade-off line of cutting conditions.

It is worth noting that the trade-off line represents the optimal region in the machinability space.

6.3.1 Optimization algorithm

The optimization of the two objective functions is conducted in three steps:

1- A three level full factorial design of experiments is conducted, and experiments are carried out to get values of the objective functions.

2- A meta-model (Kriging model) is used to fit a continuous surface through the discrete experimental outcomes (Goovaerts, 1997).

3- An evolutionary multi-objective optimization method is applied to the continuous functions (from step 2) that spreads a population of search points on the trade-off line of cutting conditions (Zitzler et al., 1999).

Figure 6-3 and Figure 6-4 show the outcomes of the optimization algorithm. As can be seen in the figures, there are three clusters of points on the trade-off space that are named zone 1 to 3. Figure 6-3 shows those zones in the cutting parameters space, while Figure 6-4 shows them in the objective functions space.

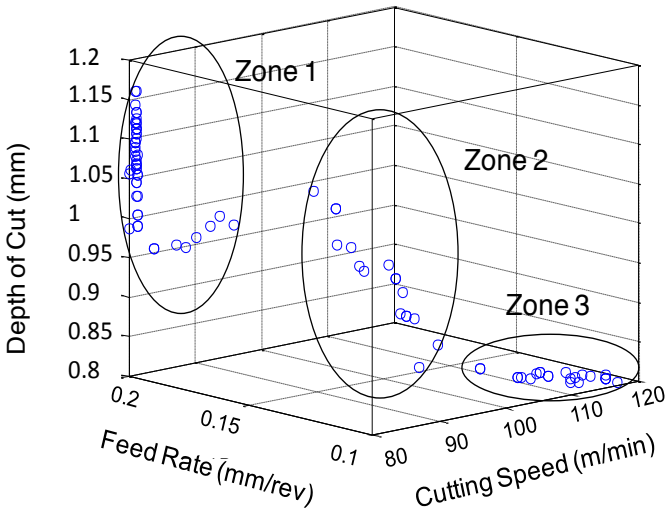

Figure 6-3: Three trade-off zones in cutting parameters space

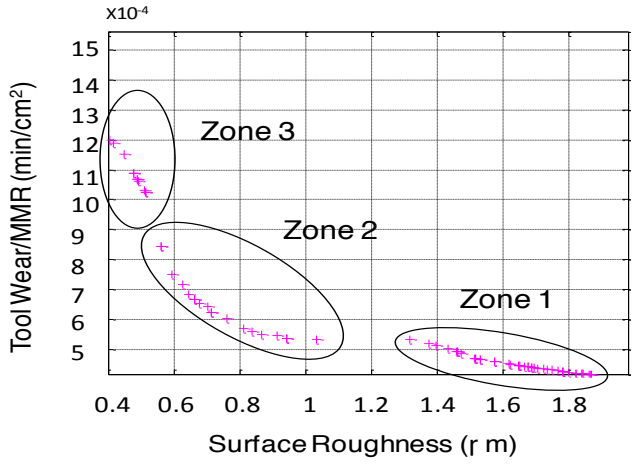

Figure 6-4: Three trade-off zones in objective function space

Looking at Figure 6-3 from a different perspective as shown in Figure 6-5, it can be realized that in each zone one of the cutting parameters can almost be assumed constant. Each of zones 1 and 2 corresponds to a specific feed rate; 0.2 mm/rev and 0.15 mm/rev respectively. On the other hand, zone 3 could be assumed at a fixed depth of cut of 0.8 mm.

Since there are three cutting parameters and a corresponding objective function, this makes four-dimensional space that is impossible to visualize. Keeping one of the cutting parameters constant allows better visualization of the objective functions.

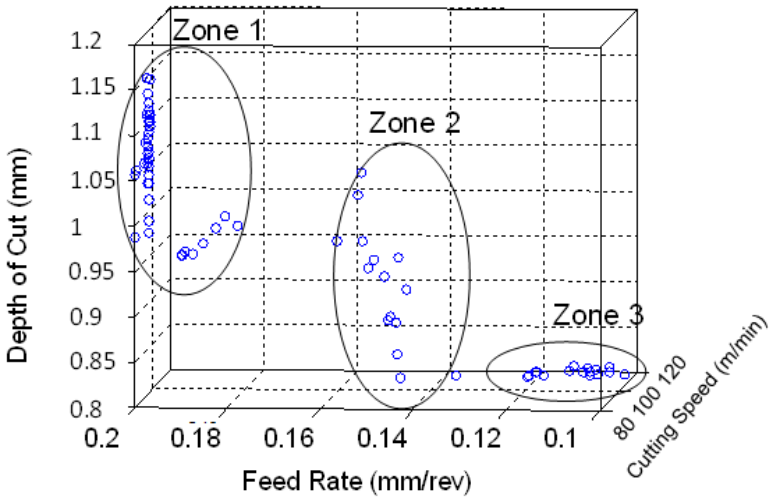

Figure 6-5: The trade-off zones in cutting parameters space from another perspective

For zone 1, Figure 6-6 (a) and Figure 6-6 (b) show the three-dimensional plots of the normalized tool wear and surface roughness, respectively. Additionally, the corresponding contours are shown in Figure 6-7 (a) and Figure 6-7 (b).

The 3D plots show that near to a cutting speed of 80 m/min and a range of depths of cut between 0.95 mm and 1.15 mm, the normalized tool wear exhibits a steep gradient towards its minimum value. Both objective functions become higher above the cutting speed of 80 m/min. Therefore, the trade-off line lies near the boundary of 80 m/min. The trade-off line is extended towards speeds higher than 80 m/min, since the normalized tool wear tends to be constant, whereas the surface roughness gets its lowest values.

Considering the trade-off zones in the objective space (Figure 6-4), zone 1 mostly corresponds to the lowest tool wear. Since tool wear is significantly affected by the cutting speed, the location of

the trade-off line mostly towards the lowest cutting speeds could be reasonably explained; at lower cutting speeds, lower tool wear is expected. On the other hand, considering the contradictory effect of cutting speed on the tool wear and surface roughness, the extension of trade-off line towards the higher speeds could be further explained.

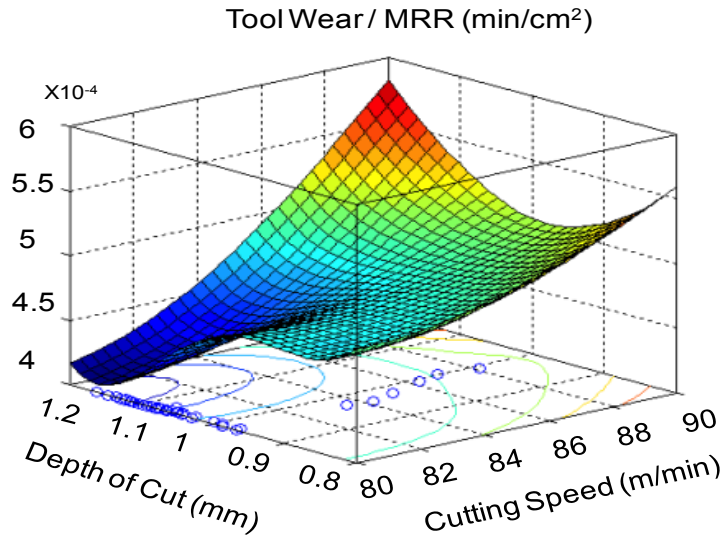

(a)

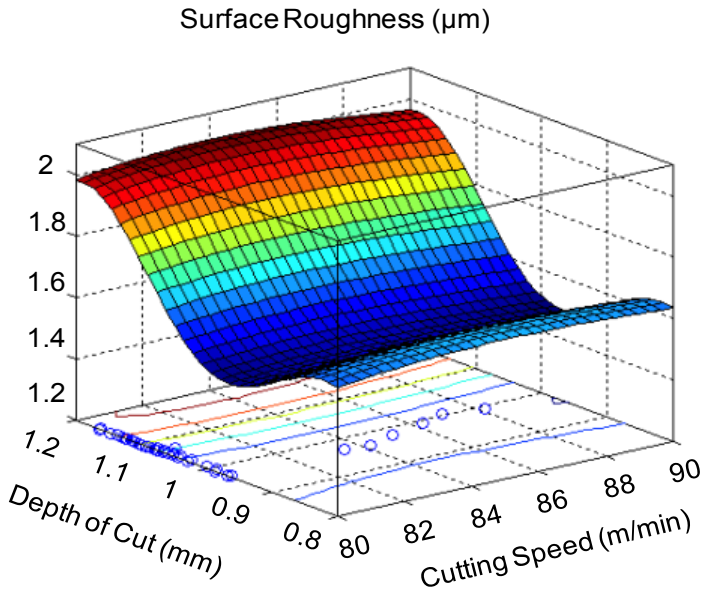

(b)

Figure 6-6: Three-dimensional plots of (a) the tool wear/MRR, and (b) the surface roughness (for zone 1 at feed rate= 0.2 mm/rev)

For zone 1, the above mentioned trend is seen as 2-dimensional contours in Figure 6-7 (a) and Figure 6-7 (b) for tool wear rate and surface roughness, respectively.

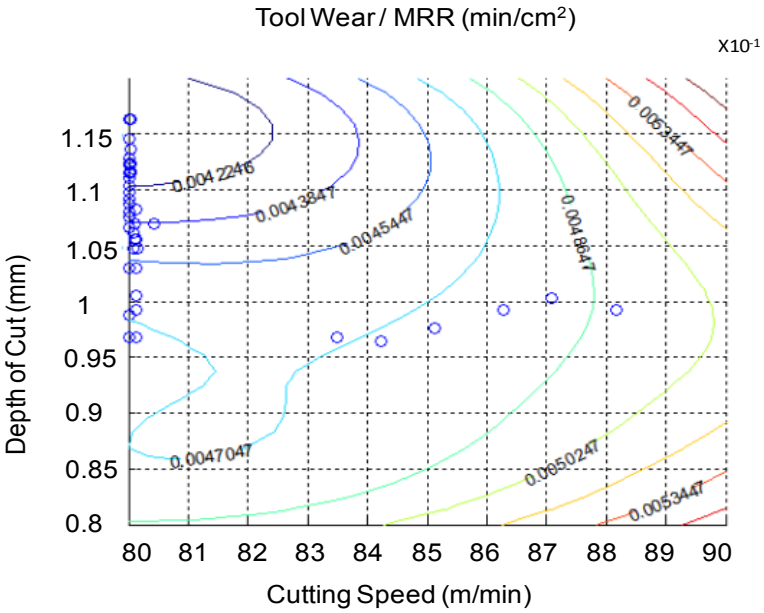

(a)

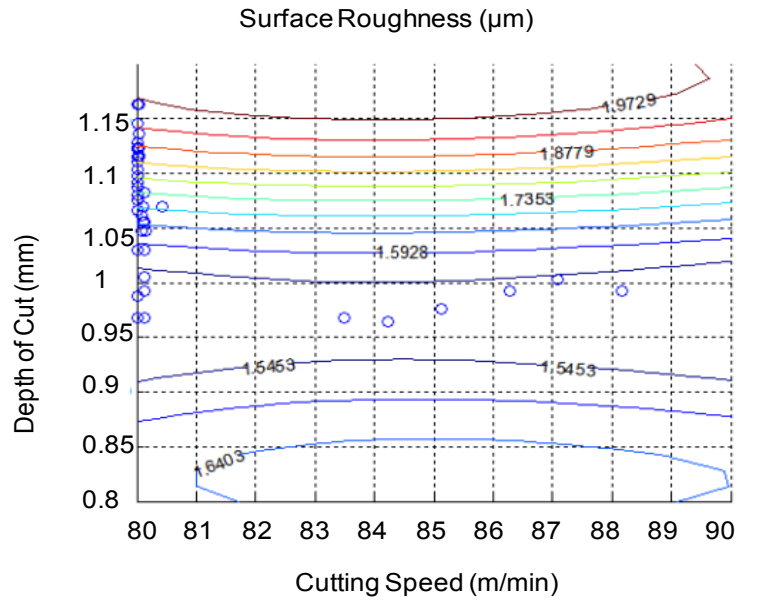

(b)

Figure 6-7: Contours of (a) the tool wear/MRR, and (b) the surface roughness (for zone 1, at feed rate= 0.2 mm/rev)

For zone 2, similar results are shown in Figure 6-8 (a) and Figure 6-8 (b). The two objective functions are competing against each other in this zone. The trade-off points are therefore found at the steepest gradient of both functions.

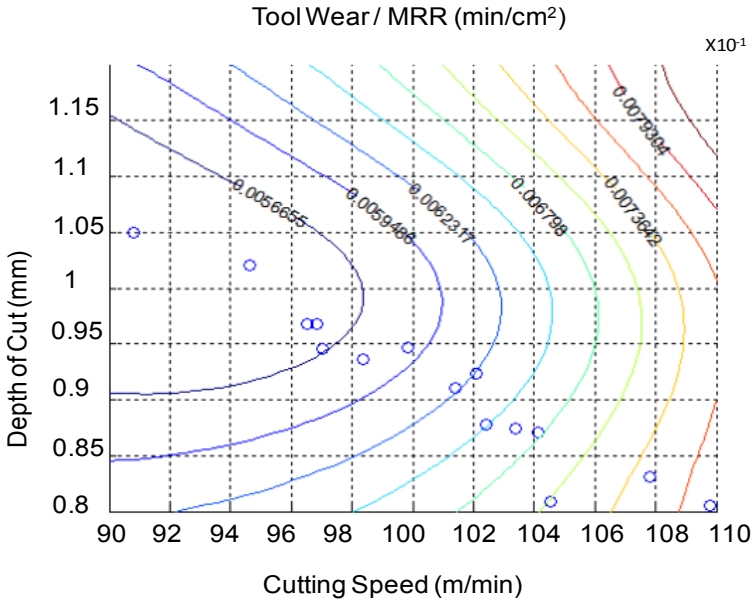

(a)

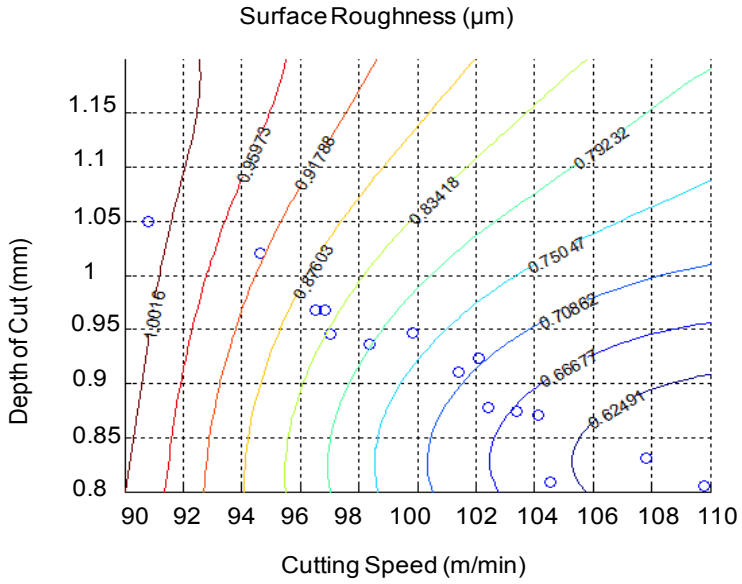

(b)

Figure 6-8: Contours of (a) the tool wear/MRR, and (b) the surface roughness (for zone 2, at feed rate= 0.15 mm/rev)

As mentioned earlier, the hard and abrasive reinforcing particles in MMCs are detrimental to the cutting tools and are responsible for higher tool wear and surface roughness. Cavities and scratches are generated on the tool face and workpiece surface, due to the tool- particle interaction which occurs during machining MMCs. This can be seen in Figure 6-9, which shows SEM images of the tool flank face and workpiece surface during turning Ti-MMCs at conditions correspond to zone 2. This phenomenon was, nevertheless, observed in all three different zones.

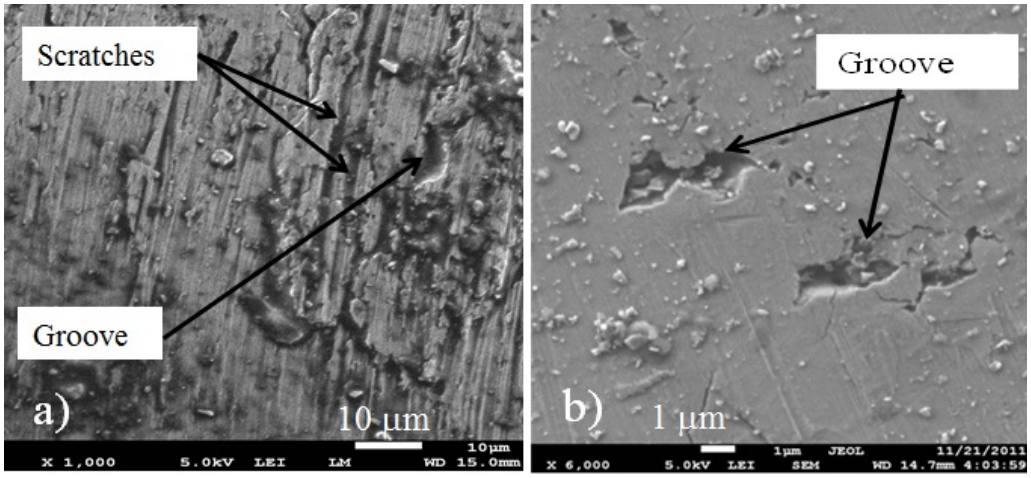

Figure 6-9: Grooves and scratches generated on (a) the tool flank face and (b) the workpiece surface during turning Ti-MMCs at v=100 (m/min), f= 0.15 (mm/ rev) and a_p= 1 (mm)

Figures 10 (a) and 10 (b) show the contours of the two objective functions for zone 3. The two objective functions are coping with each other in this zone. It is worth noting that although the two functions compete, no trade-off points were found above a feed rate of 0.12 mm/rev, since there are other subspaces (in zones 1 or 2) which dominate this sub-zone.

It is also noted that the trade-off points are found along the steepest gradient of the normalized tool wear function. Considering the trade-off zones in the objective space (Figure 6-4), zone 3 almost corresponds to the lowest surface roughness, which is expected to be obtained when machining with high cutting speeds and low feed rates and depths of cut.

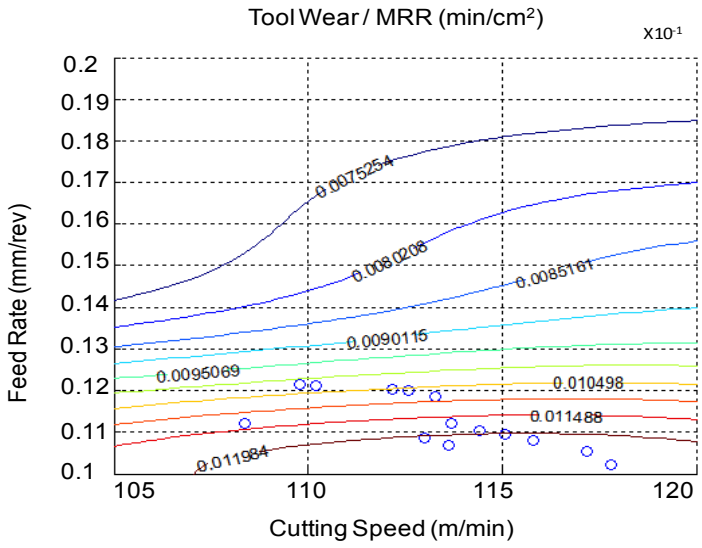

(a)

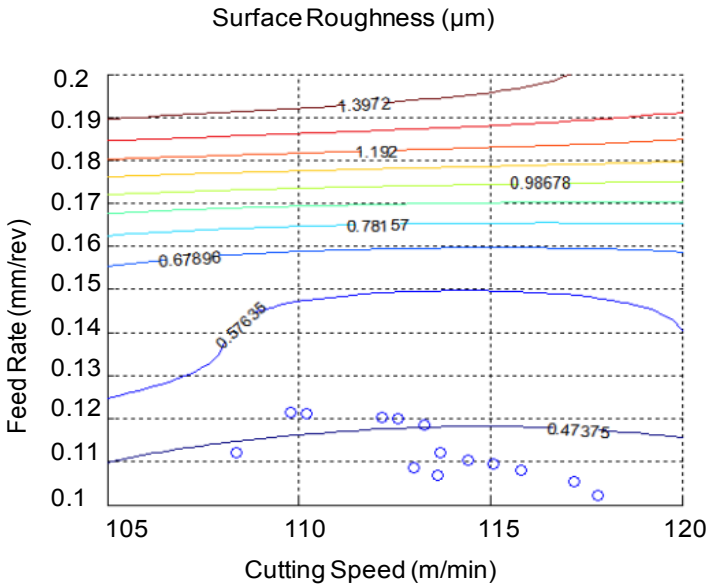

(b)

Figure 6-10: Contours of tool wear/MRR, and (b) Contours of surface roughness (zone 3, for depth of cut = 0.8 mm)

6.4 Conclusions

In this paper, multi objective optimization has been performed to find the combinations of cutting conditions that produce minimum tool wear and surface roughness, while preserving the highest productivity.

The optimization results were grouped into three different zones. The selection of the zone of operation depends on the design requirements and manufacturing constrains. For example, if cost and the productivity are of highest priority while surface roughness is tolerated (as in roughing operation), then the zone 1 would be of interest. On the other hand, when surface quality is of prime importance, then zone 3 would be the choice. Excluding these two extreme conditions, zone 2 provides a compromise between surface quality and productivity

6.5 Acknowledgment

The authors thank the Dynamet Technology Inc. for providing the Ti-MMC material, and Seco Tools for supplying the inserts. The authors acknowledge the Canadian Network for Research and Innovation in Machining Technology (CANRIMT) for their financial support, and the Aerospace Manufacturing Technology Center (AMTC) of the National Research Council Canada (NRC) for its valuable contribution to this work.

6.6 References

Bhushan, R. K., Kumar, S., & Das, S. (2010). Effect of machining parameters on surface roughness and tool wear for 7075 Al alloy SiC composite. *International Journal of Advanced Manufacturing Technology, 50*(Compendex), 459-469.

Davim, J. P., Pramanik, A., Arsecularatne, J. A., & Zhang, L. C. (2008). Machining of Particulate-Reinforced Metal Matrix Composites *Machining* (pp. 127-166): Springer London.

Goovaerts, P. (1997). *Geostatistics for natural resources evaluation*. New York: Oxford University Press.

Karthikeyan, R., Ganesan, G., Nagarazan, R. S., & Pai, B. C. (2001). A critical study on machining of Al/SiC composites. *Materials and Manufacturing Processes, 16*(Compendex), 47-60.

Kishawy, H. A., Kannan, S., & Balazinski, M. (2005). Analytical modeling of tool wear progression during turning particulate reinforced metal matrix composites. *CIRP Annals - Manufacturing Technology, 54*(Compendex), 55-58.

Li, X., & Seah, W. K. H. (2001). Tool wear acceleration in relation to workpiece reinforcement percentage in cutting of metal matrix composites. *Wear, 247*(Compendex), 161-171.

Pramanik, A., Zhang, L. C., & Arsecularatne, J. A. (2008). Machining of metal matrix composites: Effect of ceramic particles on residual stress, surface roughness and chip formation. *International Journal of Machine Tools and Manufacture, 48*(15), 1613-1625. doi: DOI: 10.1016/j.ijmachtools.2008.07.008

W. H. Cubberly, R. B. (1989). Tool and Manufacturing engineers handbook

Zitzler, E., & Thiele, L. (1999). Multiobjective evolutionary algorithms: a comparative case study and the strength Pareto approach. *Evolutionary Computation, IEEE Transactions on, 3*(4), 257-271. doi: 10.1109/4235.797969

Chapter 7 GENERAL DISCUSSION

The general discussion of the thesis, highlighting the most important results of each phase of the study, is provided below.

In the first phase of this work, tool wear mechanism of CBN inserts during machining of Ti-MMCs was investigated for the first time in this study. Three different zones were identified on the CBN flank and rake surfaces during wet machining at relatively high cutting speeds:

An adhered layer consisted of vanadium, titanium and carbon which came from the workpiece material. This layer consisted of two different areas: a sticking area near the cutting edge, and a sliding area located beyond the sticking area till the ultimate contact point between the workpiece/chip and the tool. SEM results showed that some material is also pushed outside the contact region. The EDS analysis revealed traces of oxidation outside of the contact region and around the adhered layer.

A black zone located on the margin of the contact zone. This zone found to be a discontinuity between the non-oxide components inside the contact zone and the oxide contaminated materials outside of the contact zone. Embrittlement of the titanium alloy in the oxide contaminated areas resulted in generation of this discontinuity between the adhered materials.

A white zone surrounding the entire material adhered to the tool. The entire material was surrounded by carbon and boron particles. The clustered material behind these particles appeared as a white zone on the worn surfaces.

Similar morphology was observed on the tool flank surface during machining with different cutting conditions and during dry machining tests as well.

The dominant oxidation mechanism during machining of Ti-MMCs found to be oxidation of magnesium outside the tool/chip contact region, where exposed to oxygen.

The oxide area formed on the tool flank face during coolant through machining was limited to the area between the black and white zones. However, during dry machining, this area was much larger and was not limited to the white zone anymore. Oxygen contamination in titanium alloys results in their embrittlement and reduction of their mechanical properties. Thus, cracks and inclusions could be generated in their structures. The black zone in the tool wear surface is

simultaneously under oxidation and abrasion mechanisms. Therefore, as a result of the tool abrasion, the brittle material in this area was removed from the tool surface during the cutting operation. Investigations performed on the workpiece machined surface also revealed the formation of cracks and cavities on the oxide contaminated area. Formation of different in-situ products, which could result in the embrittlement of titanium alloys during the machining process, was investigated via XRD analysis. Formation of titanium nitride (TiN) and titanium boride (TiB) was confirmed through XRD analysis of the generated chips after machining process.

Agglomeration of boron particles of the tool around the white zone was observed during wet and dry machining on the tool flank face. Very high local temperature is generated in the cutting zone during machining of Ti-MMCs, which could be attributed to a very low thermal conductivity of titanium alloy matrix and the CBN tools. Thus, excessive thermal and mechanical stresses in addition to the severe abrasion wear resulted in the debonding of boron particles. During the machining process, they found to be pushed outside of the contact zone and clustered around the worn area. This fact could inversely affect the cutting performance of these inserts during machining of Ti-MMCs. Debonded TiC particles from the workpiece material were also found around the tool flank worn areas during wet and dry machining conditions. The clustered material behind these particles appeared as a white zone around the worn area.

Such debonding of boron elements was not observed on the rake face of the worn CBN insert. During coolant through machining, the TiC particles were found around the worn area and similar morphology with three different zones was observed on the tool surface. During dry machining conditions TiC particles were pushed away to the corners of the tool flank face. Thus, such distinct black and white layers were not observed on the rake face during dry machining. The adhered material was just blocked behind the carbide particles in the corners of the worn area. Also, similar to the flank face, during dry machining of Ti-MMCs, the oxide area formed around the worn zone was much larger comparing to the wet machining conditions.

Fire hazard was mentioned as a significant issue during machining of Ti-MMCs. The responsible oxidation mechanism is reported for the first time in this paper. Furthermore, the embrittlement of titanium alloy as a result of oxygen contamination was discussed for the first time. The effect on the wear surface morphology and more importantly on the quality of the workpiece material

was also discussed. Thus, inert gas shielded conditions are recommended during machining Ti-MMCs in order to prevent any contamination.

The results of this study also suggest that low content CBN inserts may not be a good choice for machining of Ti-MMCs. High amounts of Al_2O_3 binder in this insert result in a low thermal conductivity; around 40-50 W/mK. The workpiece material also inherits very low thermal conductivity around 5.8 W/mK. Thus, extremely high temperatures are generated in a small area around the cutting zone, which on one hand will induce a chemical mechanism such as oxidation and on the other hand will result in reduction of the interfacial bonding strength between CBN particles and the ceramic binders, leading to debonding during the machining process.

At the second phase of this study, survival analysis was performed in order to estimate the remaining life of inserts during the machining process. At the first step, standard cutting conditions based on the recommendation of the material suppliers were selected. A novel approach was proposed to obtain the transition time between different states of tool wear. Each state of tool wear was analyzed as a separate case, having its own criterion. A Weibull distributions with two parameters (β, η), representing the survival functions were developed based on the experimental data for all inserts and for each state separately. Corresponding probability density function and reliability functions in addition to the mean time to failure (MTTF) were calculated for each state separately. Mean Residual Life (MRL) function was used to predict the transition times between each state. Furthermore, the sojourn time for each state was also obtained from the mean residual life to failure of each state, given that the observation time is equal to zero for state one and equal to $MTTF_1$ and $MTTF_2$ for the second and third states, respectively.

At the second step, a proportional hazards model (PHM) with a Weilbull baseline was developed to estimate the between-state transition times under different cutting conditions during the machining process. This model is based on the fact that the failure rate of a random variable is dependent on *time*, which reflects the aging phenomenon, in addition to *variables* which describe the operating environment. The effect of aging is reflected in the baseline and variables built the second term of the model. Cutting speed and feed rate were added as variables of the model. A similar methodology, as for the first step, was performed to obtain the transition time between each state of tool wear under variable cutting conditions. A specific data layout based on a

complete series of experiments were required to construct the model. The accuracy of the model was validated with the results obtained from the experiments. It was shown that the novel model is well capable of accurately predicting the progressive states of tool wear.

Another advantage of proportional hazards model is that different uncontrollable variables such as tool wear itself can contribute to the model. Taking this advantage, at the third step of this phase, for the first time an accurate model was developed for estimating the remaining life of worn inserts under different cutting conditions, using the current tool wear value as the input. Maximum flank wear length at the transition point between the second and third state of tool wear was chosen as the failure criterion. The results of this study showed that this transition occurs at a very low tool wear value comparing to the other materials during machining of Ti-MMCs and the tool is worn out extremely fast after reaching this point. The model is capable of predicting the remaining life of inserts to this point at any desired cutting condition and at any desired tool wear level. Unlike the other models presented before, the real amount of tool wear is used as the input of the model. Thus, only a simple tool wear measurement is required to find the remaining life of the insert under any desired cutting condition. The accuracy of the model was validated with the experimental results. The results confirmed the validity and reliability of the model.

A complementary analysis was also performed to find the optimum cutting conditions which result in minimum tool wear and surface roughness while preserving the highest productivity. The independent parameters were cutting speed, feed rate and depth of cut. The response parameters were the surface roughness and the tool wear rate. The kriging meta-modeling technique was also used to fit the model to the response parameters in the multi-dimensional space. An evolutionary multi-objective optimization was performed in turn in order to find the optimum cutting conditions. The optimization results were grouped into three different zones in the parameter space. The selection of the zone of operation depends on the design requirements and manufacturing constraints. Multi-objective optimization has not been performed on this material previously. Thus, this information could be considered as a very valuable data for manufacturers.

7.1 Originality of the work and contribution to knowledge

There is a significant lack of data regarding the machinability of Ti-MMCs. Severe tool wear, very short tool life and low surface quality are the main drawbacks of employing this class of materials. Thus, several experimental and analytical investigations were performed to address these issues during machining of Ti-MMCs. The main contributions of this study are as follows:

- For the first time, a detailed analysis was performed to investigate the tool wear mechanisms of CBN inserts during turning of Ti-MMCs. CBN inserts, as the second hardest available tools, could be considered as a potential alternative for costly PCD tools for machining of Ti-MMCs. Yet, there is no literature available regarding the wear mechanisms of these inserts during machining of Ti-MMCs. This study highlights the formation of a unique wear morphology on the CBN surfaces. An in-depth microstructural analysis was performed to discover the responsible wear mechanisms.
- Chemical wear mechanisms, especially the oxidation mechanisms during machining of Ti-MMCs were not studied before. The oxidation rate is so severe that fire hazard should be considered an important issue during machining of this class of material. This mechanism was studied in this investigation for the first time.
- The effect of embrittlement of the titanium workpiece alloy during the machining process and the impact on the tool and workpiece surface morphologies were studied for the first time. Microstructural analysis of the machined surface revealed several brittle fractures, cracks and cavities on the oxygen contaminated areas. This phenomenon was studied in this work and the different responsible mechanisms were investigated.
- A novel model was proposed for modeling the progressive states of tool wear under different cutting conditions. Since this model is based on the theory of probability, it could account for considerable variability of tool wear data originating from the non-homogenous distribution of reinforcing particles. Furthermore, the effect of aging in addition to the influence of cutting parameters is considered in this model. Thus, the model is very suitable for tool life estimation during machining of Ti-MMCs. Furthermore, this is the first model proposed to estimate the time to reach different states of tool wear. This study could not only be of interest for various academic studies, also its

results could be valuable data for industrial applications. The second transition point is considered as an important criterion for tool replacement in any machining operation. This is even more crucial for machining of Ti-MMCs, since the tool wears out drastically beyond this point. Thus, reliable estimation of this point could significantly contribute to productivity improvement by reducing the huge cost associated with sub-optimal replacement of tools.

- Another more advanced novel method is developed for estimating the remaining life of worn inserts under different cutting conditions. This is the first model of its kind, which considers the current tool wear data as the input and provides the remaining life at any tool wear level. Thus, merely by knowing the existing tool wear value, the model is capable of estimating the remaining life at any desired cutting condition. This could contribute to safe and reliable reuse of worn tools and in turn to cost reduction and productivity increase. Furthermore, the second tool wear transition point was considered as the failure criterion for tool replacement, which adds value to the model in terms of its accuracy and applicability.
- For the first time, multi-objective optimization is performed in order to find the optimum cutting conditions that result in minimum tool wear and surface roughness while preserving the highest productivity during machining of Ti-MMCs. The results contribute significantly in quality and productivity increase of the machining process.

Chapter 8 GENERAL CONCLUSIONS

This study focused on the tool wear and tool life analysis of cutting inserts during machining of Ti-MMCs, due to the crucial impact of this study on the machinability of this class of material. The general conclusions drawn from experimental and analytical investigations are listed below.

- Three different zones were identified on the CBN flank and rake surfaces during wet machining at relatively high cutting speeds: an *adhered layer* on the tool worn surfaces composed of work-piece materials such as Ti, Al, C and V adhered to the tool surface inside the contact region, *a black zone* found on margin of the contact region. SEM analysis showed that this zone was in fact a discontinuity between the non-oxide components inside the contact zone and the oxide contaminated materials outside the contact zone; and *a white zone* surrounding the entire materials adhered to the tool.
- High metallic interlocking between the workpiece elements and the tool resulted in generation of an adhered layer inside the contact region which consisted of two different areas: a sticking area near the cutting edge and a sliding area which is located beyond the sticking area till the ultimate contact point between the workpiece and the tool. It was further shown that some material was pushed outside of the contact region.
- Energy Dispersive Spectroscopy (EDS) analysis of the tool surfaces revealed that reaction between magnesium and oxygen is the primary oxidation mechanism which occurs during machining of Ti-MMCs. Very high affinity of magnesium with oxygen constantly resulted in the oxidation of magnesium outside the tool/chip contact region, where exposed to oxygen.
- Contamination of the titanium alloy matrix with oxygen outside the contact region was resulted in its embrittlement and reduction in mechanical properties. Therefore, around the contact region, simultaneous abrasion and oxidation mechanisms resulted in the brittle fracture and debonding of adhered materials from the tool. Thus, a distinct discontinuity was formed within the materials adhered to the tool around the contact region, which appeared as a black zone.
- The EDS analysis also revealed that extremely high temperatures at the contact region in addition to the severe abrasion wear on the tool flank face resulted in reduction of the

bond strength of the tool boron particles on the tool flank face during wet and dry machining conditions. Thus, some boron particles were deboned and pushed out in the direction of the cutting force and agglomerated around the tool worn area. Debonded TiC particles from the workpiece material were also found around the tool worn area. The clustered material behind these barriers appeared as a white zone on the worn surfaces. The debonding of boron particles was not observed on the tool rake face during dry and wet machining conditions. During wet machining conditions TiC particles surrounded the worn area. Thus, a similar morphology with three different zones was observed on the tool rake face after wet machining. The TiC particles were pushed to the corners of the tool worn zone during dry machining conditions. Hence, no white and black zones were observed in this conditions on the tool rake face.

- During the dry machining of Ti-MMCs, the oxide area was bigger and was not limited to the white zone in both flank and rake faces.
- SEM analysis of the workpiece machined surface revealed traces of severe oxidation and brittle fracture in the oxide areas, suggesting that the embrittlement of titanium alloy could also be considered as a root cause of poor surface quality of the finished parts.
- No compatibility between the CBN pattern and HBN pattern was observed via XRD analysis of the tool worn surfaces, suggesting no transformation occurred during neither wet nor dry cutting conditions.
- A new model based on a proportional hazards model (PHM) with a Weibull baseline is developed in order to estimate all the progressive states of tool wear under different cutting conditions during turning of Ti-MMCs. One of the advantages of employing the PHM as the predictive model for tool life estimation is that the effects of aging and cutting parameters are taken into consideration, resulting in high accuracy of the model. Furthermore, this statistical model could account for considerable variability of the tool wear data which occurs during machining of MMCs. The results of the model were validated by the experimental results. The results are were very well compatible. Since each state of tool wear was analyzed as an individual case, an adjusted function was derived and used for calculating the time between transition points. Thus, the evolution of different phenomena occurring at each state was also reflected in the model.

- Another substantial advantage of PH models is that different uncontrollable variables such as tool wear could be added to the model. Taking the advantage of this aspect, a more advanced novel method was proposed for tool life estimation of worn inserts under different cutting conditions. Since the current tool wear data itself was added to the model as the input variable, merely by having the tool wear of a worn insert, the model is capable of predicting its remaining life till failure at any desired cutting conditions. The accuracy of the results were validated via experiments, showing a very good agreement.
- A complementary study was also performed in order to find the optimum cutting conditions which resulted in minimum wear, minimum surface roughness and highest productivity, using multi-objective optimization algorithm. Three different optimized zone were obtained on the parameter space. The selection of desired zone depends on the manufacturers` priority and constraints in terms of surface quality and tool wear level.

8.1 Recommendations for Future Research Work

Tool wear, chip morphology, surface integrity and optimization are considered as the most important topics for any machinability analysis. Since Ti-MMC is a new class of material, they suffer from significant lack of knowledge and data in regarding to their machinability.

Different tools could be investigated in order to find the best alternative for the costly PCD tools. High content CBN inserts could be considered as a very good potential, due to their high thermal conductivity and high hardness and wear resistance.

Tool life estimation is also considered as an important data for any machinability analysis. Different controllable and uncontrollable variables could be added to the proposed model in this study. Thus, tool life estimation could be performed for different operations such as roughing operations with different depth of cuts, using the same model. Furthermore, other uncontrollable variables such as temperature and cutting forces could be added to the model in order to investigate the effect of these parameters on the tool life.

Comprehensive investigation of chip morphology could lead to better understanding of different phenomena occurring during machining of Ti-MMCs.

Phase and martensitic transformations during machining of Ti-MMCs has been also studied previously (Aramesh et al., 2012). Phase transformation is considered as the thermal root cause of machining induced residual stresses. This study could be completed via investigating the residual stresses created on the machined surface. This is an area which has huge potentials for investigations and will contribute in understanding and improving the surface integrity during machining of this class of materials.

Multi objective optimization could also be performed for different operations such as semi-finishing and finishing operations in order to obtain the desired range of cutting conditions which result in minimum tool wear, surface roughness and maximum productivity. The results would be a valuable data for the manufacturers.

BIBLIOGRAPHY

Abkowitz, S., & Fisher, H. (2011). Breakthrough claimed for titanium PM. *Metal Powder Report, 66* (6), 16-21.

Angseryd, J., & Andrén, H. O. (2011). An in-depth investigation of the cutting speed impact on the degraded microstructure of worn PCBN cutting tools. *Wear, 271*(9–10), 2610-2618. doi: http://dx.doi.org/10.1016/j.wear.2010.11.059

Ao, Y., & Qiao, G. (2010). Prognostics for drilling process with wavelet packet decomposition. *The International Journal of Advanced Manufacturing Technology, 50*(1-4), 47-52.

Aouici, H., Yallese, M. A., Chaoui, K., Mabrouki, T., & Rigal, J.-F. (2012). Analysis of surface roughness and cutting force components in hard turning with CBN tool: Prediction model and cutting conditions optimization. *Measurement, 45*(3), 344-353. doi: 10.1016/j.measurement.2011.11.011

Aramesh, M., Balazinski, M., Attia, H., & Kishawy, H. (2012). An experimental investigation on the deformation process during cutting titanium metal matrix composites (Ti-MMCs). Paper presented at the *First international conference on virtual machining process technologies CIRP sponsered conference (VMPT 2012)*, Montreal, Canada.

Aramesh, M., Shaban, Y., Balazinski, M., Attia, H., Kishawy, H. A., & Yacout, S. (2014). Survival Life Analysis of the Cutting Tools During Turning Titanium Metal Matrix Composites (Ti-MMCs). *Procedia CIRP, 14*(0), 605-609. doi: http://dx.doi.org/10.1016/j.procir.2014.03.047

Aramesh, M., X. Rimpault, H. K. Zdzislaw, & Balazinski, M. (2013). Wear Dependent Tool Reliability Analysis during Cutting Titanium Metal Matrix Composites (Ti-MMCs). *SAE Int. J. Aerospace, 6*(2), 492-498. doi: 10.4271/2013-01-2198

Aramesh, M., Y. Shaban, S. Yacout, M. H. Attia, Kishawy, H. A., & M.Balazinski. (2015). Survival life analysis applied to tool life estimation with variable cutting conditions when machining titanium metal matrix composites (Ti-MMCs). *Machining Science and Technology, in press*.

Astakhov, V. P. (2006). *Tribology of Metal Cutting*: Elsevier.

Astakhov, V. P. (2013). Tribology of Cutting Tools. In J. P. Davim (Ed.), *Tribology in Manufacturing Technology* (pp. 1-66): Springer Berlin Heidelberg.

Astakhov, V. P. (2014). Machinability: Existing and Advanced Concepts *Machinability of Advanced Materials* (pp. 1-56): John Wiley & Sons, Inc.

Banjevic, D., Jardine, A. K. S., Makis, V., & Ennis, M. (2001). A control-limit policy and software for condition-based maintenance optimization. *INFOR, 39*(1), 32-50.

Barry, J., & Byrne, G. (2001). Cutting tool wear in the machining of hardened steels. Part II: Cubic boron nitride cutting tool wear. *Wear, 247*(2), 152-160. doi: 10.1016/s0043-1648(00)00528-7

Baruah, P., & Chinnam, R. B. (2005). HMMs for diagnostics and prognostics in machining processes. *International Journal of Production Research, 43*(6), 1275-1293.

Bejjani, R. (2012). Mashinability and modeling of cutting mechanism for titanium metal matrix composites. *Doctarate degree dissertation*, Polytechnique Montreal.

Bejjani, R., Aramesh, M., Balazinski, M., Kishawy, H., & Attia, H. (2011). Chip morphology Study of Titanium metal matrix composites. Paper presented at the *23rd Canadian Congress of Applied Mechanics*.

Bejjani, R., M. Balazinski, B. Shi, H. Attia, & Kishawy, H. (2011). Machinability and chip formation of Titanium Metal Matrix Composites (Ti-MMCs). *Int. J. of Advanced Manufacturing Systems, IJAMS, 13*(1).

Benkedjouh, T., Medjaher, K., Zerhouni, N., & Rechak, S. (2013). Health assessment and life prediction of cutting tools based on support vector regression. *Journal of Intelligent Manufacturing*, 1-11. doi: 10.1007/s10845-013-0774-6

Berthelot, J.-M. (1999). *Composite materials mechanical behavior and structural analysis*. New York: Springer.

Bhattacharyya, P., Sengupta, D., & Mukhopadhyay, S. (2007). Cutting force-based real-time estimation of tool wear in face milling using a combination of signal processing techniques. *Mechanical Systems and Signal Processing, 21*(6), 2665-2683.

Bhaumik, S. K., Divakar, C., & Singh, A. K. (1995). Machining Ti-6Al-4V alloy with a WBN-CBN composite tool. *Materials & Design, 16*(4), 221-226. doi: http://dx.doi.org/10.1016/0261-3069(95)00044-5

Bhushan, R. K., Kumar, S., & Das, S. (2010). Effect of machining parameters on surface roughness and tool wear for 7075 Al alloy SiC composite. *International Journal of Advanced Manufacturing Technology, 50*(Compendex), 459-469.

Bindal, M. M., Singhal, S. K., Singh, B. P., Nayar, R. K., Chopra, R., & Dhar, A. (1991). Synthesis of cubic boron nitride using magnesium as the catalyst. *Journal of Crystal Growth, 112*(2-3), 386-401. doi: 10.1016/0022-0248(91)90314-u

Bonifacio, M., & Diniz, A. (1994). Correlating tool wear, tool life, surface roughness and tool vibration in finish turning with coated carbide tools. *Wear, 173*(1), 137-144.

Braun, W. J., Miller, M. H., & Schultze, J. F. (1999). The development of machine-tool force reconstruction for wear identification. Paper presented at the *Proceedings of the 17th International Modal Analysis Conference*.

Brun, M., Lee, M., & Gorsler, F. (1985). Wear characteristics of various hard materials for machining SiC-reinforced aluminum alloy. *Wear, 104*(1), 21-29.

Byrne, G., Dornfeld, D., & Denkena, B. (2003). Advancing Cutting Technology. *CIRP Annals - Manufacturing Technology, 52*(2), 483-507. doi: Doi: 10.1016/s0007-8506(07)60200-5

Chiou, S.-Y., Ou, S.-F., Jang, Y.-G., & Ou, K.-L. (2013). Research on CBN/TiC composites Part1: Effects of the cBN content and sintering process on the hardness and transverse rupture strength. *Ceramics International, 39*(6), 7205-7210. doi: http://dx.doi.org/10.1016/j.ceramint.2013.02.066

Ciftci, I., Turker, M., & Seker, U. (2004). CBN cutting tool wear during machining of particulate reinforced MMCs. *Wear, 257*(9), 1041-1046.

Clark, R. K., & Unnam, J. (1983). Residual mechanical properties of Ti-6Al-4V after simulated Space Shuttle reentry. *NASA Technical Memorandum*.

Cook, R. J., & Lawless, J. F. (2007). *The statistical analysis of recurrent events*: Springer.

Cuppini, D., D'Errico, G., & Rutelli, G. (1990). Tool wear monitoring based on cutting power measurement. *Wear, 139*(2), 303-311.

Dabade, U. A., Joshi, S. S., Balasubramaniam, R., & Bhanuprasad, V. (2007). Surface finish and integrity of machined surfaces on Al/SiCp composites. *Journal of Materials Processing Technology, 192*, 166-174.

Dai, L. H., Liu, L. F., & Bai, Y. L. (2004). Effect of particle size on the formation of adiabatic shear band in particle reinforced metal matrix composites. *Materials Letters, 58*(11), 1773-1776. doi: 10.1016/j.matlet.2003.10.050

Das, D. K., Mishra, P. C., Singh, S., & Thakur, R. K. (2014). Tool wear in turning ceramic reinforced aluminum matrix composites—A review. *Journal of Composite Materials, 0*(0), 1-13.

Das, S., Chattopadhyay, A., & Murthy, A. (1996). Force parameters for on-line tool wear estimation: a neural network approach. *Neural networks, 9*(9), 1639-1645.

Davim, J. P. (2002). Diamond tool performance in machining metal–matrix composites. *Journal of materials processing technology, 128*(1), 100-105.

Davim, J. P. (2008). *Machining: fundamentals and recent advances*: Springer.

Davim, J. P., & Astakhov, V. P. (2008). Tools (Geometry and Material) and Tool Wear *Machining* (pp. 29-57): Springer London.

Davim, J. P., Pramanik, A., Arsecularatne, J. A., & Zhang, L. C. (2008). Machining of Particulate-Reinforced Metal Matrix Composites *Machining* (pp. 127-166): Springer London.

Daymi, A., Boujelbene, M., Salem, S. B., Sassi, B. H., & Torbaty, S. (2009). Effect of the cutting speed on the chip morphology and the cutting forces. *Archives of Computational Materials Science and Surface Engineering, 1*(2), 77-83.

de Agustina, B., Rubio, E. M., & Sebastian, M. A. (2014). Surface roughness model based on force sensors for the prediction of the tool wear. *Sensors (Switzerland), 14*(4), 6393-6408. doi: 10.3390/s140406393

DeVor, R. E., Anderson, D. L., & Zdeblick, W. J. (1977). TOOL LIFE VARIATION AND ITS INFLUENCE ON THE DEVELOPMENT OF TOOL LIFE MODELS. *Journal of Engineering for Industry, Transactions of the ASME, 99 Ser B*(3), 578-584.

Dimla Snr, D. E. (2000). Sensor signals for tool-wear monitoring in metal cutting operations—a review of methods. *International Journal of Machine Tools and Manufacture, 40*(8), 1073-1098. doi: http://dx.doi.org/10.1016/S0890-6955(99)00122-4

Dimla Sr, D. E., & Lister, P. M. (2000). On-line metal cutting tool condition monitoring.: I: force and vibration analyses. *International Journal of Machine Tools and Manufacture, 40*(5), 739-768. doi: http://dx.doi.org/10.1016/S0890-6955(99)00084-X

Ding, W. F., Xu, J. H., Fu, Y. C., Xiao, B., Su, H. H., & Xu, H. J. (2006). Interfacial reaction between cubic boron nitride and Ti during active brazing. *Journal of Materials Engineering and Performance, 15*(3), 365-369. doi: 10.1361/105994906x108747

Ding, X., Liew, W., & Liu, X. (2005). Evaluation of machining performance of MMC with PCBN and PCD tools. *Wear, 259*(7), 1225-1234.

Dobrzański, L., & Dołżańska, B. (2010). Hardness to toughness relationship on WC-Co tool gradient materials evaluated by Palmqvist method. *Archives of Materials Science and Engineering, 43*(2), 87-93.

Ezugwu, E. O., Da Silva, R. B., Bonney, J., & Machado, A. R. (2005). Evaluation of the performance of CBN tools when turning Ti-6Al-4V alloy with high pressure coolant supplies. *International Journal of Machine Tools & Manufacture, 45*(9), 1009-1014. doi: 10.1016/j.ijmachtools.2004.11.027

Farhat, Z. N. (2003). Wear mechanism of CBN cutting tool during high-speed machining of mold steel. *Materials Science & Engineering A (Structural Materials: Properties, Microstructure and Processing), A361*(1-2), 100-110. doi: 10.1016/s0921-5093(03)00503-3

Feng, D., Lijuan, Z., & Zhengjia, H. (2011). On-line monitoring for cutting tool wear reliability analysis. Paper presented at the *2011 9th World Congress on Intelligent Control and Automation (WCICA 2011), 21-25 June 2011*, Piscataway, NJ, USA.

Gadelmawla, E. S., Al-Mufadi, F. A., & Al-Aboodi, A. S. (2014). Calculation of the machining time of cutting tools from captured images of machined parts using image texture features. *Proceedings of the Institution of Mechanical Engineers, Part B: Journal of Engineering Manufacture, 228*(2), 203-214. doi: 10.1177/0954405413481291

Godfrey, T. M. T., Wisbey, A., Goodwin, P. S., Bagnall, K., & Ward-Close, C. M. (2000). Microstructure and tensile properties of mechanically alloyed Ti–6A1–4V with boron additions. *Materials Science and Engineering: A, 282*(1–2), 240-250. doi: http://dx.doi.org/10.1016/S0921-5093(99)00699-1

Gokulachandran, J., & Mohandas, K. (2012). Predicting remaining useful life of cutting tools with regression and ANN analysis. *International Journal of Productivity and Quality Management, 9*(4), 502-518. doi: 10.1504/IJPQM.2012.047195

Goovaerts, P. (1997). *Geostatistics for natural resources evaluation*. New York: Oxford University Press.

Grzesik, W. (2008). *Advanced machining processes of metallic materials: theory, modelling and applications*: Elsevier.

Heath, P. J. (2001). Developments in applications of PCD tooling. *Journal of Materials Processing Technology, 116*(Compendex), 31-38.

Hitomi, K., Nakamura, N., & Inoue, S. (1978). reliability analysis of cutting tools (78 - WA/PROD-9).

Hosseini, A., & Kishawy, H. A. (2014). Cutting Tool Materials and Tool Wear *Machining of Titanium Alloys* (pp. 31-56): Springer.

Hosseini, A., Kishawy, H. A., & Hussein, H. M. (2014). Machinability of Titanium and Its Alloys *Machinability of Advanced Materials* (pp. 95-118): John Wiley & Sons, Inc.

Hotta, M., & Goto, T. (2008). Densification and microstructure of Al2O3-cBN composites prepared by spark plasma sintering. *Journal of the Ceramic Society of Japan, 116*(1354), 744-748.

Huang, S., Tan, K., Wong, Y., De Silva, C., Goh, H., & Tan, W. (2007). Tool wear detection and fault diagnosis based on cutting force monitoring. *International Journal of Machine Tools and Manufacture, 47*(3), 444-451.

Hung, N. P., Loh, N. L., & Xu, Z. M. (1996). Cumulative tool wear in machining metal matrix composites Part II: Machinability. *Journal of Materials Processing Technology, 58*(1), 114-120. doi: http://dx.doi.org/10.1016/0924-0136(95)02115-9

Hung, N. P., Venkatesh, V. C., & Loh, N. L. (1998). Cutting tools for metal matrix composites. *Key Engineering Materials, 138-140*(Compendex), 289-325.

Jardine, A., Banjevic, D., & Makis, V. (1997). Optimal replacement policy and the structure of software for condition-based maintenance. *Journal of Quality in Maintenance Engineering, 3*(2), 109-119.

Jawahir, I., & Wang, X. (2007). Development of hybrid predictive models and optimization techniques for machining operations. *Journal of Materials Processing Technology, 185*(1), 46-59.

Jemielniak, K., Szafarczyk, M., & Zawistowski, J. (1985). Difficulties in tool life predicting when turning with variable cutting parameters. Paper presented at the *CIRP Annals 1985: Manufacturing Technology, Annals of the International Institution for Production Engineering Research. 35th General Assembly of CIRP.*, Palermo, Italy.

Kainer, K. U. (2006). *Metal matrix composites: custom-made materials for automotive and aerospace engineering*: John Wiley & Sons.

Kannan, S., Balazinski, M., & Kishawy, H. (2006). Flank wear progression during machining metal matrix composites. *Journal of Manufacturing Science and Engineering, 128*(3), 787-791.

Kannan, S., Kishawy, H. A., & Balazinski, M. (2006). Flank Wear Progression During Machining Metal Matrix Composites. *Journal of Manufacturing Science and Engineering, 128*(3), 787-791. doi: 10.1115/1.2164508

Karandikar, J., McLeay, T., Turner, S., & Schmitz, T. (2013). Remaining useful tool life predictions using Bayesian inference. Paper presented at the *ASME 2013 International*

Manufacturing Science and Engineering Conference collocated with the 41st North American Manufacturing Research Conference.

Karthikeyan, R., Ganesan, G., Nagarazan, R. S., & Pai, B. C. (2001). A critical study on machining of Al/SiC composites. *Materials and Manufacturing Processes, 16*(Compendex), 47-60.

Kishawy, H. A., Kannan, S., & Balazinski, M. (2005). Analytical modeling of tool wear progression during turning particulate reinforced metal matrix composites. *CIRP Annals - Manufacturing Technology, 54*(Compendex), 55-58.

Kishawy, H. A., M. A. Elbestawi. (1997). Effect of process parameters on chip morphology when machining hardened steel. Paper presented at the *ASME*.

Kleinbaum, D. G., & Klein, M. (1996). *Survival analysis*: Springer.

Klim, Z., Ennajimi, E., Balazinski, M., & Fortin, C. (1996). Cutting tool reliability analysis for variable feed milling of 17-4PH stainless steel. *Wear, 195*(1-2), 206-213. doi: 10.1016/0043-1648(95)06863-5

Klimczyk, P., Figiel, P., Petrusha, I., & Olszyna, A. (2011). Cubic boron nitride based composites for cutting applications. *Journal of Achievements in Materials and Manufacturing Engineering, 44*(2), 198-204.

Knight, W. A., & Boothroyd, G. (2005). *Fundamentals of metal machining and machine tools* (Vol. 69): CRC Press.

Komanduri, R., & Brown, R. H. (1981). On the mechanics of chip segmentation in machining. *Journal of engineering for industry, 103*(Compendex), 33-51.

Komanduri, R., & Schroeder, T. A. (1984). High speed machining. Paper presented at the *Presented at the Winter Annual Meeting of the American Society of Mechanical Engineers.*, New Orleans, LA, USA.

Kramer, B., & Von Turkovich, B. (1986). A comprehensive tool wear model. *CIRP Annals-Manufacturing Technology, 35*(1), 67-70.

Lahiff, C., Gordon, S., & Phelan, P. (2007). PCBN tool wear modes and mechanisms in finish hard turning. *Robotics and Computer-Integrated Manufacturing, 23*(6), 638-644. doi: 10.1016/j.rcim.2007.02.008

Lee, J., Kim, D., & Lee, S. (1998). Statistical analysis of cutting force ratios for flank-wear monitoring. *Journal of Materials Processing Technology, 74*(1), 104-114.

Li, X., & Seah, W. K. H. (2001). Tool wear acceleration in relation to workpiece reinforcement percentage in cutting of metal matrix composites. *Wear, 247*(Compendex), 161-171.

Liang, S., & Dornfeld, D. (1989). Tool wear detection using time series analysis of acoustic emission. *Journal of Manufacturing Science and Engineering, 111*(3), 199-205.

Lin, H., Liao, Y., & Wei, C. (2008). Wear behavior in turning high hardness alloy steel by CBN tool. *Wear, 264*(7), 679-684.

Lin, H. M., Liao, Y. S., & Wei, C. C. (2008). Wear behavior in turning high hardness alloy steel by CBN tool. *Wear, 264*(7-8), 679-684. doi: 10.1016/j.wear.2007.06.006

Lin, W. (2008). The reliability analysis of cutting tools in the HSM processes. *Archives of Materials Science and Engineering, 30*(2), 97-100.

Liu, H., & Makis, V. (1996). Cutting-tool reliability assessment in variable machining conditions. *IEEE Transactions on Reliability, 45*(4), 573-581. doi: 10.1109/24.556580

Luo, S. Y., Liao, Y. S., & Tsai, Y. Y. (1999). Wear characteristics in turning high hardness alloy steel by ceramic and CBN tools. *Journal of Materials Processing Technology, 88*(1–3), 114-121. doi: http://dx.doi.org/10.1016/S0924-0136(98)00376-8

Mallock, A. (1881). The action of cutting tools. *Proc. Roy. SOC London*, 127-139.

Mamalis, A., Kundrak, J., & Horvath, M. (2002). Wear and tool life of CBN cutting tools. *The International Journal of Advanced Manufacturing Technology, 20*(7), 475-479.

Marksberry, P., & Jawahir, I. (2008). A comprehensive tool-wear/tool-life performance model in the evaluation of NDM (near dry machining) for sustainable manufacturing. *International Journal of Machine Tools and Manufacture, 48*(7), 878-886.

Martin, K. (1994). A review by discussion of condition monitoring and fault diagnosis in machine tools. *International Journal of Machine Tools and Manufacture, 34*(4), 527-551.

Mashinini, P. M. (2010). Process window for Friction Stir Welding of 3 mm Titanium (Ti-6Al-4V). *Research dissertation*, Nelson Mandela Metropolitan University.

Mathew, P. (1989). Use of predicted cutting temperatures in determining tool performance. *International Journal of Machine Tools and Manufacture, 29*(4), 481-497.

Mazzuchi, T. A., & Soyer, R. (1989). Assessment of machine tool reliability using a proportional hazards model. *Naval Research Logistics, 36*(6), 765-777.

Miracle, D. B., & Donaldson, S. L. ASM Handbook, Volume 21 - Composites (pp. 1019): ASM International.

Monteiro, S. N., Skury, A. L. D., de Azevedo, M. G., & Bobrovnitchii, G. S. (2013). Cubic boron nitride competing with diamond as a superhard engineering material–an overview. *Journal of Materials Research and Technology, 2*(1), 68-74.

Murray, J. (1986). The Mg− Ti (Magnesium-Titanium) system. *Bulletin of Alloy Phase Diagrams, 7*(3), 245-248.

Negishi, H., K. Aoki. (1976). Investigations on reliability of carbide cutting tools. *Precis Machining, 42*(6), 578-589.

Nikham, S. A., R. Khettabi, V. Songmene. (2014). Machinability and machining of titanium alloys: a review. In J. P. Davim (Ed.), *Machining of titanium alloys*.

Odelros, S. (2012). Tool wear in titanium machining.

Oh, Y. T., Kwon, W. T., & Chu, C. N. (2004). Drilling torque control using spindle motor current and its effect on tool wear. *The International Journal of Advanced Manufacturing Technology, 24*(5-6), 327-334.

Orhan, S., Er, A. O., Camuşcu, N., & Aslan, E. (2007). Tool wear evaluation by vibration analysis during end milling of AISI D3 cold work tool steel with 35 HRC hardness. *NDT & E International, 40*(2), 121-126.

Papoulis, A. (1990). *Probability & statistics* (Vol. 2): Prentice-Hall Englewood Cliffs.

Patiño Rodriguez, C. E., & Francisco Martha de Souza, G. (2010). Reliability concepts applied to cutting tool change time. *Reliability Engineering & System Safety, 95*(8), 866-873. doi: http://dx.doi.org/10.1016/j.ress.2010.03.005

Paulo Davim, J., & Monteiro Baptista, A. (2000). Relationship between cutting force and PCD cutting tool wear in machining silicon carbide reinforced aluminium. *Journal of Materials Processing Technology, 103*(3), 417-423. doi: Doi: 10.1016/s0924-0136(00)00495-7

Poulachon, G., Moisan, A., & Jawahir, I. S. (2001). Tool-wear mechanisms in hard turning with polycrystalline cubic boron nitride tools. *Wear, 250*(1–12), 576-586. doi: 10.1016/s0043-1648(01)00609-3

Pramanik, A., Zhang, L. C., & Arsecularatne, J. A. (2008). Machining of metal matrix composites: Effect of ceramic particles on residual stress, surface roughness and chip formation. *International Journal of Machine Tools and Manufacture, 48*(15), 1613-1625. doi: DOI: 10.1016/j.ijmachtools.2008.07.008

Ravi, A. M., Murigendrappa, S. M., & Mukunda, P. G. (2014). Experimental investigation on thermally enhanced machining of high-chrome white cast iron and to study its machinability characteristics using Taguchi method and artificial neural network. *The International Journal of Advanced Manufacturing Technology*, 1-16. doi: 10.1007/s00170-014-5752-4

Ravindra, H., Srinivasa, Y., & Krishnamurthy, R. (1993). Modelling of tool wear based on cutting forces in turning. *Wear, 169*(1), 25-32.

Recht, R. F. (1964). Catastrophic thermoplastic shear. *J. Appl. Mech., 86*, 189. doi: citeulike-article-id:1981937

Rittel, D. (2009). A different viewpoint on adiabatic shear localization. *Journal of Physics D: Applied Physics, 42*(21). doi: 10.1088/0022-3727/42/21/214009

Salonitis, K., & Kolios, A. (2014). Reliability assessment of cutting tool life based on surrogate approximation methods. *International Journal of Advanced Manufacturing Technology, 71*(5-8), 1197-1208. doi: 10.1007/s00170-013-5560-2

Seshan, S., Guruprasad, A., Prabha, M., & Sudhakar, A. (1996). Fibre-reinforced metal matrix composites - a review. *Journal of the Indian Institute of Science, 76*(Compendex), 1-14.

Shaw, M. C. (1984). *Metal cutting principles*: Clarendon press Oxford.

Shaw, M. C., & Vyas, A. (1993). Chip formation in the machining of hardened steel. *CIRP Annals - Manufacturing Technology, 42*(Compendex), 29-33.

Sikdar, S. K., & Chen, M. (2002). Relationship between tool flank wear area and component forces in single point turning. *Journal of Materials Processing Technology, 128*(1), 210-215.

Songmene, V., & Balazinski, M. (1999). Machinability of graphitic metal matrix composites as a function of reinforcing particles. *CIRP Annals - Manufacturing Technology, 48*(Compendex), 77-80.

Srivatsan, T., & Lewandowski, J. (2006). Metal Matrix Composites *Advanced Structural Materials* (pp. 275-357): CRC Press.

Tail, M., Yacout, S., & Balazinski, M. (2010). Replacement time of a cutting tool subject to variable speed. *Proceedings of the Institution of Mechanical Engineers, Part B (Journal of Engineering Manufacture), 224*(B3), 373-383. doi: 10.1243/09544054jem1693

Taylor, F. W. (1906). On the art of cutting metals. *Proceedings of the American Society of Mechanical Engineers, 28*(3).

Umbrello, D., Hua, J., & Shivpuri, R. (2004a). Hardness-based flow stress and fracture models for numerical simulation of hard machining AISI 52100 bearing steel. *Materials Science and Engineering: A, 374*(1), 90-100.

Umbrello, D., Hua, J., & Shivpuri, R. (2004b). Hardness-based flow stress and fracture models for numerical simulation of hard machining AISI 52100 bearing steel. *Materials Science and Engineering: A, 374*(1–2), 90-100. doi: http://dx.doi.org/10.1016/j.msea.2004.01.012

W. Grzesik, B. K., A. Ruszaj. (2010). Surface integrity of Machined surface. In J. P. Davim (Ed.), *Surface integrity in machining*. London: Springer.

W. H. Cubberly, R. B. (1989). Tool and Manufacturing engineers handbook

Wager, J. G., & Barash, M. M. (1971). Study of the Distribution of the Life of HSS Tools. *Journal of Manufacturing Science and Engineering, 93*(4), 1044-1050. doi: 10.1115/1.3428041

Wager, J. G., M.M. Barash. (1971). Study for distribution of the life of HSS tools. *ASME, J. Eng. Ind., 73*, 295-299.

Wang, K.-S., Lin, W.-S., & Hsu, F.-S. (2001). A new approach for determining the reliability of a cutting tool. *The International Journal of Advanced Manufacturing Technology, 17*(10), 705-709.

Wang, K. S., Lin, W. S., & Hsu, F. S. (2001). A New Approach for Determining the Reliability of a Cutting Tool. *The International Journal of Advanced Manufacturing Technology, 17*(10), 705-709. doi: 10.1007/s001700170114

Wang, M., & Wang, J. (2012). CHMM for tool condition monitoring and remaining useful life prediction. *The International Journal of Advanced Manufacturing Technology, 59*(5-8), 463-471. doi: 10.1007/s00170-011-3536-7

Wanigarathne, P., Kardekar, A., Dillon, O., Poulachon, G., & Jawahir, I. (2005). Progressive tool-wear in machining with coated grooved tools and its correlation with cutting temperature. *Wear, 259*(7), 1215-1224.

Wenfeng, D., Jiuhua, X., Zhenzhen, C., Honghua, S., & Yucan, F. (2010). Effects of Heating Temperature on Interfacial Microstructure and Compressive Strength of Brazed CBIN-AlN Composite Abrasive Grits. *Journal of Wuhan University of Technology - Materials Science Edition, 25*(6), 952-956.

Wong, T., Kim, W., & Kwon, P. (2004). Experimental support for a model-based prediction of tool wear. *Wear, 257*(7–8), 790-798. doi: http://dx.doi.org/10.1016/j.wear.2004.03.010

Xie, L.-J., Schmidt, J., Schmidt, C., & Biesinger, F. (2005). 2D FEM estimate of tool wear in turning operation. *Wear, 258*(10), 1479-1490.

Xuan-Troung, D., R. Mayer, M. Balazinski. (2014, November 14-20, 2014). Chaotic Tool wear during machining of titanium metal matrix composites (TiMMCs). Paper presented at the *2014 ASME International Mechanical Engineering Congress and Exposition*, Montreal, Canada.

Yanming, Q., & Zehua, Z. (2000). Tool wear and its mechanism for cutting SiC particle-reinforced aluminium matrix composites. *Journal of Materials Processing Technology, 100*(1), 194-199. doi: 10.1016/s0924-0136(99)00405-7

Yen, Y.-C., Söhner, J., Lilly, B., & Altan, T. (2004). Estimation of tool wear in orthogonal cutting using the finite element analysis. *Journal of Materials Processing Technology, 146*(1), 82-91. doi: http://dx.doi.org/10.1016/S0924-0136(03)00847-1

Zhang, G. F., Tan, Y. Q., Zhang, B., & Deng, Z. H. (2009). Effect of SiC particles on the machining of aluminum/SiC composite. Paper presented at the *13th International Manufacturing Conference in China, IMCC2009, September 21, 2009 - September 23, 2009*, Dalian, China.

Zhou, J., Andersson, M., & Ståhl, J.-E. (1995). A system for monitoring cutting tool spontaneous failure based on stress estimation. *Journal of materials processing technology, 48*(1), 231-237.

Zitzler, E., & Thiele, L. (1999). Multiobjective evolutionary algorithms: a comparative case study and the strength Pareto approach. *Evolutionary Computation, IEEE Transactions on, 3*(4), 257-271. doi: 10.1109/4235.797969

APENDIX I: LIST OF PUBLICATIONS

Journal Papers:

1- M. Aramesh, Y. Shaban, S. Yacout, M. H. Attia, H. A. Kishawy, M. Balazinski, "Survival life analysis applied to tool life estimation with variable cutting conditions when machining titanium metal matrix composites (TI-MMCs)", Accepted; in press in *Machining Science and Technology,* 2014.

2- M. Aramesh, H. Attia, H. A. Kishawy, and M. Balazinski, "Tool wear mechanisms of CBN inserts during cutting titanium metal matrix composites (Ti-MMCs)," submitted to *International Jourrnal of Machine Tools and Manufacture,* 2015.

3- M. Aramesh, H. Attia, H. A. Kishawy, M. Balazinski, "Estimating the remainig tool life of used inserts using a proportional hazard model", submitted to *CIRP Journal of Manufacturing Science and Technology* , 2015.

4- M. Aramesh, X. Rimpault, H. K. Zdzislaw, M. Balazinski, "Wear Dependent Tool Reliability Analysis during Cutting Titanium Metal Matrix Composites (Ti-MMCs)", *SAE Int. J. Aerospace,* vol. 6, pp. 492-498, 2013.

5- M. Aramesh, Y. Shaban, M. Balazinski, H. Attia, H. A. Kishawy, and S. Yacout, "Survival Life Analysis of the Cutting Tools During Turning Titanium Metal Matrix Composites (Ti-MMCs)", *Procedia CIRP,* vol. 14, pp. 605-609, 2014.

6- M. Aramesh, B. Shi, A. O. Nassef, H. Attia, M. Balazinski, and H. A. Kishawy, "Meta-modeling Optimization of the Cutting Process During Turning Titanium Metal Matrix Composites (Ti-MMCs)", *Procedia CIRP,* vol. 8, pp. 576-581, 2013.

7- Y. Shaban, M. Aramesh, S. Yacout, M. Balazinski, H. Attia, H. A. Kishawy, S. Yacout, M. Balazinski, H. Attia, and H. Kishawy, "Optimal replacement times for machining tool during turning titanium metal matrix composites under variable cutting conditions", Accepted; in press in *Journal of Engineering Manufacture,* 2014, *DOI: 10.1177/0954405415577591*

8- Y. Shaban, M. Aramesh, S. Yacout, M. Balazinski, H. Attia, and H. Kishawy, "Optimal replacement of tool during turning titanium metal matrix composites", accepted; in press in *Industrial Engineers Journal*.

Conference Papers:

1- R. Bejjani, M. Aramesh, M. Balazinski, H. Kishawy, and H. Attia, "Chip morphology Study of Titanium metal matrix composites," in *23rd Canadian Congress of Applied Mechanics*, 2011, pp. 499-502.

2- M. Aramesh, M. Balazinski, H. Attia, H. Kishawy, and R. Bejjani, "A study on phase transformation and particle distribution during machining titanium metal matrix composites," in *26th Annual Technical Conference of the American Society for Composites 2011 and the 2nd Joint US-Canada Conference on Composites*, 2011, pp. 2183-2195.

3- R. Bejjani, M. Balazinski, H. Attia, M. Aramesh, and H. Kishawy, "Segmentation and shear localization when turning TiMMC (Titanium Metal Matrix Composites)," in *26th Annual Technical Conference of the American Society for Composites 2011 and the 2nd Joint US-Canada Conference on Composites*, 2011, pp. 2196-2211.

4- M. Aramesh, M. Balazinski, H. Attia, and H. Kishawy, "An experimental investigation on the deformation process during cutting titanium metal matrix composites (Ti-MMCs)," in *First International Conference on Virtual Machining Process Technologies CIRP sponserod conference (VMPT 2012)*, Montreal, Canada, 2012.

5- M. Aramesh, B. Shi, M.Balazinski, H. Attia, H. Kishawy "On the tribological aspects of machining of titanium metal matrix composites (Ti-MMCs)," presented in *Second International Conference on Virtual Machining Process Technologies, CIRP sponsored conference (VMPT 2013)*, Hamilton, Canada, 2013.

6- M. Aramesh, Y. Shaban, M. Balazinski, H. Attia, H. A. Kishawy "Tool life prediction via survival life analysis of the cutting inserts during turning titanium metal matrix composites (Ti-MMCs)," presented in *Third International Conference on Virtual Machining Process Technologies (VMPT 2014),* Calgary, Canada, 2014.